

*Rock Engineering and Ground Control*



## South African Mining Industry in the New Millenium and New Technologies For The Future

R.G.Gürtunca

*Miningtek, CSIR, Johannesburg, Republic of South Africa*

**ABSTRACT;** The South African Mining Industry has always been faced with immense challenges to mine safely and profitably. The current situation in the mining industry, particularly, gold, coal and platinum group metals are discussed. The new research initiatives and some emerging technologies that will provide solutions to those challenges are also described in the paper.

### 1 INTRODUCTION

The South African mining industry can look back at a century in which it has proved to be the economic mainstay of South Africa and in many ways of some of us neighboring states. However, a number of new challenges face the mining industry as we enter the next millennium, which have necessitated the creation of major initiatives to ensure sustainability of this industry in the long term.

South Africa is rich in mineral reserves as listed in Table 1 and also produces significant amounts of gold, coal, platinum, palladium and rhodium. The total revenue generated by the South African mining industry in 2001 was around R116 billion (about \$15 billion USA) and about 80 per cent of the total revenue is generated from exporting these minerals.

The paper reviews the current situation in the mining industry, particularly gold, coal and platinum group metals and discusses some of the challenges facing those three mining sectors to stay competitive well into the new millennium. The paper also describes the new research initiatives and some emerging technologies that will provide solutions to those challenges.

### 2 CURRENT SITUATION IN THE MINING INDUSTRY

#### 2.1 Gold mining industry

Gold production in South Africa has decreased from 1 200 tonnes in 1970 to 395 tonnes in 2001. There are three major reasons for the reduction on gold output: low productivity, high costs coupled with a low gold price and depletion of high grade gold reserves.

The need for gold producers to go ahead with mine restructuring and re-organization, coupled with a low gold price led to the reduction of workers employed by the gold mines from about 500 000 in 1987 to about 200 000 in 2001.

Safety has always been a key priority for South African gold mining industry. Safety statistics, quoted as reportables per 1 000 people at work per year, improved consistently since the 1960s to the 1980's. However, for the last 10 years these statistics have remained stubbornly constant with little improvement. Improvement is undoubtedly possible through the implementation of current technologies and systems.

At present, only 5% of production occurs below three kilometers and it is estimated (Willis, 1997) that some 40% of total South African production will be sourced from below these depths by 2015, assuming a favourable economic environment.

#### 2.2 Coal mining industry

The South African coal mining industry produces about 225 million tons of coal and about 65 million tons of it is exported. South Africa is the third largest hard coal exporting country and the fourth largest hard coal producer in the world. South Africa ranks fifth largest coal reserves in the world and these reserves are sufficient to last for about 180 years at current run of mine production rates. Almost half of the coal production is from opencast operations. The underground mining methods are bord and pillar, stoop recovery and longwall mining.

Coal meets three quarters of South Africa's primary energy needs. In 2001, 88,2 million tones (nit) of coal was burnt at Eskom power stations and total

electricity sold was 171 7222 Gwh of which 91,4 percent was generated by coal-fired power stations

The South African coal industry employed an average of 51 000 workers in 2001. The average pro-

ductivity figures at coal mines is 4 845 saleable tonnes per employee

Table I Total mineral sales and exports for South Africa

Commodity	Total sales R1 000	Export sales R1 000	Percentage of exports to total sales <t	World Rank	Percentage of World Reserves <A
<b>Precious metals</b>					
Gold	29 011 598	28 651 912	98.8	1	40
PGMs	11 170 849	29 181 009	88.0	1	56
Silver	141 721	116 956	96.6		
Sub total	62 524 170	58 171 577	91.0		
<b>Other Metals</b>					
Chromium	1 002 109	177 286	17.6	1	68
Copper	1 927 165	870 108	45.1		
Iron ore	4 128 901	1 444 701	81.4		
Zinc	115 912	91 764	80.9		
Manganese	1 101 440	877 819	67.4	1	81
Nickel	1 809 686	707 110	19.1		
Other metallic	148 297	61 758	18.1		
Sub total	10 611 712	6 414 566	60.5		
<b>Non metallic minerals</b>					
Coal	26 524 190	16 956 659	61.9	5	11
Fluorspar	274 901	220 221	80.1	1	12
Vein chert	128 782	125 096	97.1	2	40
Granite	717 192	677 698	94.5		
Other non metallic	187 716	192 868	57		
Sub total	11 012 801	18 172 544	58.6		
Miscellaneous*	12 011 915	8 164 275	67.9	2	10
Total	116 222 600	90 941 262	78.2		

\* Includes strategic and minor commodities not otherwise enumerated

Source: Minerals Bureau 26 July 2002

Employment levels on Chamber of Mines member collieries have declined by more than 25 per cent since 1991 despite a more than 20 per cent increase in total output during the same period. This is attributable to increased mine mechanization and aggressive efforts to reduce costs, which improves the South African coal industry's international competitiveness.

Concerns over the quality of the environment at global, national and regional levels and tighter environmental constraints are increasingly pressuring the producers and users of fossil fuels to clean up and reduce pollution. The important environmental issues are increased coal extraction, cleaner coal preparation, closure of coal mines and coal combustion.

### 2.3 Platinum group metals (PGM)

Platinum group metals are platinum, palladium and rhodium. South Africa's proportion of the world's production of PGMs amounted to 46 per cent in 2001 and about 229 tons were produced. The generated revenue of about R13 billion (i.e. \$4 billion USA) in 2001. The South African platinum production is planned to increase by almost 100 per cent by the year 2010.

Although PGM prices are at record high, the platinum mining industry has a few challenges ahead of them. The industry's cost structures are heavily weighted to the mining operation.

Operating costs can be typically 65% - 75% mining, 8-12% concentrating, less than 10% smelting and about 10% refining (Cramer, 2000). The underground mining operations have to increase productivity by using mechanization and reducing labour involvement underground. The Achilles heel of the platinum industry in South Africa is its high

mining costs and, in this respect particularly, its high proportion of labour in those costs. The industry must break out of the low level of training, the unskilled job content, and large numbers required underground (Cramers, 2000).

### 3 NEW MINING TECHNOLOGIES USED IN SOUTH AFRICA

#### 3.1 Dispersed Bagged Stone Dust Passive Barrier System

The prevention of the propagation of coal dust explosions by means of explosion-suppression systems in underground coal mines is a very important activity. For many years, the most commonly used passive barrier system was the Polish Light Barrier. This type of barrier system was developed mainly for long, single-entry mining practices. As the basic design of this barrier system did not change over the past 5 decades, its suitability to modern day mining practices was questioned. Besides this, the installation cost of these barriers is high and they are difficult to install and maintain, making them more of a hindrance than a benefit to modern day underground coal mining practices.

This led the Kloppersbos Test Facility of CSIR: Miningtek to develop a new method of building passive stone dust barriers (Du Plessis et al, 2000). The new system, the bagged stone dust barrier, is based on an array of specially manufactured bags suspended from the roof containing the stone dust. What makes this barrier system different from similar concepts is the newly developed method of rupturing the bags during a coal dust explosion. This is achieved by the special closing mechanism of the bag, and balancing the stone dust content with the void in the bag. Testing of the barrier has shown it to be just as effective, or more so, than conventional barriers, while offering advantages in terms of minimum pressure requirements for operation, improved operational time, reduced costs and ease of installation and maintenance.



Figure 1. Array of dust bags installed in the 200 m test gallery at Kloppersbos

In the development phase of the new system, the bags were tested extensively in the 200 m coal dust explosion gallery at Kloppersbos (Figure 1). The barrier was evaluated against a baseline explosion, which developed a dynamic pressure of 20 kPa with a flame length of 236 in. With the new barrier system installed, the flame length was shortened by at least 100 m, with the static pressure less than half of the base explosion, and the dynamic pressure less than a quarter. From the tests, it became evident that these bags could be made to rupture and spread stone dust when subjected to smaller forces than those required for the more commonly used Polish Light Barrier.

To gain international acceptance of the new South African bagged barrier system and prove its ability to effectively inhibit the propagation of a coal-dust explosion, further testing was carried out at the DMT's Tremonia test gallery in Germany and at the U.S. National Institute for Occupational Safety and Health's (NIOSH) Pittsburgh Research Laboratory Lake Lynn Experimental Mine. This proved the bagged stone dust barrier system to be effective in stopping flame propagation in small (5 m" cross-section at Kloppersbos), medium (12 ft" cross-section at Lake Lynn Laboratory) and large (20 ft" cross-section at Tremonia) explosion galleries. It also proved that that system is effective in stopping coal dust explosions in the multiple entries. Through these extensive test programmes questions such as what influence mine size would have on the design and operation of the bagged barrier was successfully resolved. Furthermore, the question of whether the bagged barrier system would operate in bord-and-pillar workings was positively answered. It has to be remembered though that barrier operation still depends on the type and strength of the explosion to be extinguished and that there are limits to the operational extremes of all barrier designs.

The new bagged stone dust barrier system has been implemented in South Africa and Australia and is considered well suited to modern-day underground coal mining practices. In South Africa, approximately 90 % of all underground coalmines are currently using the new dispersed bagged barrier system.

#### 3.2 CADSminc in Mine Layout Design

A mine layout forms the basis of mine scheduling and production planning. Prior to the implementation of a scheduling procedure, a layout has to be arrived at, therefore. The CADSminc tool, an AS&T-GMSI proprietary software package, has the ability to design and schedule very complex mine layouts for tabular deposits, and the ability to generate multiple scheduling scenarios by varying numerous input parameters (Vieira, 2003).

CADS mine is a mineral resource management tool that provides the user with graphical interfaces for mine planning. It integrates three-dimensional mine layout design and mine-wide layout scheduling in the same three-dimensional space.

CADSmine has two separate modules, namely: the mine design module and the scheduling module. The mine design module generates CAD-type three-dimensional models that represent underground workings through the use of graphical interface MicroStation®. Mine planners are able to create complex layout designs against the background of a geological model and overlaying valuation information. The scheduling module processes certain "sequential rules" in order to output production results in graphic or text format, which include numerous performance variables such as: the time required to develop tunnels, the time required to prepare and mine stopes, amount of rock removed, amount of gold removal, etc.

### 3.3 Minsim 2000

MinSim 2000 is an efficient, three-dimensional mine layout analysis package built around a linear elastic boundary element solution utilising displacement discontinuity elements (MinSim 2000 Manual, 2003). It facilitates the analyses of mine layouts through the full life of mine for tabular ore bodies on a regional-scale, including haulage locations, sloping sequence and regional support strategies. The suite is highly optimised for solving underground tabular mining problems such as the Wilwatersrand gold and Bushveld platinum deposits and is applicable to multi-reef geometries. Although MinSim was originally designed for hard-rock, deep-level mining situations, it has been modified to address other underground tabular mining situations including shallow workings and soft seams such as coal.

MinSim computes the solution in two stages: During the first stage the interaction between significant surfaces, such as mined out seams and faults, is established. Thereafter, stresses, displacements and other design criteria (e.g. average pillar stress, energy release rate and excess shear stress) at predefined points of interest within the model. The results for any chosen variable can be viewed as either two-dimensional sheets or in true 3D. It is important to note that, since the solution methodology assumes the rock mass to be linear, elastic, homogeneous and isotropic, the program is not capable of modelling rock failure and plastic deformation.

MinSim 2000 has been designed to be flexible and extendable enabling future developments and to ensure that MinSim 2000 does not exist in isolation. MinSim 2000 integrates visualisation of stress-strain analysis with recorded mine seismicity as shown in Figure 2. A significant amount of work has been un-

dertaken towards developing integration with mine scheduling software to enable the evaluation and comparison of proposed mining layouts and schedules.

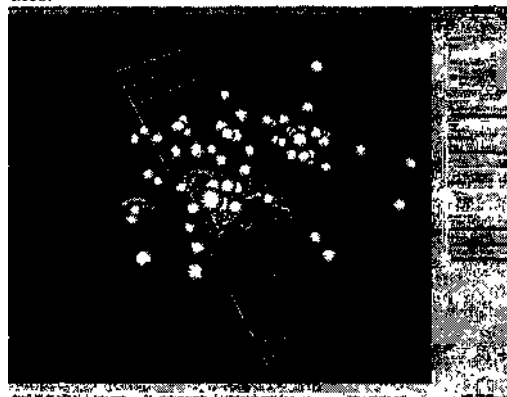


Figure 2. MinSim 2000: integrated visualisation of stress-strain analysis with recorded mine seismicity

Within the realm of numerical modelling tools available to rock mechanics engineers, MinSim 2000 is a user-friendly package. It is, however, designed for use by experienced rock mechanics engineers as its use assumes a significant degree of rock mechanics experience and education. MinSim has been an indispensable mine design and analysis tool within the South African rock mechanics fraternity since the early 1980s and is currently the most widely used tool of this nature in south Africa

### 3.4 Thin Sprawl Linings (TSL)

According to the accident statistics, the rock related accidents (rockfalls and rockbursts) are the major cause of injuries and fatalities in South African underground mines and the majority of these accidents are due to rockfalls. The investigations of accidents caused by rockfalls showed that many of these accidents could have been prevented if there was an effective areal support coverage between support units.

If the rock is highly fragmented, support units such as tendons or mine poles (i.e. elongates) do not provide adequate rock reinforcement and the potential for separation of rock from the rock surface, due to gravity and/or seismicity, exists. In tunnels, the most conventional way of overcoming this problem is the use of mesh and lace as an attachment to the rock surface. Increasing use of shotcrete (or fibrecrete), which has the advantage that it provides immediate support to the substrate, is also made. However, these conventional support components have some disadvantages. The application of mesh and lace is expensive and time consuming, while the required shotcrete thickness results in logistical

problems due to large material volumes which need to be supplied. In addition, the use of these support types in narrow stoping horizon (e.g. 1.2 m) is almost impractical.

CSIR/Miningtek has been carrying out a research programme on alternative support types in the form of "Thin Sprayed Lining" (TSL) for more than a decade (Yilmaz et al, 2003). To date, a series of laboratory and *in-situ* tests has been conducted and a significant amount of knowledge on the support effects of TSLs has been gained. Figure 3 shows the spraying application of TSL.

Currently, the research team is focusing on the development of the standard testing methodologies for TSL products as well as the determination of the required physical properties of these products. Additionally, a series of comparative evaluation of the support performance of these products in various mining environments is being carried out. Once rational testing procedures are developed, the support requirements in different mining environments are defined and the support effects of TSLs are quantified, it is believed that South African mining industry will use TSLs more effectively and widely, and significantly safer working environments will be created.



Figure 3. Spraying application

### 3.5 Borehole Radar Research at Miningtek

The driver for borehole radar is the need for advance information about the topography of the reef horizon ahead of mining. If mechanization is introduced, face advance rates will increase while the number of faces will decrease, so the cost of losing a face to an

unexpected fault becomes far higher. Borehole radar is an application of Ground Penetrating Radar (GPR) in a borehole. The borehole allows the excellent high resolution capability of GPR to be employed over significant distances with respect to the target.

Recent research at Miningtek has concentrated on the development and application of a state of the art borehole radar - the Aardwolf BR40 (Figure 4). The tool digitizes down the borehole with instantaneous sampling at up to 400 MSa/s. It is designed to operate in boreholes of 48 mm or less diameter, up to 1000 m long. The bandwidth is 40 MHz, which translates to a range of better than 50 m in typical Witwatersrand Quartzites or Bushveld Igneous Complex rocks. The first results achieved with the system, in October 2001, are for the surface test site illustrated in Figure 5. The borehole starts above the Ventersdorp Contact Reef (VCR), crosses the reef at 50 m, then travels away from the VCR in the foot-wall quartzites at a relative angle of 15°. The VCR reflector is clearly visible in Figure 6, together with other reflectors due to bedding planes in the quartzite. The system has since been applied successfully at a number of underground sites.

### 3.6 Goafwani

The investigations Canbulat and Jack, (1998) into the falls of ground fatalities concluded that pillar extraction is the least safe method in South Africa collieries. This highlighted a need for a device that can provide timely warnings of large goafing in pillar extraction sections. Large goafing in this environment is a safety threat and also has the potential economic loss by trapping the continuous miner.

Such a device should provide enough warning for the operator to withdraw the continuous miner and to ensure that everyone is protected by a safety barrier. Ideally, all large goafing should be preceded by an alarm.

CSIR-Miningtek developed a stand-alone warning device, called GoafWarn (Figure 7) to provide early warning of pending goafing. The warning algorithm is based on the temporal behaviour of the micro-seismicity in the immediate roof area.

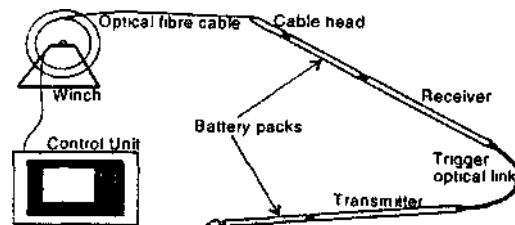


Figure 4. The Aardwolf BR40 borehole radar system.

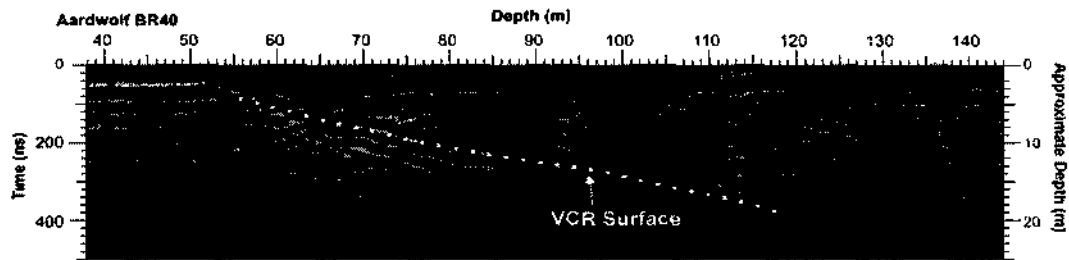


Figure 6. Results from the test site

The basic specifications for GoafWam are as follows:

- An integrated and digital seismic event detection device with local storage and decision-making.
- An early warning goaf alarm based on the temporal behaviour of the recorded seismicity.
- Effective discrimination between man-made vibration and seismic events associated with failure in the roof strata.
- Portable and easy to install - no communication cabling or power connection required.
- Intrinsically safe.

### 3.7 A New Mine Ventilation Software VUMA

Effective tools are essential for the practical and efficient design of mine ventilation and cooling systems, to enable both the development and the interactive simulation of mine layouts. To satisfy these requirements, new technology that was developed to assist mine operators in optimising thermal conditions is the mine ventilation and cooling network simulation program, VUMA-network, developed as a joint initiative by the South African Council for Scientific and Industrial Research (CSIR) and Bluhm Burton Engineering.



Figure 7. Goafwam

VUMA-network simulation software is specifically designed and developed to assist underground ventilation control engineers and practitioners in planning, designing and operating mine ventilation systems. VUMA-network is an interactive network simulation program that allows for the simultaneous modelling of airflow, air thermodynamic behaviour, as well as gas and dust emissions in an underground mine (Figure 8). The program includes user-friendly interfaces and three-dimensional graphics designed to facilitate the construction and analysis of networks, as well as perform "what-if" and optimisation studies. The software is Windows-based and produces full thermodynamic simulations for the opera-



lion of underground environmental control systems. Ventilation for all major mining configurations, including coal deposits, massive ore bodies and tabular ore bodies, are provided for.

### *J.S Activation of Rock Culling*

Activation is a method of superimposing an oscillatory motion on mechanical rock breaking tools, such as disk cutters, saws and drum cutters. The additional oscillation has shown to reduce operating forces to a third to cutting without activation.

The principles and benefits of activation have been researched for many years and are well documented. As a result of activated roller cutting tests on granite (Knickmeyer and Banmami, 1981), experimental results of hydraulic activated roller cutting tests (Kaci, 1993) and tests on vibrating tool coal cutting (Yuanchang, 1996), some parameters, i.e. influence of vibration frequencies, vibration amplitude, vibration wave length in cutting object, culling pitch, relative direction between vibration and cutting, and relative direction between cutting and bedding, have been more clearly defined. These studies also concluded that the vibration cutting method could significantly reduce the main culling force and specific energy consumption. Some of the advantages of activation are summarized as follows (Williscud., 2001):

- much higher breaking rate than /or similar non-activated devices,
- tool heating is significantly reduced, resulting in up to 10 times lower tool wear,
- reduced fines and more lumpy product.
- reduced frictional ignition (coal).
- very high production rates possible in hard rock.
- much lighter and smaller mining machines possible for similar production rates, and
- much lower installed power.

Although activation and its benefits have been known for a long time, no applications materialized because the generated oscillations either caused destructive vibrations in the machine or else required massive vibration damping equipment. This has been overcome by a recent patent, which provides an internal rotating counterweight, thus permitting simple and smaller cutter designs. If this technology is demonstrated to be successful, it could revolutionize hard rock mining. For the first time, a method would be available to economically mechanize and eventually automate the rock breaking operation in all rock conditions.

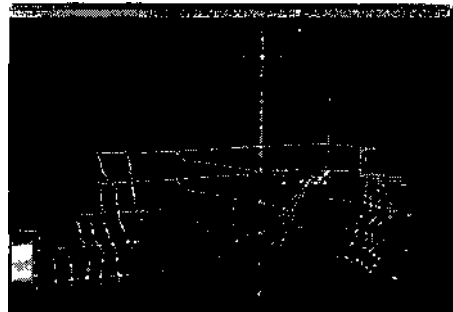


Figure 8. 3-D View of mine ventilation network

CSIR: Miningtek has made a considerable investment in laboratory testing facilities to enable testing of mechanical rock breaking methods, such as activated rock cutting. The project involved both laboratory testing of platinumiferous orebodies and conceptual design of a long-wall type machine. A prototype machine was commissioned and tested underground at the Townlands Business area, Anglo Platinum Ltd.

This mining system consists of a movable sprocket driven machine body mounted on a steel plate conveyor that runs parallel to the mining face. The machine body is equipped with a head arrangement incorporating two tungsten carbide activated rock cutting discs (Figure 9). The cutter head units can be engaged to cut the orebody in controlled forward motion along 30 m of the mining face. The machine body is also fitted with a drum equipped with rock cutting picks, behind the activated cutting discs, to maintain the hangingwall and footwall stop dimensions.

Subsequent to initial problem solving and the identification and implementation of the necessary technological developments, the individual components were manufactured and tested overseas. Concurrent with this South African made components were developed and manufactured. Special lubricants that surpassed German specifications for the unique equipment were also developed and produced in South Africa.

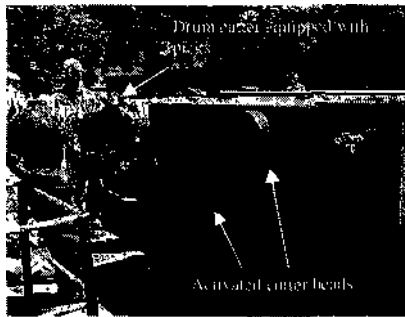


Figure 9. The Hard Rock Miner (HRM) with a head arrangement incorporating a set of two tungsten carbide activated rock cutting discs (cutter heads) and a drum equipped with rock cutting picks.



Figure 10. The conveyor system equipped with a row of hydraulic cylinders and sprags.

A conveyor system, linked to the activated rock cutting machine, is equipped with a row of hydraulic cylinders and props (sprags) that allow the conveyor to be shifted forward in a snake-wise manner and locked in position, respectively, after the completion of each cut (Figure 10). Broken rock is ploughed onto the steel plate conveyor that delivers the rock to conventional materials handling equipment and a belt conveyor system in one of the gullies.

In July 2001, all the components of the system were completed and delivered to South Africa. The system was then assembled on surface for full compatibility testing, simulating as far as possible conditions that would be experienced underground.

The underground test programme commenced in September 2001. The main outcome of the testing programme is that no fundamental technological reason to doubt the ability of the technology to succeed could be found and proven after three main bearing failures. Bearing failures can be overcome. It is possible to increase the bearing load carrying capacity

to the required limit as measured underground. It is also highly recommended that a new generation activated disc cutter has to be redesigned and may include design changes to the hard rock miner.

## REFERENCES

- Canbulat. I. and Jack. B.W. . 1998. Review of current design methodologies to improve the safety of roof support systems, particularly in the face area, in collieries. *SIMRAC Final Project Report*. COL 328, December.
- Chambei of Mines of South Africa Annual Report for 2001
- Cramers. LA. 2000. Presidential Address : Platinum perspectives. *SAIMM Journal*, volume 100. No. 5 September pp. 273-280.
- Du Plessis. J.J.L., Weiss. E.S. and Cashdollar K.L. Bagged 2000. Stone Dust Barrier Evaluations in a Bord and Pillar Mine. *SIMRAC Final Project Report COL 501*. CSIR Division of Mining Technology, Johannesburg, South Africa
- Kaci. M.V. . 1993. Aktivierte losetechnik zur gewinnung von kohle und nebegestein. *Gleuckaif Forschungshefte* 54. N5. pp 205-209
- Knickmeyer. W. and Baumann. L. 1981. Activated roller cutters as a means of lock breakage - Initial tests results and future applications. *Proceedings of the rapid excavation and tunnelling conference*. Volume 2. pp 1370-1381.
- MmSim 2000 *Training Manual*. CSIR Mining Technology Division. 2003.
- Vieira. F. *Personal communication* at/on. 2003.
- Vogt. D R. A 2002. Slimline boiehole radar for in-mine use. m 9<sup>th</sup> Int. Conf. on Gmünd Penetrating Radar. *Proceedings of SPIE*. Vol. 4758. pages 31-36.
- VUMA 2002. *Training Manual* CSIR Mining Technology Division.
- Willis. R.P.H 1997. Towards an integrated system for deep level mining using new technology. *Prot. 4<sup>th</sup> Int. Svmp on Mine Mechanisation and Automation*. Brisbane, vol. 2. pp. A9-14.
- Willis, R.P.H., Guler. G., and Kramers. P 2001. Non-explosive continuous mining methods being developed by CSIR: Miningtek. SAIMM Colloquium 22 February 2001 - *Mining Methods & Occupational Hygiene for the new millennium*. Miningtek Report No: 2001-0052. Johannesburg.
- Yilmaz. H., Saydam. S. and Topper. A.Z. . 2003. Emerging support concept: Thin spray on lineis. *The 1<sup>st</sup> Int. Mining congress and Exhibition of Turkey*. Antalya, Turkey.
- Yuanchang. J. 1996. Research of vibration coal cutting mechanism. *Journal of China Coal Society* Vol.21, No. 2. pp 153-157

## Emerging Support Concept: Thin Spray-on Liners

H. Yılmaz

*University of the Witwatersrand, School of Mining Engineering, Johannesburg, RSA*

S. Saydam

*University of the Witwatersrand, School of Mining Engineering, Johannesburg, RSA*

*Doku: Eylül University, Department of Mining Engineering, Izmir, Turkey*

A. Z. Toper

*Rock Engineering Programme, CSIR Division of Mining Technology (Miningtek), Johannesburg, RSA*

**ABSTRACT:** Accidents resulting from rockfalls occur frequently in the vicinity of active mining faces where workers spend most of their time. Installation of conventional surface support methods has been successful in overcoming this problem. However, they are expensive, time consuming, and their thickness results in logistical problems due to large material volumes. "Thin Spray-on Liner (TSL)" is an emerging alternative surface support system with remote, rapid and easy spraying techniques. The support action of TSL is still not well understood. Currently, there is no standard test methodology for TSLs and it is not possible to evaluate the quality and performance capabilities of TSL products. Assessment of TSL performance would be possible once the design standards and requirements are determined. Only then, will more effective use of TSL be possible in any support design. This paper reviews the development of TSL as a support concept, current testing procedures and gives a brief description of the research work undertaken by the authors.

### I INTRODUCTION

Rock related accidents are the major cause of injuries and fatalities in underground mines around the globe. The effect of rock related accidents on the fatality rates is up to 65% in South African gold mines (Erasmus 2000). More accidents occur in the vicinity of active faces, (production excavations or development ends), where workers spend most of their time. One of the major causes of instability is the lack of support coverage at these locations. Support tendons do not provide adequate rock reinforcement for fragmented rock and pieces of rock from the excavation boundary can easily be separated due to gravity.

Increasing the use of surface support methods, such as mesh, shotcrete or fibrecrete, near the face would reduce the risk of rockfall injuries; however, these support components have disadvantages. Application of mesh is expensive and time consuming, while the required shotcrete thickness results in logistical problems due to large material volumes which need to be supplied.

Total elimination of rock related accidents is not possible by strict measures on ground support as human involvement in mining activity cannot be eliminated with current technology. An emerging alternative surface support system in the form of "Thin Spray-on Liners (TSLs)" has the potential to reduce accident levels and to increase productivity

by minimising interference on the mining activities due to remote and rapid spraying techniques.

TSLs have been used in civil engineering for many years and is a recently growing support concept still lacking widespread application in the mining field. TSL can be applied easily and much faster after a new opening is excavated and their distance to face can easily be adjusted. Although the support action of TSL is not well understood, quick application with high areal coverage enables early reaction against ground movement. The initiation and propagation of fractures are prohibited and loose blocks are maintained in place at the early stages of face exposure. Rock strength and therefore excavation stability can be improved particularly for jointed rockmass. TSL design standards and requirements are not clearly available yet. Additionally, there is no standard test methodology for TSL support and it is not possible to evaluate the quality and performance capabilities of TSLs in the market. There is no reliable correlation between laboratory results and field results whether on surface or underground. Once rational procedures are developed and acceptable parameters are derived, more effective use of TSL will be possible in support design.

## 2 HISTORY AND BACKGROUND

TSL materials for ground support were initially intended to be used as an alternative to rock bolts and mesh or shotcrete. The first tests on TSL technology were initiated in Canada in the late 1980's (Archibald et al. 1992). The fact that TSL can be generally applied onto the rock to a thickness of 3 to 5 mm enabled the realisation of numerous advantages in terms of speed of application and minimizing transportation of materials in the 1990's.

Meanwhile, South African and Australian researchers have also been exploring the use of TSLs for rock support and have conducted various field and laboratory tests. By the mid to late 1990's news of TSLs being used in Canada's hard-rock underground mines reached many other interested manufacturers of a wide variety of spray-on products. Many products were tested and it was found that most did not possess adequate physical or chemical properties. The composition of some of the products has been dramatically changed to meet performance requirements. Newer products are continuously developed, introduced and tested. Recent developments on TSL support continue to receive increasing attention by the mining industry around the world due to considerable operational benefits, with the potential to greatly reduce mining costs. There are currently about 55 mines around the world that are considering the use of TSL for rock support and this number is increasing steadily. The greatest interest is in North America, Australia, and South Africa (Tannant 2001).

## 3 COMPOSITION, PROPERTIES AND TYPES OF TSL'S

Polymer based TSL's can either be non-reactive or reactive. Reactive TSLs are made from isocyanates (polyurethanes, polyureas) and acrylates. First versions of TSL were of single component "glue emulsion" type and were not suitable due to health & safety requirements. Later on, two and three

component TSL systems were developed. Polymer based liners normally require physical combination of two liquid chemicals or a liquid and a powder phase to form liner material. Today, utilization of two-component, reactive TSL systems are increasing due to ease of application, longer shelf lives and fast curing times. Table 1 shows a list of TSL products, commercially available or under development, including some key characteristics describing each product (updated during workshop of 2<sup>nd</sup> Int. TSL seminar-Johannesburg 2002).

## 4 TESTING OF TSL

A number of laboratory and field tests have been developed over the last few years, aiming at better understanding the properties of TSLs as well as characterising its interaction with rock. According to Naismith & Steward (2002) the following requirements should be satisfied from a well-designed TSL testing procedure:

- Simple (Easily prepared sample)
- Cost effective
- Repeatable
- Practical
- Representative of relevant properties and behaviour
- Relate to in-situ performance
- Statistically valid data should be generated.

Testing could be performed to address TSL material itself or could consider both the TSL material and the substrate in order to understand both the physical behaviour and the interaction of TSL with the substrate. It should be noted that most of the tests developed for rocks cannot be applied directly for TSL testing. Firstly, stresses imposed on TSLs are a few orders of magnitude smaller than rocks. Secondly, TSLs undergo much higher deformations than rocks. In addition, the effect of environmental factors such as temperature, humidity and chemical interaction could be more significant in altering TSL properties.

Table 1 Existing TSL Products (2<sup>nd</sup> Int. TSL seminar 2002)

Product	Manufacturer	Mix Base	Material Type	Curing Speed
ArduimnTM020	Ardex	Hydraulic Cement	n.a.	Fast
Eyet mine	Mead Mining	Cement/Acrylic	Liquid/Powder	Slow
GSM CS 1251	M BT	Polyurethane -Polyurea/Acrylic	u.a.	Fast
Masterseal	M BT	Methacrylate	Liquid/Liquid	Fast
Mineguard	Mineguard Canada	Polyurethane	Liquid/Liquid	Fast
Rock Hold	Mondi Mining Supplies	Methacrylate	Liquid/Powder	Slow
Rock Weh	Spray On Plastic	Polyurea	Liquid/Liquid	Fast
Rocks; uaid	Engineered Coalings	Polyurea/Polyurethane	liquid/Liquid	Fast
Tekilx	Fosioc Inc	Cement Latex	Liquid/Powder	Slow
Tunnels; uaid	Reynolds Soil Tech	Cement Latex	Liquid/Powder/Fibre	Slow

The following mechanical properties are relevant and could be tested in defining TSL properties i.e.:

- Tensile Strength (Elongation)
- Adhesion (Bond) Strength
- Tear Strength
- Shear Strength
- Creep Behaviour
- Impact Strength (Abrasion)

Specimen preparation, speed of testing and environmental factors may change the test results. No matter which testing method is developed, the two most important factors, temperature and humidity, need to be recorded for the test duration. Another shortcoming will exist if the test does not consider any interaction between the TSL material and the applied surface.

## 5 PREVIOUS TESTS OF TSLs

Despite the significant variety of testing procedures developed, only two tests have met with the acceptance of the delegates who attended the P' Int. Seminar on Surface Support Liners in Australia (2001). They were the tensile and the direct adhesion tests. Large-scale tests were found to provide interesting results but were also found to be difficult to interpret in terms of TSL properties and behavior. TSL's tensile strength, adhesive strength and elongation capacity are properties that are important to the liner's ability to hold loose rock in place and therefore are the key factors in the determination of TSL performance. The scope and results of selected tests are reviewed and presented in the following sections.

### 5.1 Adhesion tests

The adhesion test measures the adhesion or bonding strength of a TSL attached to a rock substrate. Two types of bond strength needs to be considered: tensile and shear. Tensile bond strength is a measure of the ability of TSL to remain in contact with the rock when a tensile stress is applied normal to the rock-TSL interface. Shear bond strength is concerned with the ability to resist stresses that act parallel to the rock-TSL interface (Fig. 1). Practically, there is some combination of these stresses acting on the TSL-rock interface.

Failure may occur due to the low tensile adhesion strength between TSL and rock surface. Adhesion strength on different rock types and the factors influencing the adhesion are important test considerations

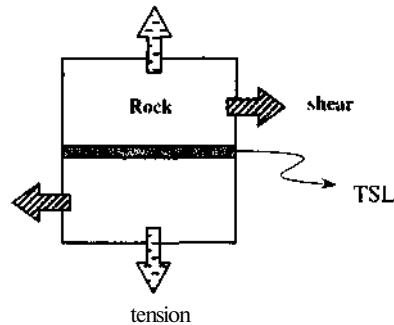


Figure 1 Debonding mechanism of TSL

### 5.2 Core adhesion test

The direct adhesion test consists of two pieces of core bonded together by TSL as shown in Figure 2. The top and bottom halves are subjected to a uniaxial pull until failure takes place at the TSL rock interface. The core adhesion test has the potential to become the main testing method in determining the bonding strength of TSL due to its simplicity. Sample preparation is an important issue in that both halves should lie along the same axis and in the direction of pull to prevent eccentric loading and premature failure.

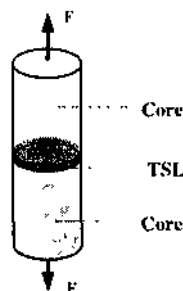


Figure 2 Core adhesion test

### 5.3 Plate-pull testing

This test consists of pulling on a test dolly embedded within TSL. A test dolly can be made from varying diameters and thicknesses of perforated steel discs that are applied to thin rock slabs (Fig. 3). Tannant et al. (1999) showed that high humidity or wet rock surfaces may significantly degrade the adhesive bond between the TSL and the rock. The TSLs bond to the rock normally increases with time, provided that the rock is firm, clean and dry. Adhesion to smooth, wet and soft rock is generally poor.

Difficulty persists in being able to produce consistently repeatable results between tests using

rock slab bonding surfaces Archibald (1992) showed that bond adhesion varies on irregular rock surfaces due to differences in substrate strength, surface roughness, porosity and degree of alteration characteristics. Therefore, he used a paving stone product that exhibits uniform strength and suitable properties.

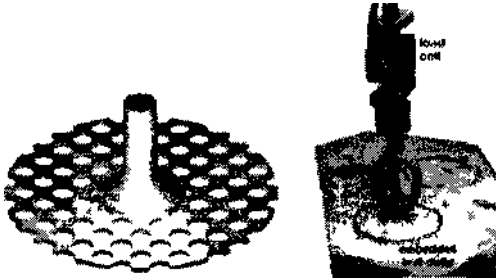


Figure 1 General view of a test dolly and typical test setup in the laboratory (Tannant et al. 1999)

Specimen preparation and testing procedures can be summarised as following (see Fig. 4 and 5),

- A test product is sprayed onto a flat surface of a cut concrete or rock surface
- A test dolly is immediately placed on the fresh, uncured coating. TSL is still in its initial liquid state and permitted to seep through the numerous perforation holes of the test dolly
- Immediately following the initial curing, TSL forms an adhesion bond with the test surface and produces an embedment bond about the pull plate
- A second coating is sprayed over the test dolly to fully embed it within the TSL
- After the test product has cured, the embedded test dolly and coating are overcured to isolate the test area from the rest of the TSL. Overcuring of the pull plate is conducted to ensure that only the bond adhesion associated with the area immediately beneath the pull plate is actually measured during pull testing.
- After 2 days of curing to the last layer of TSL, the test dolly is pulled normal to the substrate surface
- Test is continued until full release or loss of adhesion contact between the pull plate assembly and the substrate
- The adhesive strength is determined from the peak stress

The manner in which material adhesion loss occurs was shown to vary between materials assessed as can be seen by different failure modes in Figure 6 (Archibald 2001)

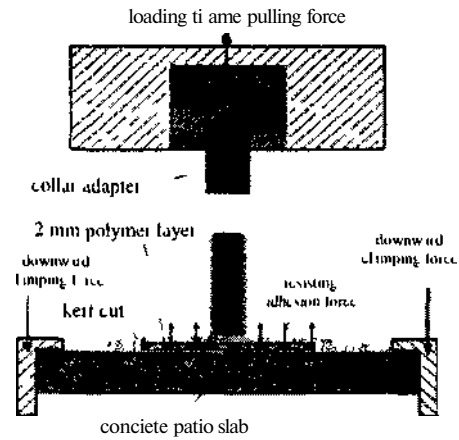


Figure 4 Adhesion pull test assembly schematic (Archibald 2001)



Figure 5 Specimen assembly prior to overcuring and at finish of adhesion bond strength test (Archibald 2001)

The test process is designed to be carried to ultimate bond failure therefore no residual adhesion bond strength is quantifiable. The location of the failure should be determined and, if it is in the bond plane, the amount of the applied material remaining should be assessed.

Underground adhesion testing of TSLs, similar to laboratory plate-pull testing, on rock and shotcrete was also performed with a range of cure times and for various moisture levels (Espley et al. 2001)

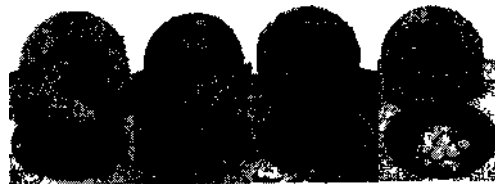


Figure 6 Typical views showing adhesion bond surfaces after completion of pull tests (Archibald 2001)

The surface substrates were cleaned prior to lining application and pull plates were embedded in the

liner for the testing. After the liner had cured, each test dolly was overcored and pulled as the loads were measured. The results indicate a correlation between surface moisture and adhesive strength - that is, the adhesion strength is decreased as the surface moisture increases.

#### 5.4 Baggage capacity test

The baggage capacity test measures loose rock supporting capacity of a deformable TSL (Swan & Henderson, 1999). An open-ended steel frame, of dimension 1.1m x 1.1m x 0.3m, is used and loaded with actual slabs of unwashed -100mm rock debris. A liner is sprayed on the "loose" rock debris surface (Fig. 7). Since the surface is discontinuous some penetration occurs between the rock fragments. After curing for the required time the frame is inverted and placed in a loading machine. A distributed compressive load is applied to the "loose" rock, thereby deforming the liner, which eventually ruptures. Repeatability of this test is questionable since the distribution of rock debris varies for each test. Preparation for a test appears to be difficult and time consuming due to the size involved.



Figure 7 Baggage load test flame & set-up (Swan & Henderson, 1999).

#### 5.5 Tensile strength and elongation tests

Standard testing method on "dog-bone" shaped pieces of plastics (ASTM D638 1998) has been selected by most of the researchers (Fig. 8) (Tannant et al. 1999, Archibald 2001, Spearing & Gelson 2002) to assess tensile properties, initial stiffness (modulus) and elongation capacity of TSL material at failure. TSLs have different rigidity properties and therefore their dimensions should have the ability to deal with rigid, semi rigid and non-rigid products. Thicknesses between 3 mm to 14 mm can be accommodated with dog-bone testing.

Multiple tests need to be performed in order to obtain reliable measurements of the tensile strength. The test specimen is clamped at each end in a tensile testing machine and then pulled. The specimen should break into two pieces on the narrow section for a valid test. The clamping can be achieved in a

number of ways; gluing, screw clamping and fixed gripping platens are some of the methods.

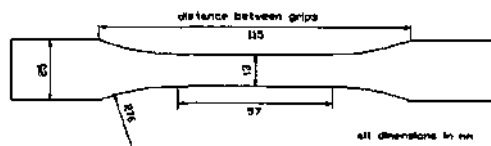


Figure 8 Shape and dimensions of a Type I test specimen using ASTM D638.

Material tensile strengths were determined either at break or yield positions along the measured load-deformation curves. The load is divided by original minimum specimen cross-sectional area at the specimen centre span to obtain the nominal tensile strength. Table 2 summarises adhesive and tensile strengths from various authors as a function of curing time.

Table 2 Adhesive and tensile strengths of various products

Product	Adhesive Strength (MPa)	Tensile Strength (MPa)
Mineguard'	0.56 (24 Hrs)	10-18(1 Hour)
Rockguard	0.43 (24 Hrs)	14-16(1 Hour)
RockWeb*	0.40 (24 Hrs)	18.5(1 Hour)
Masterseal <sup>1</sup>	0.50 (24 Hrs)	>2.0 (1 Hour)
	>() 16 (8 His)	1.0 (8 His)
Tekflex"	>0.51 (24 His)	1.74 (24 His)
	>0.65 (72 Hrs)	2.65 (72 Hrs)
GSM		
CS 1251'''	1.0(1/4 His)	17 (1/4 His)

'Aiclnbald (2001). 'Swan & Henderson (1999), '''Laceida & Rispin (2002)

#### 5.6 Pull strength determination

The plate pull test simulates the loads generated in a supporting liner when a loose block of rock moves relative to the surrounding rock (Fig. 9). The test consists of placing a solid circular plate of steel on either a concrete block or rock surface and then spraying the test material over the plate and the substrate surrounding the plate with a uniformly thick and continuous TSL. No TSL is permitted to be placed between the substrate and plate as it is not the aim of this test to measure the direct bonding strength of TSL (Fig. 10 and 11). The plate pull test

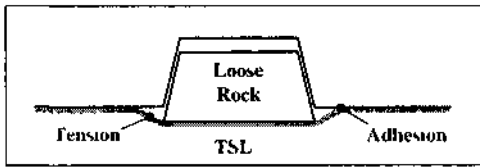


Figure 9 TSL supports the load from loose rock

procedure can be summarised as follows (Tannant et al 1999)

- Place the pull plate on a concrete or rock surface which has a diameter greater than the pull plate
- Coat the pull plate and the area surrounding the plate with TSL
- Slowly pull the plate perpendicular and away from the substrate after the required curing time

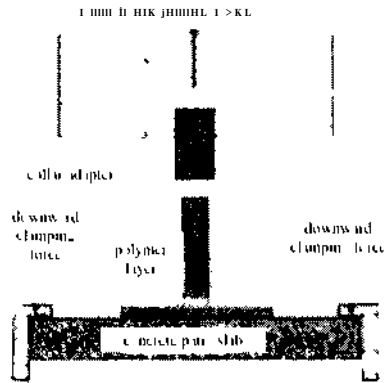


Figure 10 Pull strength test assembly schematic (Aichibald 2001)

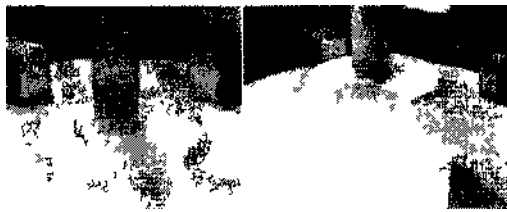


Figure 11 Test assembly condition at end of pull strength test (Aichibald 2001)

The test is completed when the load begins to drop when the plate is pulled free of the substrate. A combination of adhesion loss and tensile rupture is the expected and desired ultimate failure mode and not that of shear rupture through the TSL.

The failure modes observed during Aichibald's (2001) pull testing can be seen in Figure 12

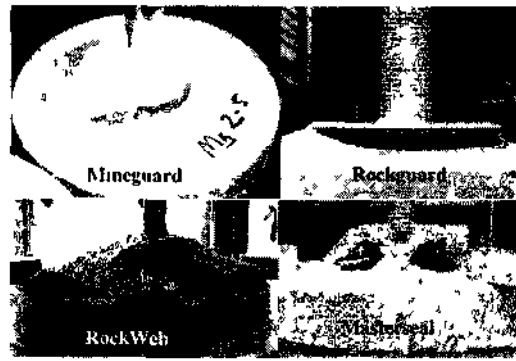


Figure 12 Typical views showing pull test failure conditions at completion of failure tests (Aichibald 2001)

### Large-scale pull test

Espley et al (1999) assessed the load carrying capacity of a TSL by coating an interlocking series of 50 mm thick hexagonal concrete paving blocks. The TSL is applied to the concrete blocks from above and left to cure. A pull-type loading is applied by a 100 mm square steel plate located in the centre and underneath the assembled paving blocks until the TSL has failed as illustrated in Figure 11.

Espley et al (1999) observed that the TSL is able to enhance the interaction between the loose blocks and thus a significant portion of the supporting function arises from block-to-block interaction.

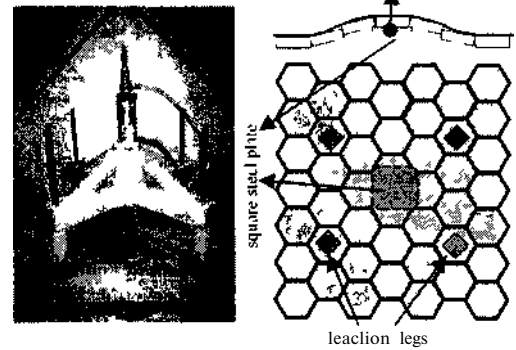


Figure 11 Test setup and typical test results from a large-scale pull test on Mineguard coated concrete blocks (Espley et al 1999)

### 5.4.1.1 MBT test

Spcaing et al (2001) performed the so-called MBT Method (Membrane Displacement Test) where the TSL is punched by a plunger at the end of a hole in a concrete slab as illustrated in Figure 14. This test is very similar to the plate pull test in terms of the



movement of the TSL i.e. punching or pulling respectively results in the same TSL behaviour.

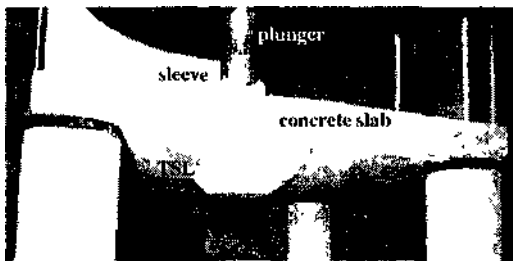


Figure 14 Punch testing setup (Speannng et al. 2001)

#### 5.9 Compression Failure Tests on Coated Samples

TSL coated cylinders of concrete and rock were tested by various researchers (Espley et al. 1999; Archibald & DeGagne, 2000) to demonstrate TSL's ability to contain and reduce the damage resulting from potential pillar-bursts. Tests were done under uniaxial loading conditions and the results demonstrated significant positive benefits at the laboratory scale in terms of non-violent post-peak failure response, and the liner's ability to absorb some of the stored strain energy (Fig. 15).

A compression failure test may not be relevant in deriving physical properties of TSLs, however it is useful to demonstrate the liner's ability to accommodate large strain ranges.



Figure 15 Coated and uncoated cylinders tested to failure (Espley et al. 1999; Archibald & DeGagne 2000)

## 6 CURRENT RESEARCH PROJECTS ON TSL TECHNOLOGY

The CSIR Division of Mining Technology (Miningtek) together with the School of Mining Engineering of the University of the Witwatersrand (WITS) in South Africa have been carrying out a research project titled "Required technical specifications and standard testing methodology for Thin Sprayed Linings" since April 2002 and will be finalised by March 2004.

The main objective of this research project is to provide realistic guidelines for the design and testing

of Thin Sprayed Linings for use as rock surface support. The project goal is to define required technical specifications for Thin Sprayed Linings as well as to propose a standard laboratory and underground testing methodology. By meeting these project objectives, mine-based Rock Mechanics Engineers will be provided with better guidelines for choosing the most appropriate TSL product for a specific environment.

The methodology adopted to achieve the project goals is as follows;

1. Identify the main rockmass failure mechanisms which can be prevented by TSL.
2. Group problem areas in the various environments into generic categories and define the required properties for TSLs in each group.
3. Identify industry and technical requirements for TSL for various environments.
4. Review previous research conducted on and results obtained from surface and underground testing of currently available TSLs.
5. Compilation of current testing procedures.
6. Identify shortcomings of current testing procedures and possible modifications.
7. Develop and propose laboratory test procedures by involving end-users and manufacturers.
8. Develop and manufacture testing equipment.
9. Carry out a sufficient number of laboratory tests for the evaluation of the proposed testing suite as well as product performances.
10. Comparison of test results in terms of the suitability of each TSL product in various environments.
11. Iterate and modify testing procedures in line with recommendations from end-users and manufacturers.
12. Report on the standard laboratory testing procedures.
13. Comparative assessment of the suitability of various TSL products in the underground environment.
14. Quantification of the support (reinforcing) effects of each product under quasi-static and dynamic loading at representative sites.
15. Comparison of both laboratory and underground results and validation of the proposed testing methodology.
16. Technology transfer.

In addition to the formal research project described above, most of mines are running small-scale comparative investigations on the evaluation of support performance of different TSL products in specific environments. Manufacturers, on the other hand, have been testing their products in a laboratory environment and based on these test results they continually modify their product properties. However, since there are no standard testing

procedures accepted and implemented by all parties, the validity of these test results may be questioned.

## 7 RECOMMENDATIONS & CONCLUSIONS

There is an urgent need for developing standard tests and testing procedures on TSLs as their application will potentially grow in the near future. Any standard test should be simple, repeatable, practical, cost effective and should relate to actual behaviour. The relevant mechanical properties of TSLs such as tensile, adhesion, tear and shear strengths could easily be addressed by simple test set-ups. Previous testing has dealt mainly with tensile and direct adhesion strengths and enough importance has not been given to shear and tear strengths as well as to creep behaviour.

TSL behaviour can differ significantly with different curing times and under different environmental conditions. Therefore, the effect of curing time, humidity and temperature on TSL behaviour should be studied as part of any testing method. The thickness of TSL and its effect on the performance behaviour are also not covered well in the previous tests and need to be addressed.

The most effective and representative of these tests or test combinations should be agreed to become standard tests through Int. collaboration of researchers on this field. Once this is done, more effective use of TSL will be possible. As the field applications grow the correlation between the laboratory and field results will become more reliable.

## ACKNOWLEDGEMENTS

This project is funded by Safety in Mines Research Advisory Committee (SIMRAC) of South Africa.

## REFERENCES

- Archibald J.F. 1992. Assessment of wall coating materials for localized wall support in underground mines. Report of Phase 4 Investigations for the Mining Industry Research Organization of Canada (MIROC), 34 pages.
- Archibald J.F. 2(H)l. Assessing acceptance criteria for and capabilities of liners for mitigating ground falls. *Mining Health and Safety Conference*, Sudbury, Ontario.
- Archibald J.F., Mercer R.A. & Lausch P. 1992. The evaluation of thin polyurethane surface coatings as an effective means of ground control. *Prat. Int. Svm. on Rock Support in Mining and Underground Construction*, Balkema, Rotterdam, pp. 105-115.
- Archibald J.F. & DeGagne, D.O. 2000. Recent Canadian Advances in the Application of Spray-on Polymeric Linings. *Mining Health and Safety Conference*, April 2000. Sudbury, Ontario.
- ASTM D638. 1998. Standard test method for *tensile properties of plastics*. American National Standard on Mechanical Properties. V. 8.01. Plastics (I): D256-D2343, April. 1998. pp. 46-58. \*
- Erasmus J. 2000. Assessment of the applicability of legislation, pertaining to the prevention of rock related accidents occurring at South African metalliferous mines. M.Sc. Research Report. University of the Witwatersrand, Johannesburg.
- Espley S., Gustas R., Heilig J. & Moreau LH 2001. Thin spray-on liner research and field trials at INCO. *Surface Support Liners: Membranes, Shotcrete and Mesh*. Australian Centre for Geomechanics, Australia.
- Espley S., Tannant D.D., Baiden G. & Kaiser P.K. 1999. Design criteria for thin spray-on membrane support for underground hardrock mining. *Canadian Ins. Of Mining and Metallurgy Annual Meeting*, Calgary.
- Laccida L., Rispin M. 2002. Current ground support membrane applications in North American underground mines. 2<sup>nd</sup> Int. Seminar on Surface Support Liners: Thin Sprayed Liners, Shotcrete, Mesh. Crowne Plaza Sandton. South Africa.
- Naismith A. & Stewart N.R. 2002. Comparative testing of ultra-thin structural liners. 2<sup>nd</sup> Int. Seminar on Surface Support Liners: Thin Sprayed Liners, Shotcrete, Mesh. Crowne Plaza. Sandton. South Africa.
- Spearing A.J.S., Ohler J. & Atogbe E. 2001. The effective testing of thin support membranes for use in underground mines. *Surface Support Liners: Membranes, Shotcrete and Mesh*. Australian Centre for Geomechanics, Australia.
- Spearing and Gelson 2002. Developments and the future of thin reactive liners since the previous conference in Australia. 2<sup>nd</sup> Int. Seminar on Surface Support Liners: Thin Sprayed Liners, Shotcrete, Mesh. SAIMM. Sandton. South Africa, Sect. 13. pp. 1-10.
- Swan G. & Henderson A. 1999. Water-based Spray-on liner implementation at Falconbridge Limited. *Proceedings CIM/AGM*, Calgary.
- Tannant D.D. 2001. Thin Spray-on liners for underground rock support. 17<sup>th</sup> Int. Mining Congress and Exhibition of Turkey. *IMCET2001*. Eds. E. Unal, B. Unver & E. Tercan. Ankara, Turkey, pp. 57-65.
- Tannant D.D., Swan G., Espley S. & Graham C. 1999. Laboratory test procedures for validating the use of thin sprayed-on liners for mesh replacement. *Canadian Ins. Of Mining and Metallurgy Annual Meeting*, Calgary, published on CD-Rom.8p
- Workshop of 2<sup>nd</sup> Int. Seminar on Surface Support Liners: Thin Sprayed Liners, Shotcrete, Mesh. SAIMM. Sandton Johannesburg. 29-31 July 2002.





## Study of Load Transfer Capacity of Bolts Using Short Encapsulation Push Test

N.I.Aziz & B.J.Webb

*Faculty of Engineering, University of Wollongong, NSW 2522, Australia*

**ABSTRACT:** A series of laboratory experiments were conducted on a variety of bolt types to examine the load transfer capacities of different profiled bolts in short encapsulation push testing. A 70 mm section of 150 mm long bolt specimen was anchored in a 70 mm long stainless steel tube using full resin encapsulation. Six types of different profiled bolts and two non-profiled bolts were tested. Bolts with higher profile were in general found to have greater shearing resistance and higher stiffness than low profile bolts. Widely spaced profiles allow greater displacement at peak shear strength, and bolts with no profiles produced very little load transfer capability. Rough surfaced plain bolts showed a significant load transfer capability in comparison to a factory supplied smooth surface bolt which supports the belief that rusted bolts have higher load transfer capability than un-rusted bolt surfaces.

### 1 INTRODUCTION

In the third Australian Coal Operators Conference, Coal 2002 (Aziz, 2002) discussed the load transfer capacity of bolt surface profile under Constant Normal Stiffness conditions (CNS). The main findings from the study were that bolts with deeper rib profiles offered higher shear resistance at low normal stress conditions while bolts with closer rib spacing offered higher shear resistance at high normal shear stress conditions. Also it was found that the peak shear stress occurred at 60 % of the profile spacing. In continuation of the work on the subject a number of studies were undertaken to examine the load transfer capacities of different profiled bolts using three different approaches. One such method involves the use of the Short Encapsulation Push Test. Unlike the tests under CNS conditions, the short encapsulation test is carried out under Constant Normal Load conditions (CNL) provided by the walls of the steel cylinder.

Questions are often asked as to why some bolts have higher and wider spaced profiles while others have shallow and narrow spaced profiles and how does each type react in different ground conditions? The answer to this question depends upon the method of testing. The most common methods used, such as the short encapsulation pull test have no way of identifying scientifically the role of profile configuration on the load transfer characteristics of the bolt. The conventional short encapsulation test tends to suffer from a variety of operational and

inherent defects, which make it difficult to produce repeatable results. Also, the short encapsulation pull test is conducted under CNL condition which generally ignore the changing nature of the confining load due to relative resin /bolt surface displacement. The only effective method of characterising the bolt profile influence is to conduct the tests under CNS conditions. Short encapsulation push test can be considered as a suitable method to examine the influence of profile configuration on load transfer capacity as the technique can be used under a controlled environment which can overcome many of the well known problems associated with the conventional short encapsulation pull testing method, even though the method embraces the principle of CNL conditions.

### 2 SHORT ENCAPSULATION PUSH TESTING

Figure 1 shows the details of the Short Encapsulation Test Cell. The cell is 75 mm long, which is 50% greater than that reported by Fabjanczyk and Tarrant(1992). The longer length cell was selected in order to permit a sufficient number of bolt surface profiles to be encapsulated in the cell. The cell consists of a machined steel cylinder with an internal groove. The groove provides grip for the encapsulation medium and prevents premature failure on the cylinder / resin interface. As opposed to pull testing, push testing involves the pushing the bolt under constant normal

load conditions through the hardened resin. With the use of a digital load cell and extensometer, a full load / displacement history could be obtained. A total of 20 cells were prepared for the study.

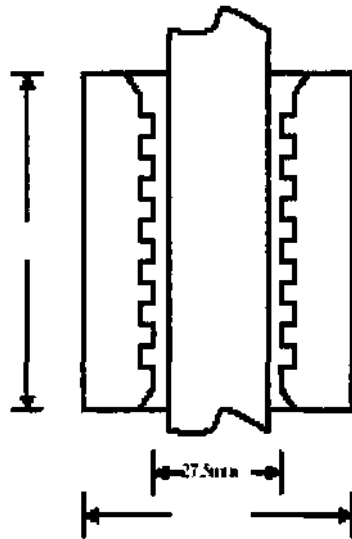


Figure 1. Push test cell

### 3 ROCK BOLT SAMPLE PREPARATION

Six types of profiled bolts and two versions of plain surface bolts were selected for the study. The first four types of the profiled bolts are Australian manufactured and widely used in Australian mines. The other two profiled types included an overseas bolt and a locally developed new bolt, yet to be marketed in Australia. The surface bolts consisted of a factory supplied bolt which was not yet profiled and a profiled bolt whose profiles were machined off in the laboratory. Table 1 shows the details of each tested bolt. For wider application in Australian mining industry, the first four bolts, namely Bolt Types T1 to T4 were called popular bolts, and the rest consisted of two profiled bolts and two plain surface bolts identified as additional bolts. For obvious reasons all the bolt types were given identification designations.

The rock bolt samples were each cut to lengths of 120mm using a mechanised saw. The equal lengths ensured that all the samples of the same type had an equivalent number of profile ribs and that the ends of each sample were square. All bolts were encapsulated into the push test cells using Fosroc

PBI Mix and Pour resin grout. The uniaxial compressive strength and shear strength of the resin used for the tests were in the order of 70 MPa and 16 MPa respectively. The encapsulated samples were allowed to harden for a minimum of seven days before being tested.

The general arrangement for testing is shown in Figure 2. Information on the load/displacement was monitored on a PC, connected to a Load cell and an LVDT of the loading system via a data logger.

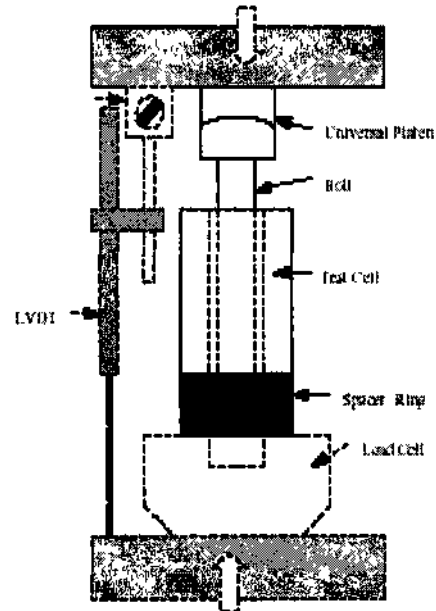


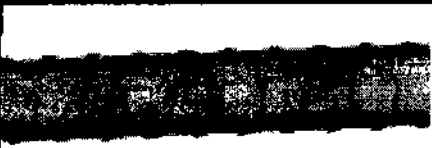

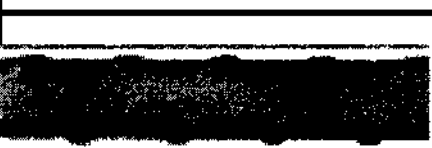
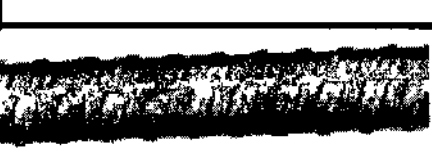


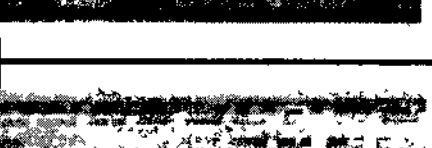

Figure 2. Instrumented push test arrangement

### 4 RESULTS AND DISCUSSION

#### 4.1 Load - displacement relationship

Figure 3 shows typical load displacement graphs of testing Type T2 bolts. The figure shows the results of four tests, and demonstrates the repeatability of the tests with a reasonable degree of confidence. Figure 4 shows the combined load displacement graphs of a group of four popular profiled bolts. Clearly, there are differences in the graphs of different bolts and one notable example is that of Bolt Type T3. This bolt had widely spaced profiles, and the peak load occurred at greater displacement than the rest of the bolts. Table 2 shows the details of the test results for the entire profiled and plain surface bolts. These results are the average values for the maximum load, shear strength, and bolt resin interface stiffness values.

Table 1 Rockbolt specifications

TYPE	T1	T2	T3	T4	T5	T6	S1 (Rough)	S2 (Smooth)
Profile centres	12.00mm	12.00mm	25.00mm	12.00mm	12.0mm	8.0mm	--	--
Profile height	1.00mm	1.60mm	0.80mm	1.50mm	1.24mm	1.5mm	<0.1mm	1.6mm
Profile angle	22.5°	22.5°	22.5°	19°	4.8°	8.8°	--	--
Profile top width	1.50mm	2.00mm	2.50mm	1.80mm	1.6mm	2.0mm	--	--
Profile base width	3.00mm	3.50mm	5.00mm	3.70mm	3.8mm	3.5mm	--	--
Samples								

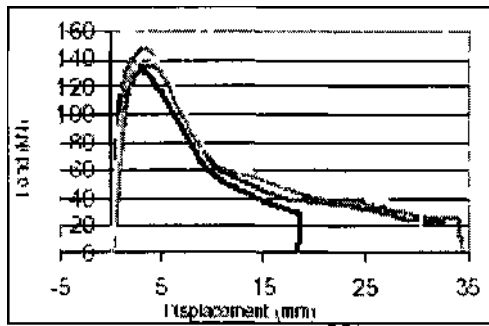


Figure 3 Load versus displacement values of Bolt T2

The peak load - displacement relations of various bolts are presented in Figure 5. The highest average peak load of 132.56 kN was that of Bolt Type T2. This was 23% greater than that achieved by the Bolt Type T4 at 102.09 kN. The difference between these two extreme values is attributed to the bolt profile heights.

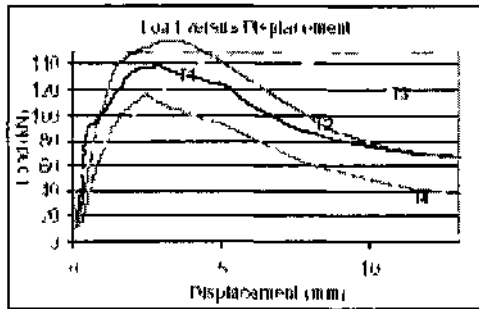


Figure 4 Load Displacement graphs of four profiles bolts

Examination of the average displacement results achieved by the bolt samples in Figure 6 showed that Bolt Type T3 achieved the highest displacement of 4.03 mm. Bolt Type T2 followed this with 2.54 mm. Bolt Type T4 achieved the lowest average displacement with 2.05 mm of displacement. Of the additional bolts tested, it was found that the Bolt Type T6 sustained a displacement of 2.37 mm at maximum load while the newly developed Bolt Type T5 achieved a displacement of 2.019 mm. Rough surfaced Bolt Type S1 achieved 1.01 mm, while smooth sulfated Bolt Type S2 achieved 0.57 mm of displacement at maximum load. A comparative study reported by A/17 Indiaratna and Dey (1999) and A/i/ (2002) between Bolt Types T1 and T3 and tested under CNS conditions has indicated that Bolt Types T1 and T3 gave similar compressive displacement patterns but at greater

displacement ranges. It is thus reasonable to suggest that wide profile bolts can accommodate greater peak load displacement than bolts with closely spaced profiles. This is considered as an advantage of Bolt Type T3 in accommodating the ground displacement without losing its load transfer capability.

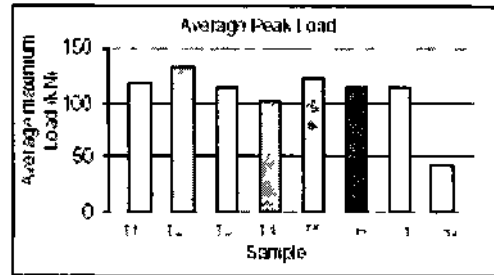


Figure 5 Average peak load of all the bolts

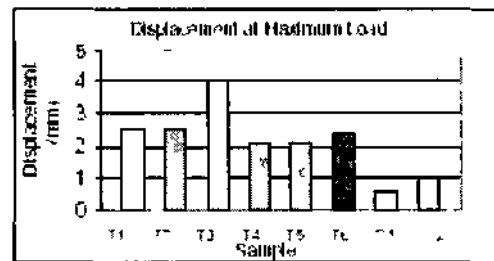


Figure 6 Displacement at peak load of all bolts

#### 4.2 Shear Strength Capacity

The average shear strength capacities achieved by each bolt type are represented below in Figure 7. It was found that Bolt Type T2 had the highest shear strength capacity of 25.89 MPa. Bolt Type T1 with an average shear strength of 22.88 MPa was 11.63% less than Bolt Type T2. The lowest shear strength value of the popular bolt type was Bolt Type T4 at 19.88 MPa, which was 23.21% less than the shear strength value of Bolt Type T2.

The rough sulfated plain bolt achieved a shear strength capacity of 22.35 MPa and the smooth plain surface bolt achieved 7.71 MPa, which was a large drop in the shear strength values with respect to rough surfaced plain bolt. Bolt Type T5 achieved 25.17 MPa, which was fractionally less than Bolt Type T2, while the overseas manufactured Bolt Type T6 with 21.76 MPa achieved a shear strength capacity 15.95% less than Bolt Type T2.



Table 2 Push test characteristics of different bolts - Average values

S.W.I.W.I: ITI'I-,	T'upular				Audit iwiml			
	'11	'12	'13	'14	'15	'16	'17	'18
örn i IV PP	11	12	13	14	15	16	17	18
We Hrtik? l kighli mtnt	fOii	1.4U	120	st.Tn	1.24	1.12	—	..
An j l'ulfile SfMuiniiuml	11.*	12.1»	25X0	Jijuu	12.CH	1.00	—	
Aw Ma\ ltm. JI k\ 1	117.12	152.51.	1 i M i	HGXW	121. »2	112"«	4.5X	11 \&i
\wi \ta Disriact-mcil 1 ram 1	2M	2M	•W	2 M	2.1»	23'»	1157	1'11
\vt Mismr Sire» t ifiKirv i VII'ul	22Ä	25.H»	*** 11	NX"!	25.IT1	21.?'>	SSSK	2\1'
\»aaiiï Syslom Slillnessi LV num	V, ~2	CI '11	2SW	W	<v.y4	47.'»«	Ti.47	112411

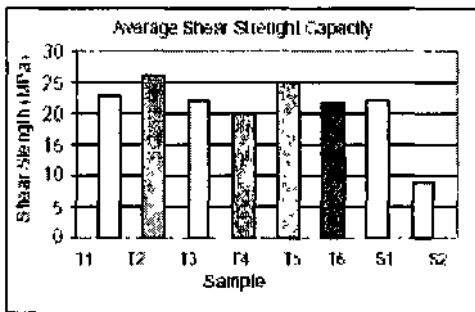


Figure 7 Average shear strength capacity

### 4.3 System Stiffness

The system stiffness is the gradient of the maximum load sustained by a bolt to the displacement at the maximum load of a fully encapsulated bolt. Expressed in kN/mm the average system stiffness for each bolt type is shown in Table 2. It is interesting to note that both smooth surfaced bolts were stiffer than the profiled bolts, however this does not mean that the plain surfaced bolts have greater load transfer capacity as the displacement at peak load was very minimal.

## 5 LOAD TRANSFER AND PROFILE DESIGN

### 5.1 Bolt Surface / Resin Interaction

Almost all the load transfer capacity between encapsulation resin and the bolt can be accepted as being attributed to the frictional effect. The level of the frictional force is dependent upon the confining pressure. The magnitude of the changes in peak shear strength with respect to applied normal load is shown in Figure 8. The graph indicates that there is an insignificant degree of cohesion bonding between the bolt surface and the resin when the vertical load approaches zero. Figure 9 demonstrates the separation of the resin from a bolt when the cast

resin was sawed axially and both halves of the resin shell came off clean from the bolt. In summary the load transfer capacity of the resin /bolt interface is a function of the applied normal load alone.

### 5.2 Profile Spacing

Examination of the average bolt profile spacings, outlined in Table 1, found that Bolt Type T3 had the greatest profile spacing with 25mm between profile centres. Bolt Type T2 had a profile spacing approximately half that of Bolt Type T3 with 12mm, while both Bolt Type T1 and Bolt Type T4 had spacings of 11 mm. The latter product had a design that is called an overlapped design that produced a general reduction in the effective shearing surface of the bolt. Bolt Type T3 design produced a bolt with a reduced circumferential profile length resulting from the absence of a central spine or 'Hash'. As can be seen from Figure 4, it was evident that the displacement required for Bolt Type T3, to achieve maximum load, was approximately 53% greater than the displacement of Bolt Type T1 and Bolt Type T4 whereas Bolt Type T2 had a peak load displacement of approximately 40%. From this it was evident that an increase in profile spacing has resulted in an increase in the displacement at maximum peak load.

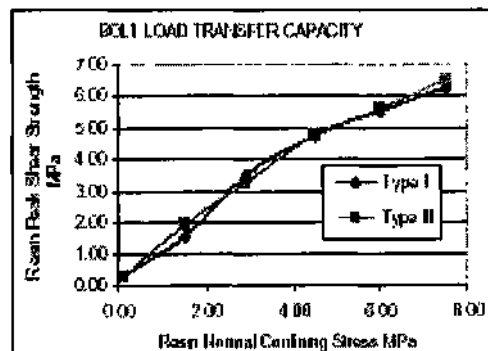


Figure 8 Resin/Bolt load shear strength under various normal confining pressures

The increased displacement required to achieve maximum load resulted in a lower system stiffness of the bolt type.

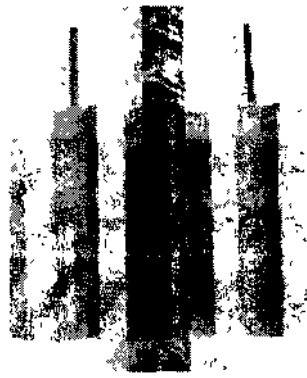


Figure 9 Resin bolt separation after bolt encapsulation

### 5.3 Profile Height

Testing of Bolt Types T3 and T1 were used to examine the effect of profile height on the shear strength capacity across the bolt resin interface. Bolt Types T1 and T3 were of the same "T" Bolt design, possessing similar profile spacings, but had different profile heights. As outlined in Table 1 Bolt Type T3 had a profile height of 1.4mm, while T1 had a height of 0.8mm. However, both Bolt Types T3 and T1 achieved shear strength capacities of 22.33 Mpa and 22.88MPa respectively. Bolt Type T2 achieved a greater shear strength capacity compared to Bolt Type T1. These results are reflected in Figure 6, which represents typical load displacement performances of Bolt Type T1 and Bolt Type T2 respectively.

### 5.4 Bolt Surface Condition

The load displacement shown in Figure 7 clearly indicates that the increase in roughness of the plain surface of the bolt has greatly influenced the shear strength capacity of the bolt. The rough finish of the bolt surface allowed additional grip to be provided between the bolt and resin interface and this reinforces the belief that rusted bolts have greater load transfer capability than a clean bolt of the same type.

## 6 PRE AND POST FAILURE BEHAVIOUR

Pre and post failure curves obtained for all the profiled bolt types show that, common to all the bolts tested, the average displacement at peak load occurred at approximately 34% of the profile

spacing as shown in Figure 4. The peak load displacement of 34% is almost 50% of the values obtained by Aziz (2002), when examining the load transfer of Bolt Types T1 and T3 bolts under Constant Normal Stiffness condition and that clearly demonstrates the influence of test technique on the result outcome.

The post peak load displacement graphs also depicted different picture for Bolt Type T3 in comparison to the rest of profiled bolts. It showed that the post peak load / displacement profile was higher than the other bolts, indicating the ability of the bolt to maintain greater load transfer capability than others.

## 7 CONCLUSIONS

Realistically the application of the Short Encapsulation Push Test technique in evaluating load transfer capability of profiled bolts cannot be accepted as a scientifically recognised credible technique, as the test is carried out under constant normal load conditions, which is not the case. The profiled bolt surfaces are not smooth, and thus the movement of profiles relative to resin surface would inevitably lead to changes in the vertical load. The application of the system on plain surface bolts is however valid. Nevertheless, the Load transfer capacity assessment is, to a certain extent, warranted because the method overcomes many of the problems associated with the conventional pull testing method, including the effect of resin gloving, host material failure and bolt yield. The test cell provided a standardized environment that allowed testing to focus on profile design only. The tests showed that:

- Rib profile height influenced the shear strength capacity of a bolt.
- Peak shear load occurred on all profiled bolts at displacements equivalent to 34% of the rib spacing, which is almost 50 % of the values obtained from testing under CNS conditions.
- Load transfer capacity between encapsulation resin and the bolt is due almost entirely to the frictional effect.
- The rough finish of the bolt surface permits additional grip between the bolt and resin interface and this enforces the belief that rusted bolt surfaces have greater load transfer capability than clean surface bolt.

## REFERENCES

Aziz N 2002 A new technique to determine the load transfer capacity of resin anchored bolts. *2012 Cool operator\* ' amfeieme*. University of Wollongong pp.176-184

A/ u NI Incl. uatiid B and Dey A 1999 Laboiatoiy study ol shea loading and bolt load tianstei mechanisms undci constant noiinal stiffness conditions *Prot IX Inknational Confereme (in Ormmil Cimrini ill Mmwi*; Moigantown WV USA, August V5 pp2W-247

Fablanc/yk M W Tan ant GC 1992 Load tianstei mechanisms in leintoicing tendons *Ulli Intel national i onfcwni c- on gitniid ionfrol m Mining*, University of Wollongong, pp 212-21



## 3-D Estimation of Stresses Around a Longwall Face by Using Finite Difference Method

N.E.Yaşıtlı & B.Ünver

Department of Mining Engineering, Hacettepe University, Ankara, Turkey

**ABSTRACT:** There is a considerable amount of lignite reserve in the form of thick seams in Turkey. It is rather complicated to predict characteristics of strata response to mining operation in thick seams. However, a comprehensive evaluation of ground behavior is a prerequisite for maintaining an efficient production especially when top coal winning by means of caving behind the face method is applied. A comprehensive modelling of deformations and induced stresses is vital for the selection of the optimum production strategy. Induced stresses around a longwall face can be determined by in situ measurements, physical models and numerical modelling techniques. In this study, numerical studies associated with numerical modelling of a longwall panel at Ömerler Underground Coal Mine have been carried out by using the software called FLAC<sup>3D</sup>. A 3-D model of the M3 panel has been prepared and associated induced stresses around the panel have been calculated.

### 1 INTRODUCTION

Characteristics of primary stresses present prior to production and secondary stresses formed after mining activity are the key factors affecting the overall stability of especially gate roadways and the face. An efficient production can only be carried out if stability of the openings is properly maintained. For this purpose, understanding of the stress distribution characteristics around a longwall panel is of vital importance.

There have been numerous attempts in estimating primary and secondary stresses around underground structures depending mainly on in situ measurements, physical and numerical models. This paper briefly presents a part of a comprehensive 3-D numerical analysis of M3 panel at Ömerler Underground Mine. The numerical model was formed by using the commercially available software called FLAC<sup>3D</sup>, based on the Finite Difference (FD) technique.

### 2 A BRIEF INFORMATION ON ÖMERLER UNDERGROUND MINE

Ömerler Underground Mine is located at the inner Aegean district of Turkey near Tunçbilek-Tavşanlı. The mine started production in 1985 and fully mechanized face was established in 1997. Average

depth below surface is around 240 m and 8 m thick coal seam has a slope of 10°. A generalized stratigraphic column showing the coal seam together with roof and floor strata is presented in Figure 1. There are three main geological units named as claystone, clayey marl and marl are present in the mine area. Physical and mechanical characteristics of coal and other units are presented in Table I.

Thickness	Lithology	Formation
1 m		Top soil
24 m	1	Calcareous marl
189 m	2	Marl
17 m	3a	Claystone
	3b	Soft claystone
8 m	4	Coal
4 m	3c	Claystone

Figure 1. A generalized stratigraphic column lit Omeiler Coal Mine

Table I. Physical and mechanical properties of coal and surrounding rocks (Destanoğlu et al., 2000; Taşkın, 1999)

Formation	Deformation Modulus (GPa)	Density (MN/m <sup>3</sup> )	Uniaxial Compressive Strength (MPa)	Tensile Strength (MPa)	Initial Strain (%)	Compressive Strength (MPa)	Modulus of Elasticity (MPa)	Poisson's Ratio
Calcareous marl	1	11(12)	2(2)	%V	47	12 s	~20	0.2(0.2)
Marl	1	>1122	16.1	1(1)	11	~11	2M0	(125)
Claystone	3.1	11(12)	144	2.1	12	1.1S	14SII	0.2(0.2)
Soft claystone	1.6	0.024	X7	1.5	1.5*		2040	
Claystone	11	0.024	20 s	15	4(1)	2.9(1)	10*S	0.2(0.2)
Coal	4	1.1(1.1)	15(15)		1S-2S		1711	0.2(0.2)

The 8 m thick coal seam has been produced by means of longwall retreat with top coal caving production method where a 2.8 m high longwall face is operated at the floor of the coal seam (Fig 2). Top slice coal having a thickness of 5.2 m is caved and produced through windows located at the top of shields. At the time of modelling, two adjacent longwall panels namely M1 and M2 had been completed and the production was carried out at M3 panel as shown in Figure 3

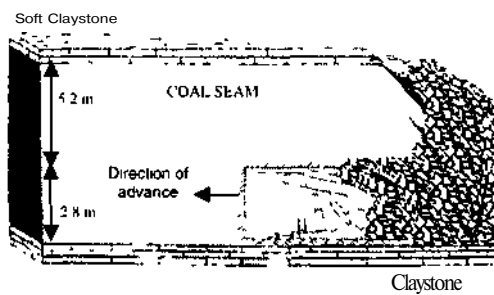


Figure 2 Longwall with top coal caving method at Ömerler Underground Mine

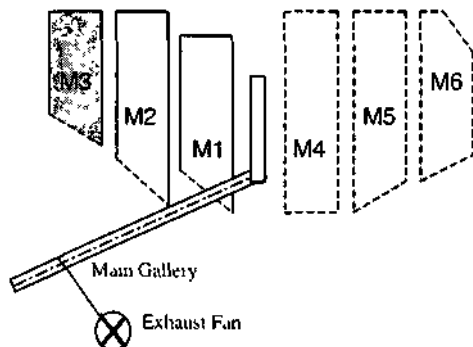


Figure 3 Plan view of Ömerler Underground Mine (Akdaş et al 2000)

### 3 MODELLING PROCEDURE IN GENERAL

Finite Difference method can be better applied to modeling of stress distribution around underground mining excavations in comparison to other numerical techniques. FLAC<sup>3D</sup> is a commercially available software that is capable of modeling in three dimension.

Modeling for estimation of stresses around the longwall panel is performed in five steps. The steps called A, B, C, D and E are as follows:

- A- Determination of boundaries and material properties,
- B- Formation of the model geometry and meshing
  - Determination of the model behavior,
- C- Determination of the boundary and initial conditions,
  - Initial mining of the program and monitoring of the model response,
- D- Reevaluation of the model and necessary modifications,
- E- Obtaining of results.

Model geometry and meshing refer to physical conditions of the district to be modeled. Model behavior is the response of a model under a certain loading condition. By means of boundary and initial conditions, physical limits of the model and original conditions are explained. At the beginning of the analysis, the model was in the form of a solid block in which gale roadways, the face and other structures were later created in the form of modifications. The modeling process is presented in Figure 4 in the form of a flowsheet.

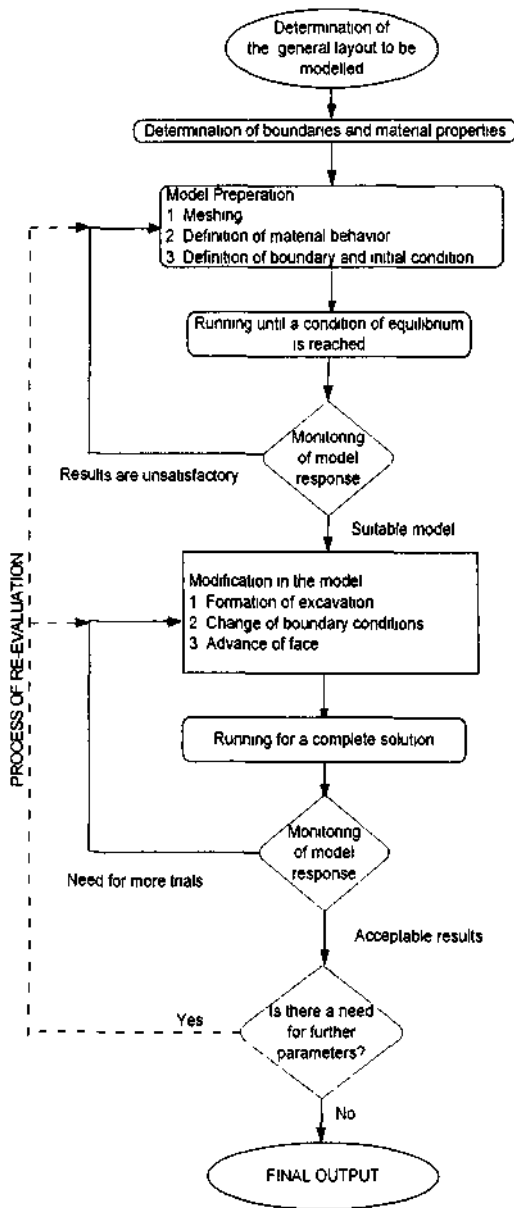


Figure 4 A general flowsheet of modelling process (Yaşıttı 2002, Unverand Yasılılı 2002, Itasca 1997)

#### 4 MODELLING OF GROUND STRESSES AROUND THE LONGWALL PANEL

A full-scale model of the M3 longwall panel and its surrounding has been prepared as seen in Figure 4. Face length, panel length and depth below surface values were taken as 90 m, 450 m and 240 m,

respectively. There was a 16 m wide rib pillar between M3 panel and the adjacent completed M2 panel. In order to efficiently estimate stress distribution around the longwall face, this area was divided in the form of a closer meshing in comparison to other regions (Fig.5).

It is crucial to properly assess material properties in order to obtain acceptable results in modelling with FLAC. Therefore, physical and mechanical properties of each geological unit must be properly determined. In general, intact rock properties are found by means of laboratory testing. However, there is an important diversity between rock material and rock mass characteristics. It is compulsory to determine representative physical and mechanical properties of the rock mass instead of intact rock material. In this study, rock material properties were converted into rock mass data by using empirical relationships widely used in the literature, i.e. Hoek and Brown (1997) failure criterion, Bieniawski's (1973; 1989) RMR classification system and Geological Strength Index (GSI) (Hoek 1995, Sönmez 2001, Sönmez and Ulusay 1999).

Modelling of caved area is another important step that affects the results. It is a well-known fact that it is a rather difficult task to model the goaf material. Therefore, the goaf was characterized by using the following expression for modulus of elasticity as suggested by Xie et al. (1999):

$$E = 15 + 175(1 - e^{-0.001t}) \quad (\text{MPa}) \quad (1)$$

where,  $t$  is time in seconds

For the goaf material in Tunçbilek Region, Kose and Cebi (1988) suggested a modulus of elasticity interval of 15-3500 MPa, whereas Yavuz and Fowell (2001) suggested a Poisson's Ratio of 0.495. These values were used for the characterization of goaf material throughout the analysis.

##### 4.1 Stress distribution around the longwall face

After formation of the model of M3 panel together with its surroundings, rock mass properties were entered and the model is solved until an equilibrium state was reached. Resulting stress distributions in horizontal ( $x$  and  $y$ ) and vertical ( $z$ ) directions are presented in Figure 6 and 7, respectively. Distribution of vertical stresses in front of the face at various distances such as 3.5, 7, 10.5, 14, 17.5 and 21 m at eight different levels of the coal seam are presented in Figure 8. As shown in Figure 8, front abutment pressures increase until a distance of 7 m from the face line reaching to a maximum stress level of 13.5 MPa. The front abutment stress was found as 2.35 times of the initial field stress of 5.75 MPa.

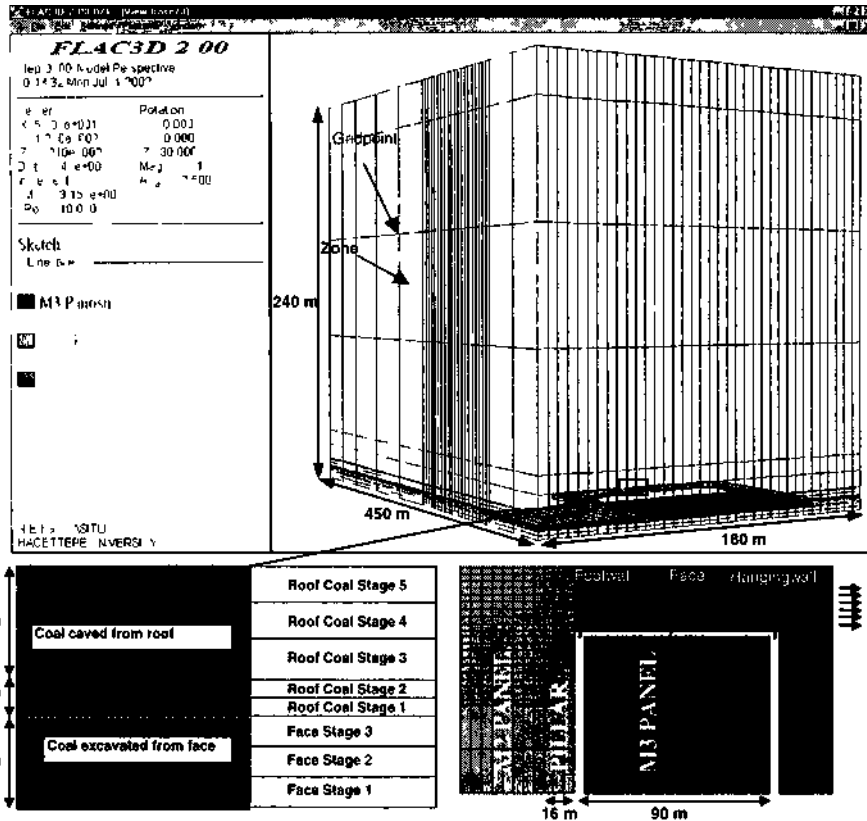


Figure 5 Omet lei Underground Mine model constructed in FLAC<sup>3D</sup> (Yaşarlı, 2002)

After leaching to its highest value front abutment stresses tend to decrease away from the face. The results of numerical modeling studies reveal that front abutment stresses are formed at the center region of the face. Due to the presence of the goaf of adjacent M2 panel front abutment stresses are higher around the footwall side in comparison to solid hanging wall side as expected. Figure 9 presents the stress distribution on axes parallel to direction of advance as shown in Figure 5. Distribution characteristics and magnitudes of front abutment stresses are found to be in good agreement with the results obtained by in situ measurements presented in the literature. After reaching to the highest front abutment pressure of 5.75 MPa at a distance of 7 m from the face, it decreases gradually to initial field stress of 5.75 MPa at a distance of 70 m away from the face.

Stresses in the goaf behind the face decrease to 0.1 MPa levels and tend to increase at the stait line of the face in a similar manner with front abutment stresses. At the face stait line of the panel, rear abutment stresses reach to the highest level at 2-3 m

inside the solid coal and decrease gradually to the field stress level at about 60 m inside the solid coal.

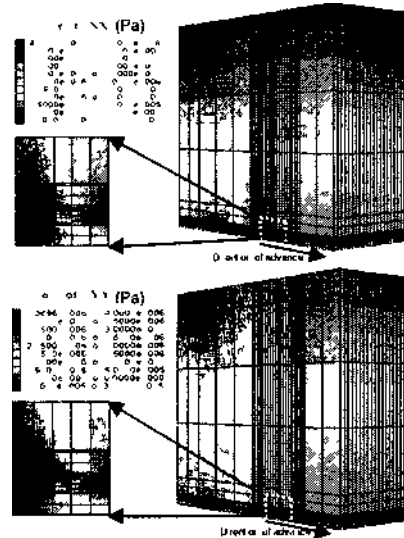


Figure 6 Secondary stresses in horizontal direction (x and y direction)



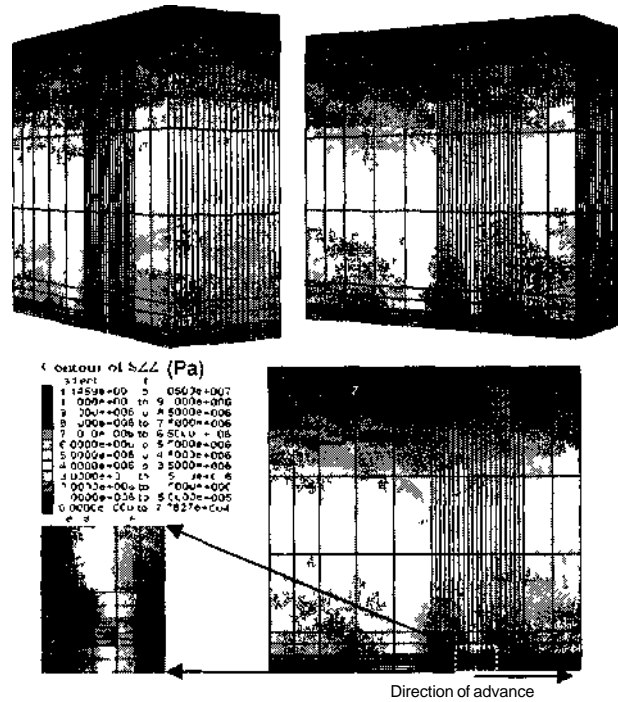


Figure 7 Secondary Stresses in vertical direction (*i* direction)

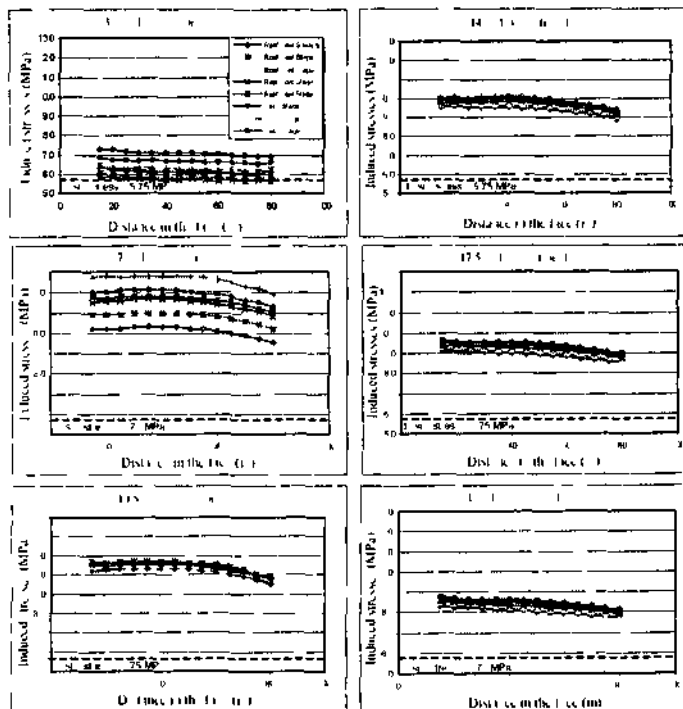


Figure 8 Secondary stresses in vertical direction

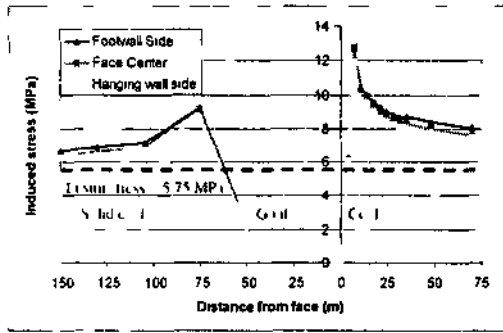


Figure 9 Veitici il Mioses tot med pat ale! to advance dnection it coal bottom

## S CONCLUSIONS

In this study preliminary results of a comprehensive 3-D modelling of a longwall panel at Ömerler Underground Coal Mine are presented. In order to maintaining a realistic modelling of stresses and displacements material properties were derived for rock mass instead of rock material by using Hoek & Brown failure criterion, RMR and GSI system and relevant empirical equations derived from the case studies. The results show that stresses around longwall faces can be successfully modelled by using FLAC<sup>3D</sup> provided that rock mass properties are input instead of rock material properties. Realistic modelling of stresses would undoubtedly be of vital importance in understanding strata response to production activity in underground operations. This is rather important for thick seam coal mining where strata response is more complex due to top coal caving behind the face.

## ACKNOWLEDGEMENTS

The authors would like to thank to Hacettepe University Scientific Researches Unit for providing (manual support and Dr. Fatih Bülent Taşkın for his kind help during in situ research.

## REFERENCES

- Akdaş H, Destanoğlu N, Öğretmen S, Yavuz M. 2000. Investigation and evaluation of pressures on powered supports in Ömerler Coal Mine. *5<sup>th</sup> National Rock Mechanics SMII/MMUIII Isparta Turkey* pp 119-121 (in Turkish).
- Biemawski ZT. 1971. Engineering classification of jointed rock masses. *Tunis S A J Insit Orlif*, 15 pp 115-144.
- Bieniawski ZT. 1989. *International Rock Mass Classification*. John Wiley & Sons, New York, 251p.
- Destanoğlu N, Taşkın TB, laştepe M, Öğretmen S. 2000. *GLI Tunçbilek Ümeilei \eialti Mekcmi:us\on Uygulanma*. Kozan Otset Ankara, 211 s.
- Hoek E. 1991. Strength of rock and rock masses. *ISRM News Journal*, Vol 2, No 2, pp 4-16.
- Hoek E and Brown FT. 1997. Practical estimates of rock mass strength. *Int J of Rock Mech and Mm Sa*, 14(8) pp 1165-1186.
- Itasca. 1997. *Usa Manual For FLAC<sup>3D</sup> Va 2.0*. Itasca Consulting Group, Minneapolis.
- Sönmez H. 2001. Investigation on the applicability of the Hoek-Brown criterion to the failure of (the fissured clay). PhD Thesis Hacettepe University, Ankara, 215 p. (in Turkish).
- Sonmez H and Ulusay R. 1999. Modifications to the Geological Strength Index (GSI) and then applicability to stability of slopes. *Int J of Rock Mech and Mm Sa*, 16(6) pp 741-760.
- Taşkın FB. 1999. Optimum Dimensioning of Pillars Between Longwall Panels in Tunçbilek Mine. PhD Thesis Osmangazi University, Eskişehir, 149 p. (in Turkish).
- Unver B and Yaşar NE. 2002. The Simulation of Stiblexel Caving Method Using in Thick Coal Seam by Computer. Hacettepe University Scientific Research Unit, Project No 00 02 602 008, 148 p. (in Turkish).
- Yaşar NE. 2002. Numerical Modelling of Longwall With Top Coal Caving. MSc Thesis Hacettepe University, Ankara, 215 pp. (in Turkish).
- Yavuz H and Fowell RJ. 2001. Softening effect of coal on the design of yield pillars in FLAC and Numerical Modeling in Geomechanics. *Proc of Int 2 International FLAC Conference* Lyon, France, D. Bilhuc et al. (eds), 11st A A Balkema pp 111-120.

## Fracture Toughness Analysis of Ankara Andésite

S. Şener & L. Tutluoğlu

Minin/; Engineering Department, Middle East Technical University, Ankara, Turkey

**ABSTRACT:** Fracture toughness, which is the resistance offered by a rock material against crack propagation is a material property used in the design of rock drilling equipment, rock bursting, hydraulic fracturing, wellbore stability and stability of jointed rock masses. Hollow Brazilian cylindrical core specimens were used in order to study mode-I fracture toughness behavior Ankara andésite. The load-displacement curves under diametrical compression were recorded and analysed for different crack propagation stages under mode-I loading. Different specimen geometries and crack initiation and propagation stages are investigated by numerical modeling using a boundary element program TDLCR, a finite element fracture analysis code FRANC 2D/L and a large deformation finite difference program FLAC. Comparison of the results of different numerical modeling techniques is provided in this work.

### I INTRODUCTION

Fracture will always have a wide- ranging importance to scientists. In solving great many engineering problems, understanding the mechanics and mechanisms of rock fracture is a key element.

Fracture mechanics is primarily used to prevent and predict catastrophic failure of structures of man-made materials such as metals, plastics, and ceramics. Before the development and integration of fracture mechanics into the conventional design procedures, strength of materials approach was the only major design tool in which the stress in a structure is compared with some material strength value in order to decide whether failure will occur or not.

With the exception of a few early investigations, rock fracture mechanics is a rather recent field study. Griffith (1921) was the first to make a quantitative connection between strength and crack size. Based on his analysis Griffith found that two necessary and sufficient conditions are required for a crack growth. First, sufficient stress must be provided at the crack tip to produce a crack growth mechanism. Second, sufficient energy must flow to the crack tip to supply the necessary work done for the creation of new surfaces at the tip.

Until the late 1940s, Griffith's pioneering work (1921-1924) was not seen as having much relevance to engineering. Irwin (1957) modified the original Griffith's fracture theory and postulated surface energy characteristics of fracture, which is

measurable in a fracture test, and he introduced the concept of stress intensity factor.

Irwin observed that there are three independent kinematic movements of the upper and lower crack surfaces with respect to each other,  $K_I$  for the opening mode,  $K_{II}$  for the shear mode and  $K_{III}$  for the tearing mode.

In present day elastic fracture mechanics, the governing parameter is the stress intensity factor  $K_I$ , at least in the linear case. It is, on one hand, a measure of the singularity of the stress field at a loaded crack tip and, on the other, intimately related to the available energy release rate (Irwin 1957).

The basic relation equates  $K_I$  to a critical value, which is often taken as a material property, and called the plane strain fracture toughness,  $K_{Ic}$ . As a short definition, fracture toughness indicates the ability of rock to resist crack propagation and it is the fracture energy consumption rate required to create new surfaces. Stress intensity factor is usually determined by numerical analysis and its dimensions

are,  $\text{stress} \times \sqrt{(\text{crack length})}$ , i.e  $\text{Pa} \times \sqrt{\text{m}}$  or  $\frac{\text{N}}{\text{m}^{3/2}}$ .

Fracture toughness value is used as a parameter for classification of rock material, an index of fragmentation processes such as tunnel boring and model scale blasting and a material property in the modelling of rock fragmentation like rock cutting, hydraulic fracturing, gas driven fracturing, explosive stimulation of gas wells, radial explosive fracturing and crater blasting as well as in stability analysis and

m the interpretation of geological features (Sun 1986). The use of fracture toughness is also common in the design of rock drilling equipment and in the prediction of rock drilling forces (Krishnan 1998).

A wide variety of testing methods and specimens has been used for assessing fracture toughness of rocks. Several researchers have adopted ISRM "Suggested methods for determining the fracture toughness of rock", i.e. Chong et al. (1987), Şantay (1990), Lim et al. (1993), Kruppu (1997), Chang et al. (2002). In this study Modified Ring Test, developed by Thiercelin et al. (1986), was used for determining the fracture toughness value of Ankara andésite.

## 2 TESTING METHOD

### 2. / Rock Sample and Specimen Description

Ankara andésite blocks were obtained from a quarry near Gölbaşı region located 20 km south of Ankara. General mechanical properties of this andésite were determined first before the fracture testing and these results are summarized in Table 1.

Table I Mechanical properties of Ankara andésite

Uniaxial compressive strength	63.81 MPa
Young modulus	19.85 GPa
Indirect tensile strength	6.71 MPa
Poisson's ratio	0.146

### 2.2 Testing Apparatus

MTS 815 servo controlled hydraulic testing machine in Mining Engineering Department of Middle East Technical University was used as the loading system.

To measure the displacement in our experiments LVDT responding to the stroke movements of the actuator was used. Here the stroke LVDT capacity is  $\pm 50$  mm with  $\pm 0.01$  mm accuracy. An external 500 kN load cell with  $\pm 0.25$  kN error band was used to measure the load. Loading rate in the testing was around 0.0005 mm/sec.

### 2.3 Modified Ring Test

Modified Ring test is essentially based on hollow cylinder geometry with two diametrically opposed, flat-loading surfaces as shown in Figure 1.

In this study, andésite blocks were prepared by using two different drill bits. One has 75 mm and the other one has 150 mm diameter. For these specimens 5 mm and 18.5 mm hole radii were used, respectively.

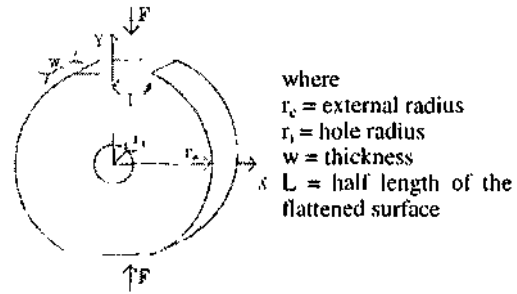


Figure 1 Modified Ring test specimen geometry 1986)

The specimen is compressed across its diameter by applying a uniform displacement at constant rate. As the tangential stress exceeds the tensile strength a crack is initiated at the top and bottom of the hole and this crack propagates vertically towards the loaded ends with increasing load. During the propagation of the crack  $K$ , changes with increasing crack length. No analytical solution is available to find this change. However, numerical modelling can generate the stress intensity factor as a function of the crack length.

## 3 NUMERICAL MODELING

The Modified Ring test for plane strain fracture toughness determination involves two phases: i) generation of laboratory load-deformation record of a specimen, and ii) numerical computation of crack-tip stress intensity factors in a model with exactly the same dimensions as the laboratory specimen (Thiercelin 1986). In this study, boundary element program TDLCR, finite element code FRANC2D/L, and finite difference program FLAC were used for modeling, analyzing, and comparing the tests numerically.

Two Dimensional Linear Crack (TDLCR) boundary element program is a displacement discontinuity type boundary element method with a main program and three subroutines. For the first crack initiation analysis, tangential stress at the top and bottom boundary of the hole is checked by comparing it to the tensile strength. When  $\sigma_c > T_n$ , a small crack with displacement discontinuity (DD) elements and one crack tip element are added to the top and bottom of the hole parallel to the applied loading. And this procedure is repeated by increasing the length of the crack along the loading axis to simulate the crack propagation. By this way, variation of stress intensity factor with increasing crack length is determined.

FRANC2D/L developed by Paul Wawrzynek at Cornell University (FRANC2D/L Catalog 1997) is an interactive program for the two-dimensional

analysis of structures. Its capabilities include elastic and elastic-plastic material response, simulation of linear elastic (LEFM) and elastic-plastic crack growth, analysis of layered structures, and a linear plate bending option.

Fast Lagrangian Analysis of Continua (FLAC) is a finite difference program and it is primarily used for geotechnical engineering applications, the code includes special numerical representations for the mechanical response of geologic materials.

#### 4 RESULTS AND DISCUSSION

A typical load-displacement curve for the Modified Ring test is shown in Figure 2.

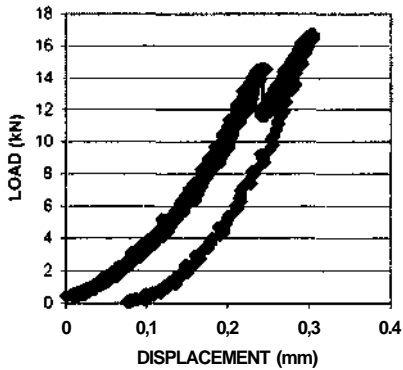


Figure 2 Load-displacement record of MTS 815 for 75 mm specimen

It is known from the experimental work and previous work by Thiercelin (1986) that once the crack is initiated it grows very fast in an unstable manner to a critical length where  $a = a_c$ .

At this point a load drop is to be observed in the load-displacement behaviour. After this critical length crack continues to propagate in a stable manner, since the crack front approaches and enters into the confined zone or high stress gradient zone of the compressive stress field under the loaded ends. This behaviour which is reflected as a drop in the load-displacement record in Figure 2 appears as a peak in the numerically generated  $K_I$  - a record of Figure 3.

Results of boundary element modeling of crack propagation using the displacement discontinuity

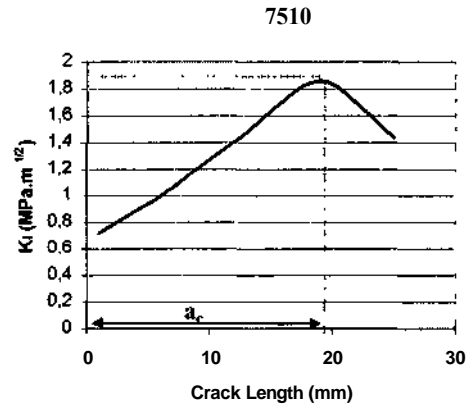


Figure 3 Variation of SIF with crack length during crack propagation

elements are presented in Table 2.  $K_I^*$  shows the normalized stress intensity factor where

$$K_I^* = \frac{K_{I, \max} \pi r_c}{F_c \sqrt{(a_c + r_c) \pi}} \quad (1)$$

is dimensionless. This normalization is done for an easy comparison of stress intensity factor to the stress intensity factor of a tensile crack of length  $(a + r_c)$  under tension  $a$  where the stress intensity factor is  $\sigma \sqrt{(a + r_c) \pi}$ .  $a_c$  corresponds to the critical stress value at the point of first load drop and  $a_c$  corresponds to the critical crack length at this drop. Stress intensity factor is  $K_{I, \max}$  at this stage.

Table 2 Results of numerical modeling of crack propagation by boundary element method

$r/r_c$ ( $\alpha$ )	$a_c$ (mm)	$\sigma_c$ (MPa)	$K_{I, \max}$ (MPa.m <sup>1/2</sup> )	$K_I^*$
<b>7510</b>				
0.133	25	52.7	2.26	2.06
0.133	22	39.94	2.04	1.723
0.133	20.5	33.54	1.87	1.451
0.133	19	30.4	1.71	1.21
0.133	14.5	25.87	1.31	0.804
<b>15037</b>				
0.247	41.5	22.76	1.92	2.86
0.247	38.5	17.59	1.76	2.33
0.247	32.5	15	1.68	2.06
0.247	26.5	12.91	1.52	1.8
0.247	23.5	10	1.07	1.19

For a general comparison, the results of numerical modeling by TDLCR boundary element method and FLAC analysis are shown in Figure 4 for 75 mm diameter and for 150 mm diameter specimens.

Displacement Discontinuity model result was closer to the experimentally measured result. For small 75 mm specimens, DD result deviate about 9 % from the mean experimental value whereas FLAC model deviation is 17 %. This deviation is reduced down to 6 % for DD modeling and 9 % for FLAC modeling for large size specimens that are 150 mm in diameter. In this figure internal hole radius  $r$ , changes between 5 mm and 18.5 mm in order to obtain different  $r/r_c$  ratios for 75 and 150 mm specimens.

For computation of  $K_{Ic}$  values following formula (Fischer, 1996) was used:

$$K_{Ic} = (\sigma_c)_{\text{min}} \left( \frac{K_{I \text{ max}}}{\sigma_c} \right)_{\text{model}} \quad (2)$$

This expression serves as to scale the numerical values by the experimental results.

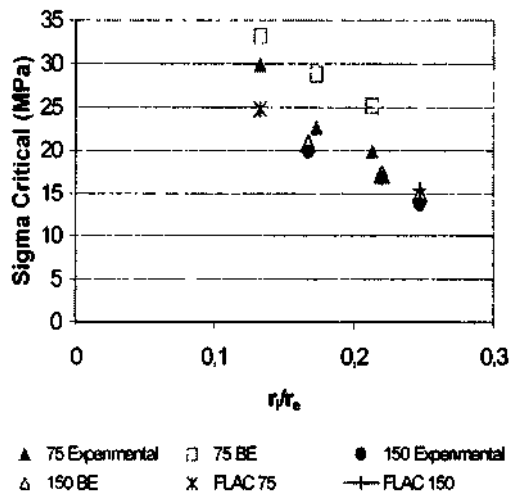


Figure 4 Comparison of OY vs  $r/r_c$  results from experiments and numerical models

$K_{Ic}$  values calculated this way are compared to  $K_{Ic}$  values of boundary element modeling in Table 3.

Table 3 Comparison of  $K_{Ic}$  and  $K_{Ic}$

	$K_{I \text{ max}} \text{ (Boundary Element)}$ $MPa\sqrt{m}$	$K_{Ic}$ $MPa\sqrt{m}$
7510	1.853	1.67
15037	1.678	1.535

## 5 CONCLUSIONS

Fracture toughness study of Ankara andésite was carried out by using hollow Brazilian cylindrical core specimens. This study involved into two parts; i ) experimental work, ii ) numerical analysis.

Modified Ring test using hollow Brazilian discs with flattened loading ends is a convenient test for the determination of mode-I fracture toughness  $K_{Ic}$ . Specimens are quite easily prepared from the rock cores of different diameters. Test procedure is simple and quick, and the load-displacement results are easy to interpret provided that a displacement controlled loading system is available such as the MTS 815 servohydraulic testing system used here.

Critical load values obtained from numerical modeling were quite close to the experimentally observed ones, especially for DD boundary element modeling being within 6-9%, FLAC models results were within 10-15% of the experimental averages. Numerical modeling predictions were better for larger size specimens for both modeling techniques.

## REFERENCES

- Chang, S.H., Lee, C.I. and Jean, S., 2002. Measurement of Rock Fracture Toughness Under Modes I and II and Mixed Mode Conditions by Using Disc-Type Specimens. *Eng. Geo.*
- Chong, K.P., Kuruppu, M.D., Kuzmaul, J.S. 1987. Fracture Toughness Determination of Layered Materials. *Eng. Fract. Mech.* Vol.28: pp. 43-54
- Fischer, M.P., Elsworth, D., Alley, R.B. and Eilgelder, T. 19%. Finite Element Analysis of the Modified Ring Test for Determining Mode I Fracture Toughness. *Int. J. Rock Mech. Min. Sci. and Geomech. Abstr.* Vol.33: pp. I-15
- FRANC2D/L 1997. Short User's Guide Version 1.4. Kansas: Kansas State University
- Griffith, A.A. 1921. The Phenomena of Rupture and Flow in Solids. *Phil. Trans. Roy. Soc. of London* A221: 163-197
- Griffith, A.A. 1924. The Theory of Rupture. *Proc. 1<sup>st</sup> Int. Congress Appl. Mech.* pp. 55-63
- Irwin, G.R. 1957. Analysis of Stress and Strain Near the End of a Crack. *J. Appl. Mech.* Vol.24: p.361
- Krishnan, G.R. 1998. Fracture Toughness of a Soft Sandstone. *Int. J. Rock Mech. Min. Sci. and Geomech. Abstr.* Vol.35: pp.695-710
- Kuruppu, M.D. 1997. Fracture Toughness Measurement Using Chevron Notched Semi-circular Bend Specimen. *Int. J. Fract.* Vol.86: pp. L33-L38
- Lin, I.L., Johnston, I.W., Choi, S.K. 1993. Stress Intensity Factors For Semi Circular Specimens Under Three Point Bending. *Eng. Fract. Mech.* Vol.44: pp.363-382
- Sun, Z. and Ouchterlony, F. 1986. Fracture Toughness of Stripa Granite Cores. *Int. J. Rock Mech. Min. Sci. and Geomech. Abstr.* Vol.23: pp.399-409
- Şantay, A.Ö. 1990. Critical Analysis of Short Rod Fracture Toughness Testing Method. *Ms. Thesis* Ankara: Middle East Technical University
- Thiercelin, M. 1986. Fracture Toughness Determination with the Modified Ring Test. *Int. Symp. on Engineering in Complex Rock Formations*. China

## An Example and Comparison of Old and New Tunnel Support Estimation Methods

C. Ağan, A. Turabik & M. M. Güven

*DSI General Directorate, Geotechnical Services and Groundwater Department, Rock and Soil Mechanics Section, Ankara, Turkey*

**ABSTRACT:** The stability of the rock structures in mining and geotechnic fields depends on the in-situ stress state and mechanical properties of the rock mass and the geometry of the structures. The stabilities and the chosen of equipments (support types, etc.) depend on the in-situ stresses. But, because of measuring difficulties and high costs, the in-situ stress measurements are very rare. They can be measure by technological methods like flat-jack, photoelasticity, hydraulic fracturing, thermal fracturing, acoustic emission, etc. But, because of high costs and difficulties of field works, they are not widely preferred by engineers.

So, for recent years, engineers began to use computer aided technologies and designs. They can be 2 or 3 dimensioned and simulate in-situ stresses, deformations, displacements, etc. But, to increase the confidence of this technology as possible as higher, the input data (E,  $\nu$ ,  $\sigma_0$ ,  $\sigma_x$ , etc.) have to be taken with in-situ experiments and studies.

But, because of high programs costs and high experience requirements, directs the engineers to simple method which is consisted of laboratory tests, old methods (Terzaghi, RMR, Q, etc) and charts in foundation design, tunnel support design, etc.

In this report, the problems and mutabilities of an injection tunnel caused by old methods will be examined. And then, the tunnel direction and support load will be designed again with computer aided simulation program to emphasize that old systems (without in-situ data) lead into errors and they must not to be preferred by engineers.

### 1 INTRODUCTION

This report is dealing about the causes and repairs of the swellings and deformations at the left side injection and transportation tunnels of Çokal Dam at Çanakkale (Figure 1). For this reason, some in-situ experiments, measurements and laboratory experiments have been done.

### 2 GEOLOGY OF STUDY FIELD

Çokal Dam field has a flysch formation with eocene aged. Formation has a gray-brown color, lateral sequenced and composed with sandstone, siltstone and claystone.

The thickness of strata are changeable between 3-12 m and their declivities are 10°-20° SE.

Sandstones are generally stable but the places where siltstones and claystones have majority, the alterations are too much. By the existence of fault



Figure 1. Deformational tunnel

zones, the alterations are increased. Sandstones are generally hard and cemented fresh surfaces that have brown-red color. Siltstones and claystones have generally thin strata and they are fragile.

The research field is in the I. grade earthquake region according to the Ministry Decision with number 96/8109 and date 18.04.1996. It is just 2 km

away to an active tault (Figure 2). This tault is a component of North Anatolian Fault zone and this zone is 60 km in length and 10 km in width. Some destructives and liquefaction effects of this fault can be observed at a distance of 200 km (Erdem and Guven 2000).

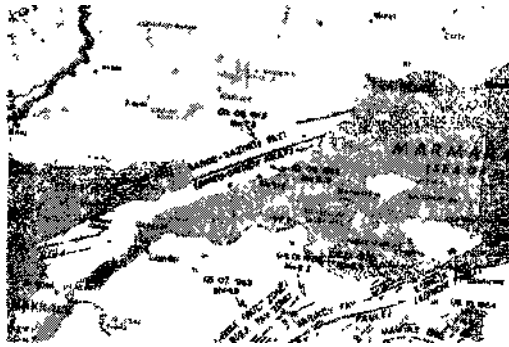


Figure 2 Tectonic map of Marmara Sea Region

Also some secondary fractures intersect with the left side tunnels (Tozak 1999). These secondary fractures altered the surrounding rocks. The leakage of surface and underground water also increases the alterations.

### 3 GENERAL SITUATION OF TUNNELS

The tunnels excavated in flysch formation. They are nearly 4,2 m in height and 4 m in width. They have horseshoe shape. Shotcrete (15 cm) + wire mesh+steel support (1-16) are used for support system. Surrounding rock was classified as 4<sup>th</sup> class according to Terzaghi.

There is no deformation that can be observed at the right side tunnels. Only low amount of sweat and drips can be observed.

At the left side tunnels, by the effects of fault, the flysch formation locally became clay. Locally, big deformations and large amount of water flow can be observed.

### 4 THE STUDIES AT THE LEFT SIDE INJECTION AND TRANSPORTATION TUNNELS

#### 4.1 Deformation studies

At first, the deformed steel supports were cut and swelled parts were sciapped. Then the aperture between each steel support elements decreased from

1 m to 0,5 m and locally to 0,25 m especially at tault zone. The steel support elements tied to each other from the bottom. Then gravel material spread to the floor.

#### 4.2 Deformation measurements

After the earthquake, which occurred at Marmara Sea on the date of 28.02 2002, total station used for deformation measurements at different sides and different places. After investigations of these measurements, it was observed that the biggest deformations (50 cm) took place at the bottom side. The bottom of steel supports became closer to each other. It was also observed that the tunnels were buried within the time.

#### 4.3 Drainage studies

By the leakage of water to the inner and surrounding parts of tunnel, it caused to swelling. Because of the fault zone, the flysch formation became clay by the time. So that the number of drainage holes increased. Perforated pipes were set to the places where the leakages can be observed. It is aimed to take the water into the tunnel and then to the outer side of tunnel. By the measurements 1 lt/sec leakage was determined.

#### 4.4 Studies for determination of the Yield zone

For determining the tunnel load, it is aimed to find the size of yield zone. Time was not enough for setting of the extensometer or other systems. So pressuremeter was chosen for this purpose. 4 locations were determined for experiments. 7 drilling holes were excavated which have 12-15 m in depth. Systematically pressuremeter experiments were done at these drilling holes.

Locations of pressuremeter experiments:

I- U-PRSK-1: It is drilled at transportation tunnel at 135 km. It is drilled at tunnel roof and the surrounding rock is strong. By the experiments, 34-40 kg/cm<sup>2</sup> limit pressure and 550-1500 kg/cm<sup>2</sup> elastic module values were obtained.

II- U-PRSK-2: 4 holes were drilled with 45° angle at transportation tunnel. It was at 208 km and at fault zone. It was seen that approximately 3 m of surrounding rock was yielded completely. By the experiments, 3-9 kg/cm<sup>2</sup> limit pressure and 50-60 kg/cm<sup>2</sup> elastic module values obtained.

III- E-PRSK-3. It was drilled at the roof of injection tunnel at 270 km. 5-13 kg/cm<sup>2</sup> limit pressure and 65-130 kg/cm<sup>2</sup> elastic module values were obtained.

IV- E-PRSK-4: It was drilled at the bottom of injection tunnel at 280 km. The experiment results were similar to the E-PRSK-3.



It can be seen that big deformations occurred at the bottom of the tunnel (Figure 3) These results confirm the burning of tunnel and the results of deformation measurements

Table 2 Evaluation of laboratory results

	Stable Points	Deformed Points
Liquid limit (LL)	28-42	42-44
Plastic index (PI)	10-23	20-23
Gain percent under #200 mesh (%)	79 CL	90-100 CI
Swelling (9f)	1.8-3.0	5-12
Swelling (kg/cm <sup>2</sup> )	0.6-0.7	1.00-2.26
Wn (%)	8-16	12-21
SC <sub>20</sub>	67-75	75-100
Gs (g/cm <sup>3</sup> )	2.78-2.80	2.77-2.80
Kind of clay	Illite	Illite

Figure 1 Deformation of yield zone by Pessuier-Li Test

#### 4.5 Laboratory test results

For determination of the kind of clay undisturbed samples were taken for experiments. Because at last seen the causes of these deformations were swelling of clay. The results and evaluation of experiment results are presented in Table 1 and Table 2.

During the spillway excavation water seepage was seen. Water sample was sent to laboratory for analysis. Within analysis 4660 µhos/cm electrical conductivity and 2990 mg/L dissolved solid materials are found. These results mean that this water seeps from depth levels.

By the results it is understood that the clay has a big swelling potential and the deformations caused by the water come from fault cracks. The earthquake also increased the deformations.

Table 1 Laboratory test results

	Plastic Clay	Clay Gavel Sand
0.075(111111)	80-90	16-40
LL (C <sub>r</sub> )	42-44	32-33
PL (%)	21-22	15-17
PI (%)	21-23	14-18
Class	CLC1	GC
Gs (g/cm <sup>3</sup> )	2.7-2.8	2.7
Wn (g/cm <sup>3</sup> )	2.1-2.3	2.2-2.3
Wn (%)	10-20	4-5
SI <sub>60</sub>	80-100	26-56
Swelling	Pessuier (kg/cm <sup>2</sup> )	-
	%	4.5-12
UCS (kg/cm <sup>2</sup> )	3-97	-

#### 5 TUNNEL ROUTE

##### 5.1 Introduction about tunnel route

Both geological investigations and field observations it is observed that these tunnels cross a lot of fault cracks. For analyzing the effects of these faults to the tunnel the directions of faults and tunnels are marked to the stereonet system in computer (Figure 4). All of the dip angles were assumed as 30°.

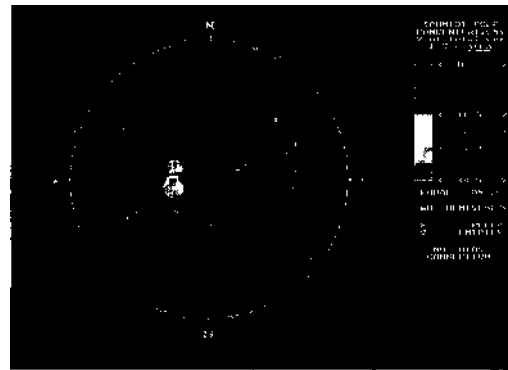


Figure 4 Orientation of fault zones

As shown in Figure 4, injection tunnel (1) is affected by only fault F5 (2). The other faults do not affect the injection tunnel. But the transportation tunnel (8) is affected by faults F2 (4), F4 (5), estimated fault (6) and Ece fault (7). This result is similar to the deformation studies results. Because, the biggest deformations had occurred at transportation tunnel (Table 3).

Table 1. Faulk ni Figure 4

Contour No	
1	Injection Tunnel
2	F5 Fault
3	F3 Fault
4	F2 Fault
5	F4 Fault
6	Estimated Fault
7	Ece Fault
8	Transportation Tunnel

### 5.2 Investigations about tunnel load, stability and deformations

Before the tunnel was excavated, the rock is determined as 4<sup>th</sup> class rock according to the Terzaghi. Referencing this system, rock load was determined as 0,7-1,0 kg/cm" and supports are selected according to this load. After these deformations, the investigations began.

Two different paths are followed. At first path, the pressuremeter experiment results are used. According to these results, 3 m of surrounding rock yielded. By calculations rock load was calculated as 6-7 kg/cm". And also, the swelling pressure found in laboratory was approximately 1,5-2 kg/cm<sup>2</sup>.

At the second path, computer program was used to find the rock load. The inputs are given in Table 4.

Table 4 Inputs, of program

Input Data	Data Values
Excavation limits	4 m width, 4 m height, horse nail section
Over burden height	Max 60 m
Material	Altered flysch
Young module	1000 kg/cm <sup>2</sup>
Poisson ratio	0,33
Specific weight	2,7 ton/m <sup>3</sup>
Cohesion	2 kg/cm"
$\phi$	30°
Characteristic-	Plastic

As shown in Figure 5, the maximum stress value is approximately 5-6 kg/cm" and it is applied to roof and the corners of bottom. During the observations at tunnel, it is seen that the maximum deformations occurred at the roof and bottom, especially at the corners. This is the evidence that, the computer analyzes are also true.

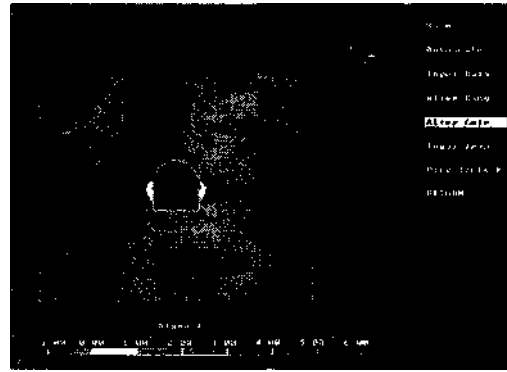


Figure 5. Vertical stress on tunnel section

## 6 CONCLUSIONS

The multilateral investigations, which are held in Çokal Dam, demonstrate that;

- Drainage studies had been done correctly
- The primitive methods (Terzaghi, Q, etc.) must not be used alone for supporting and route selection. They can be changeable from one person to another and deceptive. In today technology, these methods must be only used for controlling and confirming the studies. Because, the primitive methods are based on experiences. But, it is true that the underground is always changeable and these methods can be insufficient. For this reason, during these calculations rock and soil mechanics principles must be taken into consideration and must not be avoided from in-situ experiments for obtaining the requiring parameters. Primitive methods do not have validity at today technology.
- All of the discontinuities and faults directions must be determined before selecting the route of tunnels.
- If the working field is in the fault zone, NATM methods and circular section must be chosen. The invert concrete must not be neglected.

## REFERENCES

- Ağan, C., Turabik, A.. 2002. Çokal Baraj Sol Sahil Ulaşım ve Enjeksiyon Galenleri Kaya Mekaniği Etüt Raporu. *Enerji ve Tabii Kaynaklar Bakanlığı, Devlet Su İşleri Genel Müdürlüğü. Jeoleknik Hizmetler ve Yeraltı Suları Dairesi Başkanlığı. Kaya ve Zemin Mekaniği Şube Müdürlüğü, Rapor No:257*
- Bagualin, F., Jezequel, F.J., Shields, H.. 1978. Pressuremeter and Foundation Engineering. *Trims. Tech. Publication. Clausthal. Germany*
- Bieniawski, Z.T., 1984. *Rock Mechanics: Delikli in Mining anil Tüneli için*; A.A. Balkema Publisher

- Canadian Manual on Foundation Engineering 1975 Canada  
Pintmg and Publishing Ottawa Canada
- Erdem IU Güven M M 2000 Çanakkale Çokal Baran  
Temel Zemin Sıvılaşma Analizi Raporu *Eiuiji u Tabu  
Kımlaklı Bakanlıđı De\let Su İşlen Gencl Mudulıđu  
Jeoteknik Hizmetler ve Yecillıslau Dairesi Başkanlıđı  
Ka\at e Zemin Mekaniđi Şube Mudulıđu* Rapor No 222
- Erdoğan II Ba\kal I Erdem IU 1988 Şanlıurla-Tugav  
komutanlıđı Yerleşim Sahası Zemin Etüt Raporu  
*Ba\mluluk u. lıkan Bakanlıđı De\let Su İşlen Genel  
Mudulıđu Jeoteknik Hizmetler ve Yecillıslau Dausı  
Başkanlıđı Kastı ve Zemin Mekaniđi Şube Mudulıđu*  
Rapor No 110
- Hoek E Bray JW IW Kaya Şev Stabıletesı *TMMOB  
Jeoloji Mühendisten Odan Umulan ı* Baskı
- Obert L Duvall W I 1967 Rock Mechanics and The Design  
ot Structures in Rock John Wiley and Sons Inc
- The Menard Pressuremeter Interpretation and Application of  
Pressuremeter Test Results to Foundation Design *197s  
Sah Sails* No 26 Pans
- Tozak A Z 2000 Çanakkale-Gelholı-Gokbucl Projesı Çokal  
Barap Dolusavak Şeşleri Jeoteknik Raporu *Ener/ı ie Tabu  
KıMiaklı Bakanlıđı Detlef Su İşlen Genel Mudulıđu  
D.SI HI Bilice Mudulıđu Jeoteknik Hizmetler ve  
eiallnulau Dausı Başkanlıđı* Balıkesir
- Ulusay R 2001 Uygulamalı Jeoteknik Bilgilerı *TMMOB  
Jolou MuteniliKleu Odası Yayınları* 38 4 Baskı



## Ground Control Problems and Roadheader Drivage at Ombilin Coal Mine, Indonesia

K. Matsui & H. Shimada

*Department of Earth Resources and Mining Engineering, Kyushu University, Fukuoka, Japan*

H. Furukawa

*Japan Coal Energy Center, Tokyo, Japan*

S. Kramadibrata

*Department of Mining Engineering, Institute of Technology Bandung, Bandung, Indonesia*

H.Z. Anwar

*Indonesian Institute of Sciences (LIPI), Bandung, Indonesia*

**ABSTRACT:** In 1998, an agreement on the "Incline Project at Ombilin III" was made between JCOAL (Japan Coal Energy Center) and PTBA (PT. Tambang Batubara Bukit Asam). In this project, a development system of an incline was introduced to open a new underground coal mine, or Ombilin III that will begin mining operations in the 2000s to meet the necessary demand for increasing the production of Indonesian domestic coal. This paper discusses the ground control problems and the development performance of two main inclines at Ombilin Coal Mine.

### 1 INTRODUCTION

Indonesia produces over 80 million tons of clean coal annually and is the third largest coal exporter to Japan, about 13 million tons annually. 99% of the total production of coal is from opencut mines. It is anticipated that more opencut mines will be developed and more coal will be mined underground to fill the great demand for coal in Indonesia and the rest of the world.

In 1998, the development of a new underground coal mine began at Ombilin Coal Mine in Indonesia in order to meet the necessary demand for increasing the production of Indonesian domestic coal in cooperation with JCOAL. In this project, a development system of an incline was introduced to open a new underground coal mine, or Ombilin III that will begin mining operations in the 2000s

A joint research work at Ombilin Coal Mine that has been conducted since 1998 by Kyushu University, Japan, the Institute of Technology Bandung (ITB), Indonesia, and the Indonesian Institute of Sciences, Bandung (LIPI), Indonesia is directed primarily towards the optimal underground support system and the development of optimal underground mining methods in Indonesia. Some results of the joint research have already been reported (Shimada et al., 1998, Anwar et al., 1998, 1999a and 1999b, Matsui et al., 1999, and Kramadibrata et al., 2000).

This paper describes the ground control problems at Ombilin I and also discusses the development performance and ground control of two main inclines at Ombilin III.

### 2 COAL MINING INDUSTRY IN JAPAN AND ITS POLICY

Japan is dependent on overseas suppliers for the coal it uses (over 150 million tons). Japanese annual domestic production output is only about 1 million tons. At present, there are only one underground coal mine (Kushiro Coal Mine) and several small opencut mines in Japan.

It is anticipated that the coal extraction conditions in the coal-producing countries will deteriorate in the future. A 'Five-year Plan for Coal Technology Transfer' started in 2002 in order to achieve greater stability in the supply of coal from overseas. Under the five-year plan, Japanese advanced technology such as safety technology will be transferred in an intensive and planned manner to coal-producing countries, especially Indonesia, China and Vietnam.

Considering the necessity of development of new underground coal mines in Indonesia, an agreement on the 'Incline Project at Ombilin III' was reached between JCOAL and PTBA in 1998. In this project, a development system of incline for a new underground coal mine (Ombilin III) was introduced, consisting of a roadheader and transport system that were manufactured in Japan. From this project, it is expected that Japanese coal mining technology will be transferred to the Indonesian side.

### 3 OMBILIN COAL MINE

Ombilin Coal Mine is located at Sawahlunto Region of West Sumatra Province. Historically, the mine was established by the Dutch Company in 1892. At present Ombilin Coal Mine is owned by PTBA, which operates open pits and underground mines. The total annually production is about 1.0 million tons and 10% of the overall production is from underground mining.

The geology of coal in Ombilin Mine is Paleogene sedimentary and belongs to the Sawahlunto Formation, which consists of a sequence of brownish grey shale, siltyshale and siltstone and interbedded brown-dense quartz sandstone and coal (Koesumadinata, et al., 1981).

The existing underground coal mine is now operating at the Ombilin I, Sawahlung. Two coal seams of A and C seams are being extracted by retreat longwall caving method and room-and-pillar method. The longwall face width varies from 70 to 150 m, and the panel length is up to 400 m. The depth cover varies from 50 to 300 m. Geotechnical problems identified at Ombilin I were discussed in some previous research works (Rai, 1999 and Kramadibrata et al., 1999).

Since 1985, underground development in coal and soft to medium hard rock has been done by using roadheaders. On the other hand, drilling and blasting methods have been used for tunnel development in harder rock formations, including siltstone and sandstone

The Siaalut area, so-called Ombilin III, is being

constructed and prepared to mine A and C coal seams at a depth of about 800 m below the surface. There are two inclines, Incline 1 and Incline 2, being developed as shown in Figure 1.

### 4 GROUND CONTROL PROBLEMS AT OMBILIN MINE

The result of the geological investigation presents that the coal bearing strata at Ombilin basin consist of low strength coal shale, interbedded siltstone/shale, siltstone/sandstone and silt overlain by sandstone. In general, the immediate roof is structurally competent, but low strength from 25 to about 50 MPa. In this category, they can be classified as weak rocks. It also shows severe slaking behavior when it comes in contact with water. Nevertheless, the strength indicates an increase with an increase of distance into the roof. The immediate floor consists of interbedded sandstone/siltstone and a siltstone layer. Some problems identified at Ombilin I have been associated with uncontrollable factors such as rock mass behavior i.e. intact rock behavior, geological structure and in-situ stresses.

These coal measures rocks showed the severe deterioration of the mechanical properties and slaking behavior due to water (Anwar, et al., 1999 and Matsui et al., 2000). These effects cannot be neglected considering the roadway maintenance and the support system design.



Figure 1 Portal of Incline 1 at Ombilin •

According to Rai (1999), the deformation of the coal bearing strata in the Ombilin area has a time-dependent behavior that follows the Burger elastoplastic rheology model. At Ombilin I the roof deformation occurred varies from 7.7 mm to over 120 mm at about 300 m depth below surface, which was measured by means of extensometer (SCT, 1994). In the level of the maximum deformation, the deflection of the steel support is likely expected. This study shows that the majority deformation occurred in the clay-rich immediate strata. It is related to the shale/siltstone behavior which is found in the immediate roof, which is very weak in wet conditions.

Figure 2 shows the mechanism of roof failure at Ombilin I described by Rai (1999). Figure 2A shows a rock failure due to the laminated structure, whereas Figure 2B depicts a rock failure due to a slickenside plane, which is frequently found in laminated sandstone or siltstone. Furthermore, Figure 2C and 2D show rock failures due to joint and wedge-form

structures. Figure 2E is a representation of the inward movement of sidewalls and failure of roof rock due to the weakness of the rock mass. The inward movement can reach the order of 40-60 cm and the falling rock block can be of 20-80 cm diameter. Moreover, Figure 2F shows the inward squeezing of swelling or creeping siltstone, which causes a bending to steel support. The inward squeezing is 50-90 cm at each side.

Up to now, many measures have been tried to control the large deformation and to prevent the failure of roadway roof. Of these, roof bolting is effective and economic support system. The effectiveness of roof bolting was shown in the poor roof conditions clearly according to tell-tale monitoring and field observation. From the long-term field observation and laboratory test, however, it was revealed that although roof bolting prevented the roof fall, it could not control the roof failure and the large deformation of the poor roof.

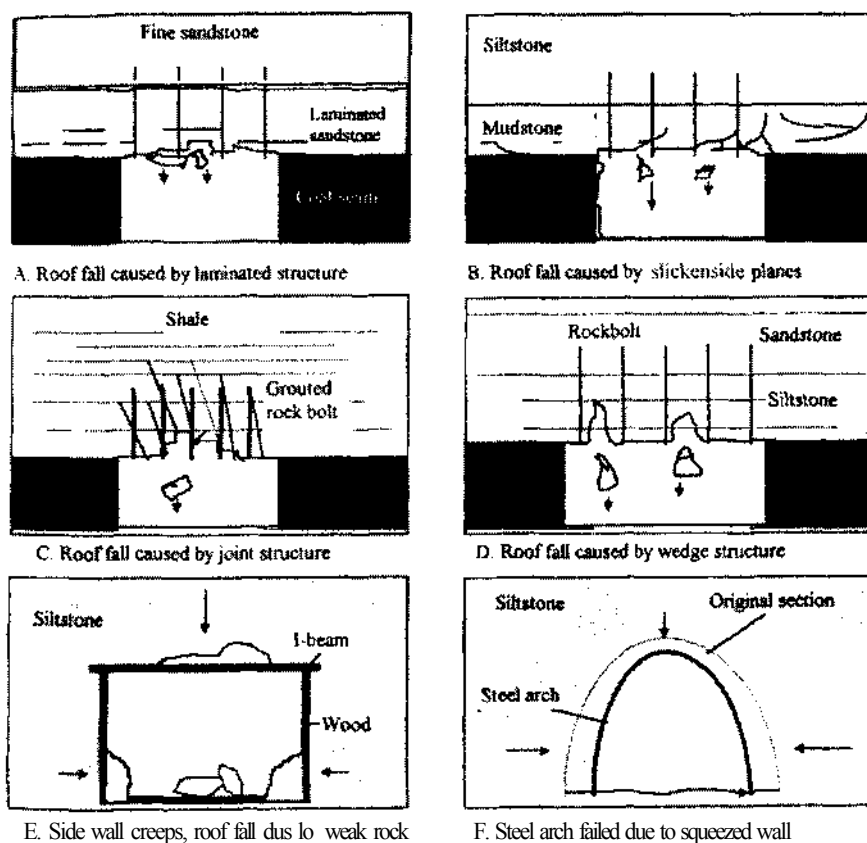


Figure 2 Failure patterns at Ombilin Coal Mine.

## 5 DRIVAGE SYSTEM OF INCLINES 1 AND 2 AT OMBILIN III

At present, serious ground control problems such as roof fall and large deformation are occurring at the two mains which are main roadways for development and extraction of the Longwall Panel 6 of Coal Seam A. The bolted main roadway is suffering from large roof deformation and roof severe falls occur in another main roadway that is supported by the three-piece-set. And rib failure is also occurring at the maingate and tailgate of the Panel 6.

Figures 3 (a) and (b) show the bolted main roadway where severe roof deformation occurred due to time-dependent and slaking behaviors of roof siltstone. It is noted that after excavation and roof bolting, the deformation of the roadway at the site was small and stable according to the tell-tale readings. However, after long stable period of about two years, the roadway roof started deforming gradually and reached to the magnitude of over 100 cm of roof settlement. According to the recommendations, three-piece-set with I-beam and wood props was installed in order to control the deformation. But the additional support could not stop the behavior. The wood props were broken and finally in order to keep the roadway open, steel arches were installed after back ripping as shown in Figure 3 (b). The height of the roof ripping was about 100 cm. The exposed bolts were seen like bamboo shoots in the same figure. The part of exposed bolt was cut off later.

It is not clear whether the installation of longer bolts or cable bolts could control the deformation in the site or not. However, it is recommended that longer bolts or cable bolts should be installed during stable period when the strata are expected to show severe time-dependent behavior.

Basically rib bolting is not used at Ombilin. From the observation, the rib was stable after excavation. About one year later or so, however, the rib started tailing gradually. Rib failure has become a serious problem at the both maingate and tailgate of the Panel 6.

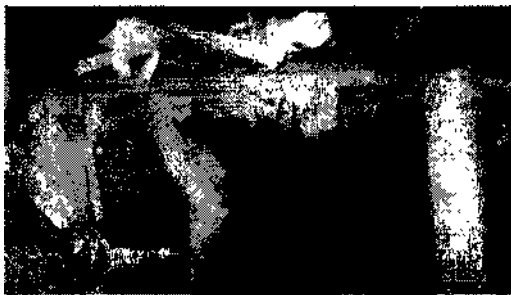
Inclines 1 and 2 at Ombilin III are being developed to drive 1550 m long inclines at a 12 degree gradient. Incline 1 will be used as a main ventilation inlet and haulage incline for underground mining. The drift of Incline 1 was started with a roadheader MRH-S220M from the surface with an open cut in July of 1998. The roadheader was manufactured at Mitsui Miike Mining Machinery Co., Ltd., Japan. The machine is capable of cutting hard rock up to 130 MPa UCS (unconfined compressive strength).

Figure 4 shows the drivage system used in Incline 1. The debris is now transported to the surface by a chain conveyor and a belt conveyor. Incline 1 is an arched shape, being of 5.0 m wide and 3.5 m high. A three-piece rigid steel arch was installed to support the roof and sidewalks at 2.0 m centers. Between the steel arches, three sets of 6 rock-bolts/W-straps were installed to reinforce the roof. The bolt was fully resin-grouted being of 2.4 m long and 22 mm in diameter. Each bolt was installed at 0.8 m centers. Toussaint-Heinzmann yielding arches were also installed at 15 m centers without roof bolting.

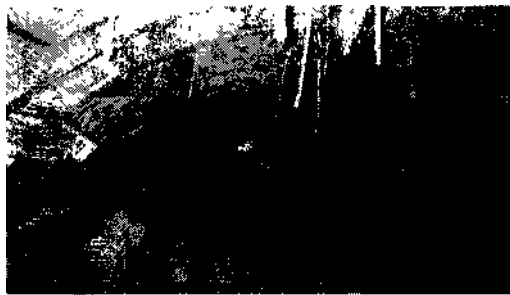
Incline 2 will be used as a main ventilation outlet incline. At the beginning, Incline 2, parallel to Incline 1, was developed by the drilling and blasting method. The distance between the two inclines is 50 m.

Concerning the support system, the shape and size of Incline 2 are almost the same as those of Incline 1. The number of blast holes that were drilled with a Jet-hammer drilling machine was 45, being 12 m long and 27 mm in diameter. It took about 2.5 hours to drill the blast holes. A medium-duty roadheader Dosco-1 is now being used in order to increase the development performance.

The development of Incline 1 so far has not been progressing well due to the presence of a soft immediate roof and floor. Floor softening and heaving is not something that can be ignored. The



(a)



(b)

Figure 3 (a) Failure of roof bolted roadway and (b) resupported by steel arches



roadheader tends to slip and sink in the softened

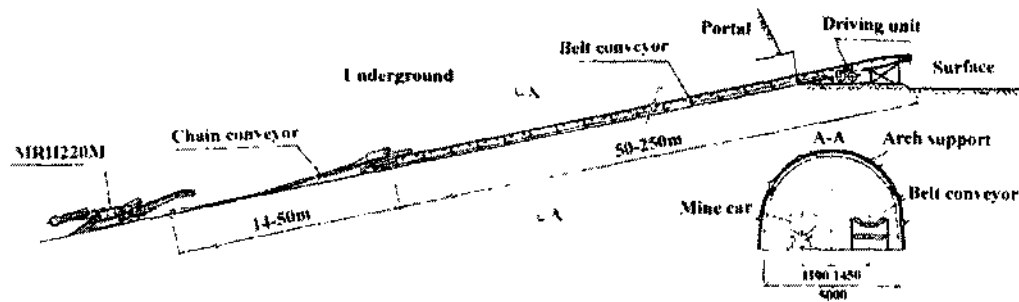


Figure 4 Drivage and transport system of Incline I at Ombilin'

floor. In relation to the poor roof, roof falls at a distance of about 121 m from the portal were apparent, and it was exaggerated at 10 m from this point when the C coal seam intersected the incline, in fact, the water trapped above the seam came out through cleats. Immediate measures were taken by reinforcing the roof by means of a double support system, including roof bolts, steel arches and cribbing. It took a couple of months to go through the fall area. During that period, heading had to be stopped. The reasons for this situation may be summarized as follows:

- 1) It is not possible to effectively predict the type and behavior of rock materials ahead.
- 2) Drainage system is not properly constructed.
- 3) Standard operating procedures are not properly practiced.

The development of Incline 2 has also not been progressing well mainly due to the drilling and blasting method. The introduction of the medium-duty roadheader Dosco-I contributes much toward satisfactory development of the operation.

## 6 RECOMMENDATIONS

According to the results of the strength tests and slaking tests, it is very important to keep the surrounding rocks dry or to reduce the water content in order to keep or increase the mechanical properties of the rocks and the rock masses. Therefore, it is important to get accurate information of the groundwater conditions at the planning stage. Advanced drilling at the heading face is quite useful for checking the groundwater and geological conditions.

Drainage is considered to be the most economical and simplest method to ensure a stable tunnel and

safe working conditions.

In order to achieve a good driving performance and good ground control of Inclines 1 and 2, the following measures should be done:

- 1) Surface geological mapping, including geological structure mapping.
- 2) Scan line survey in Inclines 1 and 2.
- 3) Progressive horizontal drilling within the inclines.
- 4) Getting rock samples around the opening for geotechnical laboratory tests.
- 5) Re-analyze the roof support requirement.
- 6) In situ stress measurements.
- 7) Establishment of a drainage system.

## 7 CONCLUSIONS

Detailed geological information is necessary in the drivage of the new inclines, Inclines 1 and 2 at Ombilin III in order to obtain good performance and ground control.

Geological disturbances such as the presence of discontinuities, faulted zones and the presence of groundwater cause problems during drivage.

Stress conditions also affect the stability of the incline and safe drivage.

Problems associated with drivage can be reduced through detailed geological and geotechnical investigations, forward planning, proper selection of measures and equipment and strict supervision.

The results obtained from this study could also be useful for controlling the stability of the incline portal and the inclines of the open pit mines because the strata tend to deteriorate when it rains.

## ACKNOWLEDGEMENTS

The authors are grateful to the managers, engineers and miners of Ombilin Coal Mine for their assistance in this study. Many thanks also go to JCOAL for giving us some important information.

This joint research work was funded by the Kyushu University Interdisciplinary Programs in Education and Projects in Research Development.

All the opinions stated in this paper are those of the authors themselves and are not necessarily those of JCOAL and the coal mine.

## REFERENCES

- Anwar. H.Z., Shimada. H., Ichinose. M and Matsui. K. 1998. Fundamental studies of the improvement of coal mine shales behavior. *Proc. of Regional Symposium in Sedimentary Rock Engineering*. Taipei, Taiwan. R O C pp.45-50.
- Anwar. H.Z., Shimada. H., Ichinose. M and Matsui. K. 1999a. Roof bolting application in longwall mining in Indonesia and Japan. *Proc. of 10<sup>th</sup> Int. Conference on Ground Control in Mining*. Morgantown, WV. USA. pp.256-262.
- Anwar. H.Z., Shimada. H., Ichinose. M and Matsui. K. 1999b. Slake-durability behavior of coal mine shales. *Proc. of '99 Int. Symposium on Mining Science and Technology*. Beijing, China, pp.343-346.
- Koesumadinata. R.P., Koesumadinata. R.P., and Matasak, T. 1991. Stratigraphy and sedimentation Ombilin basin, Central Sumatra (West Sumatra Province; Presented at the 10<sup>th</sup> Annual Convention of the Indonesian Petroleum Association. Jakarta. Department of Geology, Institute Technology Bandung.
- Kramadibrata. S., Novi. P. and Rivai. A. 1999. Determination of long term strength of silicified coal pillars by means of multistage creep test. *Proc. '99 Japan-Korea joint Symposium on Rock Engineering*. Fukuoka, Japan, pp. 371 - 380.
- Kramadibrata. S. and Matsui, K. 2000. Rock engineering problems in Indonesian mining industries. *Special lecture at National Institute for Resources and Environment*. Tsukuba. pp. 20.
- Matsui. K., Shimada. H., Ichinose. M. and Anwar. H.Z. 1999. Reinforcement of slaking-prone mine tunnel floor by grouting. *Proc. Mine Planning and Equipment Selection 1999 & Mine Environmental and Economical Issues 1999*. Dnipropetrovsk, Ukraine, pp.253-260.
- Matsui. K., Shimada. H., Ichinose. M., Kramadibrata, S., Anwar. H.Z., Furukawa. H. 2000. Drive of a new incline with roadheader at Ombilin Coal Mine. Indonesia. *Proceedings of the 10<sup>th</sup> International Symposium Mine Planning and Equipment Selection*. Athens, Greece : 83-88.
- Rai. M.A. 1999. On the assessment of tunnels stability and role of field measurements in Ombilin underground coal mines. *Proc. '99 Japan-Korea Joint Symposium on Rock Engineering*. Fukuoka, Japan, pp. 101-111.
- SCT (Strata Control Technology Pty. Ltd.) 1994. *Ombilin mines - Initial Investigation. Report No. OMB 0236/2*.
- Shimada. H., Matsui. K. and Anwar. H.Z. 1998. Control of hard-to-collapse massive roofs in longwall faces using a hydraulic fracturing technique. *Proc. 10<sup>th</sup> Int. Conference on Ground Control in Mining*. Morgantown, USA. pp.79-87.

## Slope Stability at Gol-E-Gohar Iron Mine

A. Bagherian & K. Shahrari

Department of Mining Engineering, Sluihitl Bahontir University, Kerimin, Iran

**ABSTRACT:** The progress of mining operations to deeper zones usually causes some changes in states of stresses. These changes have resulted some failures and instability problems in different parts of Gol-E-Gohar iron open pit mine. It seems that main parameters which effect the failure and instability of the mine slopes are high pressure of groundwater and system of discontinuities (faults, joins, and bedding planes), which intersect the pit walls. To overcome these problems, numerical analysis was carried out using a Fast Lagrangian Analysis of Continua (FLAC) software. To prepare the input parameters for modeling, field studies (include discontinuities mapping, point load index test, and Schmidt hammer test) and laboratory tests (to determine compressive, shear strengths, and elastic constants) were carried out. Then discontinuities orientation and laboratory tests data analysed to determine major structures, and shear strength parameters. Following pit walls modeling and safety factors have been determined. The results of analysis were in good agreement with the actual observations in the mine, and with analysis that carried out using other methods.

### 1 INTRODUCTION

The Gol-E-Gohar (GEG) Iron mine is located in 60 km southwest of Sirjan, in Kerman province of the Islamic Republic of Iran. The mine lies at a point approximately equidistant from the cities of Bandar Abbas, Shiraz and Kerman, each being approximately 280 km away. The Mine elevation is approximately 1750 meters above the sea level in an area of planar desert topography.

#### 1.1 History

Iron ore extraction in GEG goes back to at least 900 years ago, some historians believe that mining activity was carried on from 2500 years ago, the time of the great Persian Empire at Perspolis. There was remnant of a large underground excavation and a small open pit in the central part of the mine (Figure 1); it is estimated from these old mining areas about 350,000 tones of ore had been extracted during that period. Most of these old mining areas have been destroyed by recent mining activities.

#### 1.2 Exploration

In 1969 the Iran Barite Co. began exploration work at the site. Following the government policy of the day, responsibility of exploration was then delegated to the National Iranian Steel Industries Co. (NISIC),

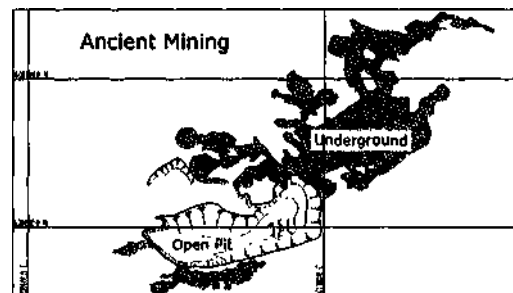


Figure 1. Ancient mining on GEG iron mine (KMC. 2001 )

a government corporation. After revolution its name was changed to National Iranian Steel Company (NISICO). NISICO in turn entered into a joint venture for development with Granges International Mining of Sweden (GIM). NISICO and GIM continued the various step of exploration and engineering planning, leading to development of an ore body, based on aerial and ground geophysical survey on an area of 75 km<sup>2</sup> at GEG in 1974. Following that, exploratory drilling began on six separate anomalies in the district in 1975 with a result of finding 6 anomalies (Figure 2), for estimating of ore quality and its reserves. Based on geophysical modeling, the total reserve in all anomalous zones was estimated about 1100 million tones (Table 1).

The detailed exploration of area I and 2 is finished and since 1994 the mine (Area I) is being extracted.

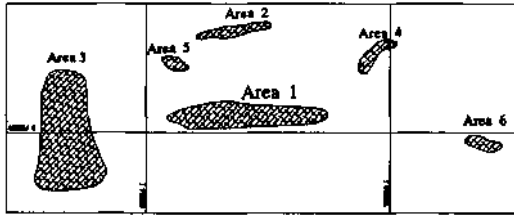


Figure 2 Anomalies of GEG non ore complex

Semi detailed exploration of Area3, the largest iron ore anomaly at GEG, has been finished and the detailed exploration program for this anomaly is being prepared. Due to the small size and high depth of the other anomalies, and more exploration on these deposits has not been planned yet.

## 2 GEOLOGY

The GEG complex (Area 1) is situated on the north-east margin of the Sanandaj-Sirjan tectonic-metamorphic belt, more precisely locally, the area is located in the marginal depression zone known as the Salt Lake of Kheirabad. The lithostratigraphy of the exposed rock units in the area comprises Paleozoic metamorphic rocks, Mesozoic and Cenozoic sedimentary rocks and Quaternary alluvial materials. The Paleozoic rocks form the basement of complex.

The ore body is generally lenticular form, greatly elongated in the east west direction, roughly parallel to the strike of the Sanandaj-Sirjan tectonic-metamorphic belt. The overall length of the ore body is 2600 m and the width at the widest section is 400 m (Figure 3).

### 2.1 Genesis of ore body and ore classification

There are a number of alternatives and conflicting concepts on the genesis of the ore body, the first of these set out by Ljung (1976), who proposed a meta-sedimentary origin, the second is that of Muecke and Golestaneh (1982-1991) who assumed a magmatic iron type genetic model, Hallaji (1992) has yielded a number of lines of evidence suggesting a metasomatic origin for deposits while Khalili (1993)

has suggested a volcano sedimentary origin for GEG iron ore.

Iron ores at GEG are classified not on lithology but exclusively on their chemical characteristics in three types, Top Magnetite, oxidized ore and bottom Magnetite:

Top Magnetite: Magnetite ore with low sulfur and phosphor.

Oxidized ore: Magnetite and Hematite with low sulfur and a little high phosphor.

Bottom Magnetite: Magnetite ore with high sulfur and low phosphor.

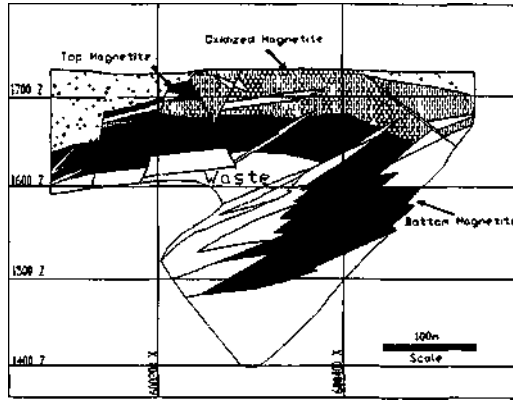


Figure 3. Geological section of GEG non mine (KMC, 2001)

### 2.2 Structural geology

The structural mapping includes all the structural features that its persistence is such that they affect at least one bench and/or those structures associated with bench-scale instabilities. The main joint systems determined using a detailed face mapping of exposure in the pit area has been summarized in Table 2, and shown in Figure 4.

It seems that faults existing in the pit area have the most effect on pit walls stability. The main orientations of faults are 203773°, 108772°, and 22762°.

Stereographic projection of the main fault systems is shown in Figure 5.

Table 1. Suinmaiv Properties of GEG Iron Ore Complex Anomalies

Ore body	Exploration Dullung (m)	Reserves (in t)		Dimension (m)		O B Thickness (in)		Grades (%)		
		Proved	Probable	Length	Width	Min	Max	Ft	P	S
Area 1	26300	265	-	2600	400	0	310	55.5	0.152	1.521
Area 2	7470	52	-	1100	200	41	199	53.1	0.146	2.308
Area 3	32340	608	-	2200	2200	84	545	53.6	0.121	1.784
Area 4	580	-	12	300	100	95	N/A	53.1	0.150	2.030
Area 5	260	-	4.5	100	100	80	N/A			
Area 6	610	-	150	1100	2400	568	N/A	50	0.090	0.084

Based on geophysical study

Table 2 Characteristics of the joint sets at the GEG mini-

Wall	Joint Sets (Dip / Dip Direction )				
	S-1	S-2	S-3	S-4	S-5
Noith	60'±87 % ± 1S	54'±9/201 ± 12			
South	82 ± 8 / 120 ± 5	85 ± 5 / 100 ± 6	82 ± 4 / 65 ± 5	80 ± 8 / 10 ± 7	56 ± 6 / 202 ± 8
East	56 ± 8 / 202 ± 10	18 ± 8 / 24 ± 9			
West	15 ± 6 / 11 ± 7	60 ± 10 / 1S ± 10			

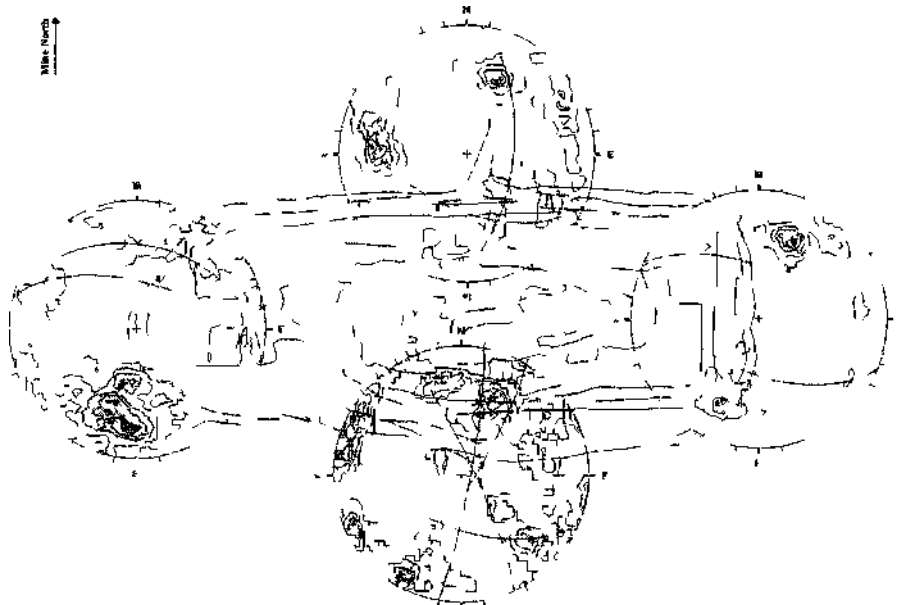


Figure 4 Stereographic projection of the main joint systems on different walls at GEG mine (Bagheian 2001)

### 2.3 Hydrology

Study of the response of groundwater flow to mining activity has begun by characterizing the porosity and permeability of the rock sequences. Rock sequences including alluvial material, paleogravels, and weathered locks. Because of the high permeability of the rock and/or intensity of discontinuities within this sequence it is considered that the surface rock mass would likely drain on pit.

Groundwater table in GEG pit area is estimated at a depth of 40 m below the ground surface. Excavation of the pit has created a drawdown of the groundwater level. It can be observed that the majority of water inflow to the pit is through the overburden excavation, and faulted zone in the body.

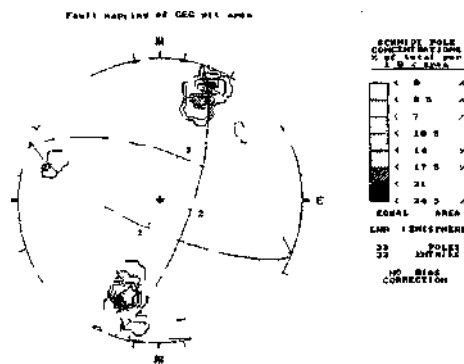


Figure 5 Fault sets in GEG pit area

## 1 MINE PLANNING

A number of geotechnical-based recommendations have been given by different consulting groups and agreed the GEG mine authorities which are summarized as below:

- The best bench height is 15 m
- The pit is approximately 1600 m long and 750 m wide in final position
- The pit overall slope angles are 45 deg in rock and waste rock and 38 deg in soil overburden

- Roads are 20 to 25 m wide with a grade of 8%.
- A 10 m wide safety bench is left at every two bench (30 m height) in the final layout.
- The overall slope height of pit is 220 m.
- The bench face angle is 60 deg.

#### 4 GEOTECHNICAL ASSESSMENT

The geotechnical evaluation of rock-mass has been done by rock-mass classification, rock materials strength obtained from the laboratory tests, and field observations of weathering. The input parameters for numerical models were obtained from characteristics obtained from above mentioned sources.

##### 4.1 Rock-mass classification

A detailed and comprehensive study was taken to determine rock-mass and structural properties for GEG iron ores and enclosed rocks.

By using the parameters collected from the structural mapping and those obtained in the laboratory and field tests, rock-mass rating (RMR) was calculated.

The average values of the geotechnical parameters are summarized in Table 3.

##### 4.2 Strength assessment

The material properties used in the analyses were derived from laboratory, field tests, and field rock-mass characterization.

- Intact rock strengths were derived from the laboratory and in pit point load tests.
- Values for the cohesion and friction angles were determined by triaxial testing in the laboratories.
- Joint strengths were determined from laboratory shear tests. Shear tests on natural joint surface, as well as on artificial saw cut surfaces, were evaluated.
- The GSI was used with the Hoek and Brown failure criteria-2002 edition (Hoek et al. 2002) to determine the instantaneous friction

angle and cohesive strength for given normal stress values.

Parameters such as  $m$  and  $s$  in the Hoek-Brown criterion were calculated assuming disturbed rock-mass condition (disturbance factor =1), since recent work has shown this category to be more appropriate for large-scale rock slopes (Sjoberg 1999). By using  $m$ ,  $s$ , GSI, and uniaxial compressive strength of intact rock ( $a_u$ ), the corresponding Hoek-Brown failure envelope was calculated assuming disturbed rock-mass conditions. The curved Hoek-Brown failure envelope was then translated to a linear Mohr-Coulomb envelope, to be used as input into the numerical models. Cohesion and friction angle for the Mohr-Coulomb model were determined using linear regression over a representative stress range of the Hoek-Brown envelope. The resulting strength values ( $c$  and  $\phi$ ) are summarized in Table 4, along with calculated compressive ( $\sigma_{tm}$ ) and tensile ( $\sigma_{tm}$ ) strength, and Young's modulus ( $E_m$ ) of the rock mass. Since no stress measurements have been carried out at GEG, the virgin stress state can only be estimated. For most models, a horizontal-to-vertical stress ratio ( $k$ ) of 1.5 was suggested (Sjoberg et al. 2001). A more detailed study on the influence of the virgin stress is outside the scope of this work.

#### 5 STABILITY EVALUATION

##### 5.1 Slope mass rating for GEG mine

For evaluating the stability of rock slopes, a classification system called Slope Mass Rating (SMR) system (Romana 1985) has been used by adding adjustment factors of joint-slope relationship and method of excavation to RMR,

$$SMR = RMR_{h,wt} - (F_1, F_2, F_3) + F_4 \quad (1)$$

Where  $F_1$ ,  $F_2$ , and  $F_3$  are adjustment factors for joint orientation with respect to slope orientation and  $F_4$  is the correction factor for method of excavation (Singh & Goel 1999).

The SMR values for pit walls, rock mass description, and stability classes are shown in Table 5. Final pit layout will locate at waste rocks.

Table 1 Average values of geotechnical parameters for intact materials

Rock Type	Density (Kil/m <sup>3</sup> )	UCS (MPa)	Poisson's Ratio	Young's Modulus (GPa)	ROD	RMR
Ore	4200-4400	85	0.20	23	80	65
waste	2600-2700	65	0.20	23	50	56

Notes:

UCS: Uniaxial Compressive Strength

RQD: Rock-Quality Designation

Table 4 Estimated rock-mass strength of GEG assuming disturbed rock mass with a stress range of  $\sigma_1 = 0-6$  MPa (Bagherian 2001)

Walk	Ore				Waste			
	North	South	East	West	North	South	East	West
$\sigma_1$	17	17	17	17	27	27	27	27
$\sigma_{ci}$ (MPa)	85	85	85	85	65	65	65	65
GSI	52	56	58	57	41	47	49	48
$\mu$	0.55	0.714	0.846	0.788	0.460	0.611	0.707	0.658
$\nu$	0.0001	0.0007	0.0009	0.0008	0.0001	0.0001	0.0002	0.0002
$\alpha$	0.505	0.504	0.501	0.504	0.509	0.507	0.506	0.507
$\beta$ (degree)	11.6	14	15.1	14.7	27.8	10.1	11.9	10.9
C (MPa)	1.25	1.40	1.48	1.44	1.02	1.15	1.21	1.18
$C_{\text{res}}$ (MPa)	1.50	2.11	2.51	2.10	0.515	0.717	0.880	0.806
$\sigma_{\text{res}}$ (MPa)	0.052	0.076	0.092	0.081	0.011	0.015	0.019	0.017
$E_{\text{res}}$ (GPa)	5.171	6.512	7.106	6.897	2.694	1.192	1.806	1.591

Table 5 SMR values and stability classes of GEG pits wall (Bagheuan 2001)

Walls	Ore				Waste			
	North	South	East	West	North	South	East	West
SMR Value	57	61	61	62	48	52	54	51
Rock Mass Description	Noimal	Good	Good	Good	Noi mal	Noi mal	Noi mal	Noi mal
Stability	Partially Stable	Stable	Stable	Stable	Partially Stable	Partially Stable	Partially Stable	Partially Stable
Failure	PI & MW	Some BF	Some BF	Some BF	PI AcMW	PJ & MW	PJ & MW	PI & MW
Probability of Failure	0.25	0.2	0.2	0.2	0.15	0.1	0.1	0.1
Notes	PI Planai along some Joint		MW Many Wedges		BF Block Failure			

### 5.2 Cut rem slope design

Initial slope design at GEG is done based on bore hole data. It seems that because of the lacking of data on that time, slope angles of pit considered very cautiously. Table 6 shows current overall slope angle of GEG pit in different soil, and rock walls. Current pit geometry shown on Figure 6.

Table 6 Current overall slope angles of pits walls

walls	Rock	Soil
North	47	32
South		41
East	48	39

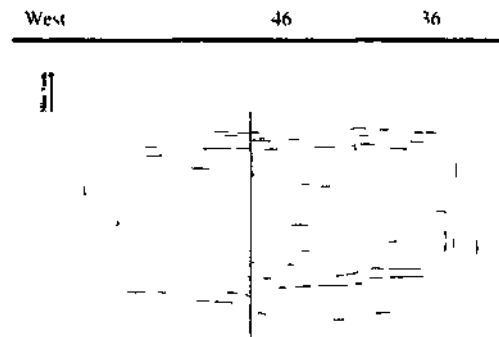


Figure 6 Horizontal map showing GEG cement pit geometry

### 5.3 Numerical modeling

Numerical modeling of the GEG pit slopes has been carried out on a number of occasions to develop a more comprehensive understanding of the slope-deformation behavior and to assess the potential for deep-seated slope-deformation mechanisms to adversely affect the current mine design.

In this paper, the south wall is analyzed, with a two-dimensional finite difference program Fast Lagrangian Analysis of Continua (FLAC) (Itasca 2001). A Mohr-Coulomb constitutive model was assigned as described to all zones with the following properties (Table 7)

Table 7 Input parameters for numerical modeling

Materials	Soil	Ore	Waste
Density (Kg/in <sup>3</sup> )	2.1M	4100	2650
Poisson's Ratio	0.3	0.3	0.3
$\phi$ (degree)	25	34	30.3
C (MPa)	0.0295	1.4	1.15
E <sub>m</sub> (GPa)	0.015	6.51	3.39

Figure 7 shows the FLAC model for the south wall

### 5.4 Modeling results

The south wall was analyzed along section 1 at current and final pit layout. The factor of safety was obtained through successive FLAC model evaluations in which the rock-mass strength was decreased incrementally until overall slope failure occurred. The ratio of the estimated strength to the failure strength defines the factor of safety in this

context. By using strength parameters, a factor of safety 1.45 predicted for south wall.

Based on the FLAC model evaluations (Figure 8 to 10), it is reasonable to expect the future south wall to remain stable.

Modeling for north, east, and west walls, yielded a factor of safety 1.40, 1.5, and 1.5 respectively (Bagherian 2003).

## 6 CONCLUSIONS

The following conclusions can be drawn, based on the stability analyses:

- The main parameters influencing the failure and instability of the mine walls are high pressure of groundwater and system of discontinuities, which intersect the pit walls.
- Based on the FLAC model evaluations, and results, it is evident that pit walls remain stable.
- FLAC model results shows that, with assuming a factor of safety of at least 1.3 against the circular-type failure the overall slope angles of pit walls could be increased.
- Because of economical importance of overall slope angles increasing, a more detailed program suggested to determine increased slope angles.
- Future analysis must consider discontinuities, using a distinct element code, like UDEC

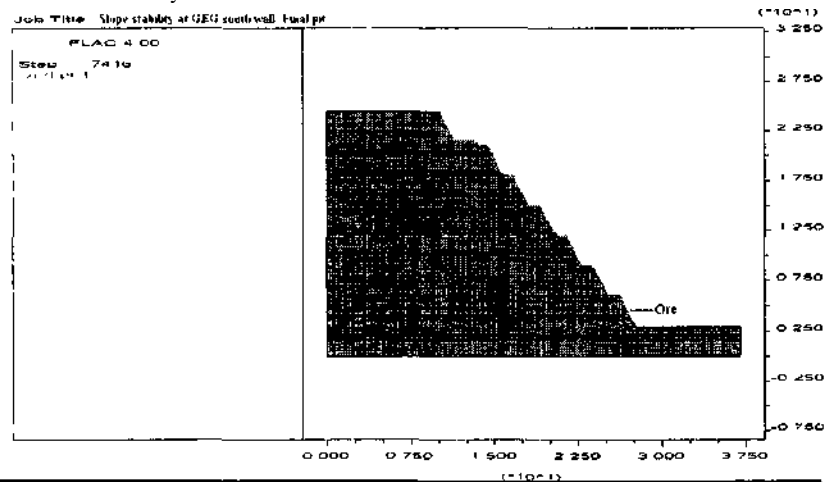


Figure 7 FLAC models used for analysis of south wall stability



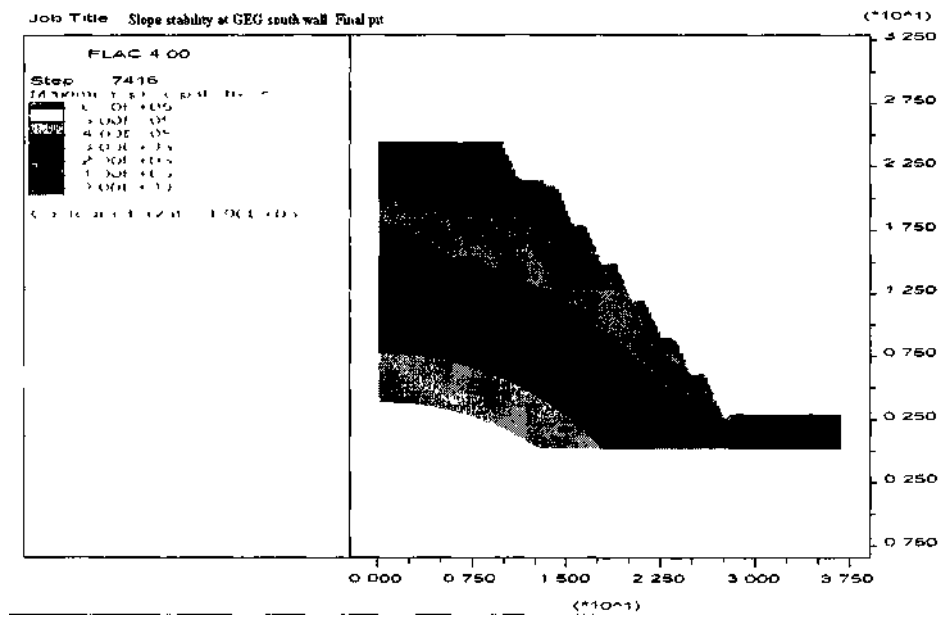


Figure 8 Result of FLAC analysis showing maximum principal stress contours for GEG south wall

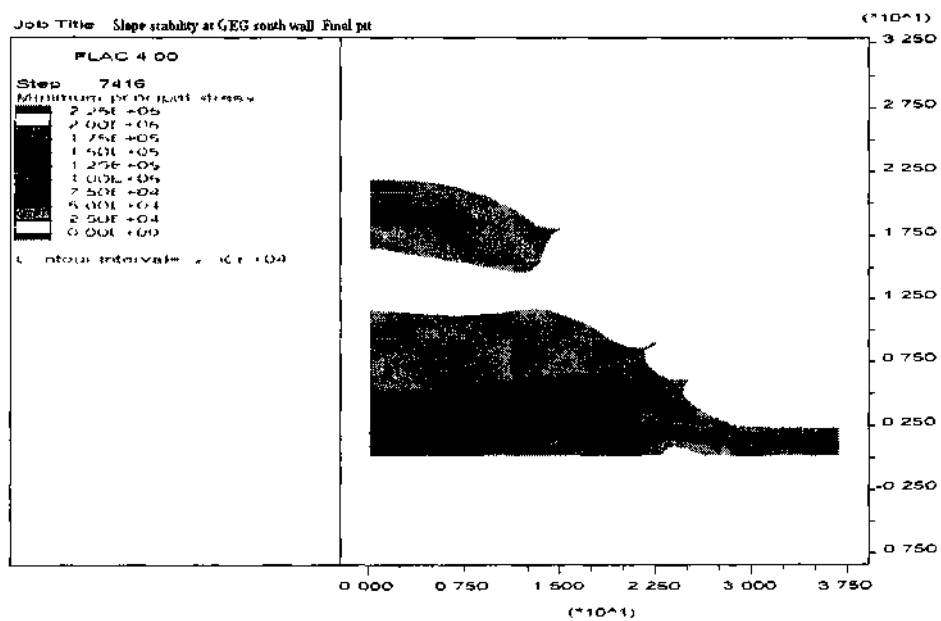


Figure 9 Result of FLAC analysis showing minimum principal stress contours for GEG south wall

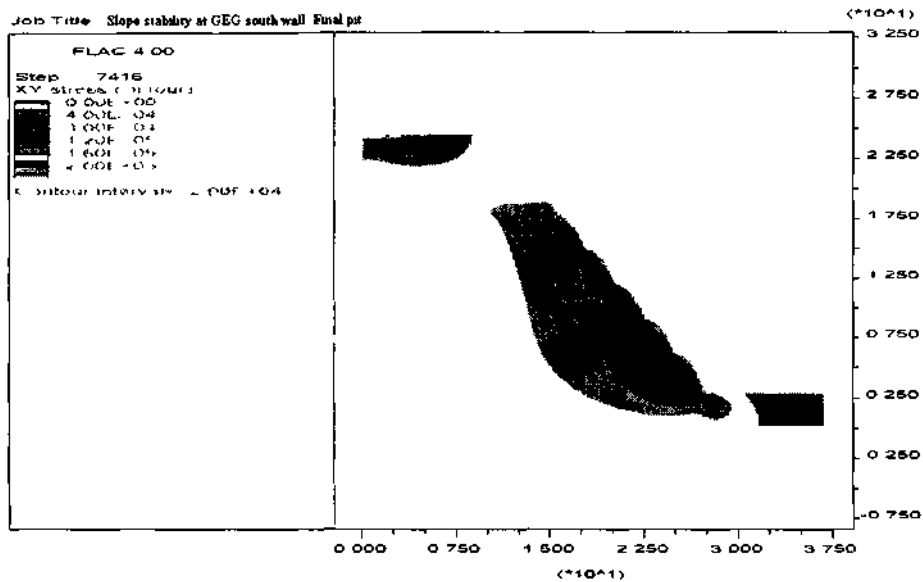


Figure 10 Result of FLAC analysis showing shear stress contours on GEG south wall

#### ACKNOWLEDGEMENT

The assistance and support by the mine staff of GEG is gratefully acknowledged. The authors also thank the engineers and geologists of GEG mine. Special thanks go to the Dr. Raesi and Azizmohamadi for permission to use their FLAC software.

#### REFERENCES

- Baghevan A. 2001. Slope stability analysis at Gol-E-Gohai iron ore mine. *Mushti of Science thesis in Mining Engineering*. Shahid Bahonar University, Kerman, Iran.
- Hoek E. 2002. Hoek-Brown failure criterion - 2002 edition. Rocscience Inc, Toronto, Canada.
- Hustulid W et al. 2001. Slope stability in Surface Mining. Society for Mining Metallurgy and Exploration Inc (SME) USA.
- ITASCA Consulting Group Inc. 2001. FLAC version 11 Manual.
- Kliche C. 1999. Rock slope stability, society for Mining Metallurgy and Exploration Inc (SME) USA.
- KMC Consulting Group Inc. 2001. An introduction to Gol-E-Gohai iron complexes.
- Romana M. 1987. New adjustment ratings for application of Bieniawski classification to slopes. *International Symposium on the Role of Rock Mechanics*, Zwickau, p. 49-51.
- Singh B. & Goel R. K. 1999. Rock mass classification: a practical approach in civil engineering. Elsevier Science Ltd, pp. 171-181.
- Sjoberg J. 1999. Analysis of large scale rock slopes. Doctoral thesis, 1999-01. Division of Rock Mechanics, LULEA University of Technology, Sweden.
- Sjoberg J et al. 2001. Slope Stability at Altuk. *4th International Symposium on Slope Stability in Surface Mining*, Denver, February 24-27.

## Rock Mass Classification Using a Computer Program-Classmass

A. H. Deliormanli & T. Onargan

Dokuz Eylul University, Mining Engineering Dept., Bornova, İzmir, Turkey

**ABSTRACT:** In this study, a computer programme coded as a ClassMass which is developed for determination of the geological strength index (GSI), rock quality index (Q) and mining rock mass rating (MRMR) is introduced. It examines the structure of the individual main and multi-level knowledge base created for each major and minor parameter for rock mass classification. ClassMass is primarily intended to work as an assistant to an engineer in planning stages in order to enable user to design underground constructions quickly.

### 1 INTRODUCTION

In rock engineering, the first major classification system was proposed over 60 years ago for tunneling with steel supports. Rock mass classifications today form an integral part of the most predominant design approach. Indeed, on many underground construction and mining projects, rock mass classifications have provided the only systematic design aid in an otherwise haphazard procedure (Bieniawski Z. T., 1989).

In this study, within the Beypazarı Trona Field-Main Drift Project, rock mass classification software which has been developed for the support design by the Dept. of Mining Engineering, Dokuz Eylül University is introduced. The system has been designed using a Visual Basic shell on a PC platform which runs under MS-Windows operation system (version 95, 98, and 2000) with min. 16 Mb RAM of memory and a 40 MB free disk space. ClassMass utilizes a multi-level knowledge base structure with a number of sub-knowledge bases; which are controlled by a main knowledge base that manages the whole system.

### 2 THE GENERAL STRUCTURE OF CLASSMASS

ClassMass utilizes a multi-level knowledge base structure with a number of sub-knowledge bases; these are controlled by a main knowledge base, which manages the whole system. The general structure of the ClassMass and input-output structure of the system are shown in Figure 1.

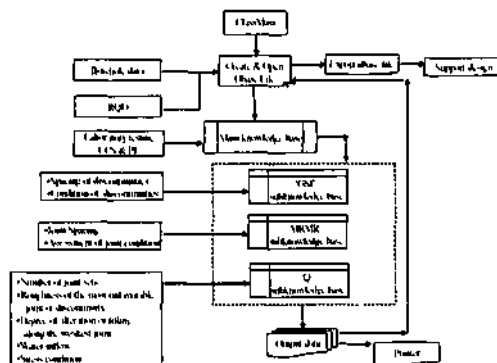


Figure 1. The general structure of the ClassMass and input-output structure of the system

### 3 THEORETICAL BACKGROUND OF THE PROGRAM

ClassMass offers GSI results with Q and MRMR. The user must provide geotechnical parameters and laboratory results to ClassMass. Therefore, engineers should investigate these factors in detail to obtain a good result from the system.

#### 3.1 Q Classification System sub knowledgebase

The Q-system of rock mass classification was developed in Norway in 1974 by Barton, Lien and Lunde, all of the Norwegian Geotechnical Institute. Its development represented a major contribution to the subject of rock mass classification for a number of

reasons the system was proposed on the basis of an analysis of over 200 tunnel case histories from Scandinavia, it is a quantitative classification (Bimawski Z T, 1989)

The Q system is based on a numerical assessment of the rock mass quality using six different parameters,

- Rock quality designation (RQD) %
- Number of joint sets
- Roughness of the most unfavorable joint or discontinuity
- Degree of alteration or filling along the weakest joint
- Water inflow
- Stress condition

The first two parameters represent the overall structure of the rock mass, and their quotient is relative measure the block size. The quotient of the third and fourth parameters is said to be an indicator of the inter block shear strength. The fifth parameter is a measure of water pressure, while the sixth parameter is a measure of a) loosening load in the case of shear zones and clay bearing rock, b) rock stress in competent rock, c) squeezing and swelling loads in plastic incompetent rock. The quotient of the fifth and sixth parameters describes the active stress. Barton et al (1974) consider the parameters  $J_n$ ,  $J_r$ , and  $J_a$ , as playing a more important role than joint orientation and if joint orientation had been included, the classification would have been less general. However, joint orientation is implicit in parameters  $J_r$  and  $J_a$ , because they apply to the most unfavorable joints (Milne et al 1998). Rates of parameters are given in Table 1.

These six parameters are grouped into three quotients to give the overall rock mass quality Q as follows

$$Q = \frac{RQD}{J_n} \cdot \frac{J_r}{J_a} \cdot \frac{1}{SRF}$$

(D)

where

RQD(%) = rock quality designation, (1 Parameter)

$J_n$  = joint set number,

$J_r$  = joint roughness number,

$J_a$  = joint alteration number,

$J_w$  = stress reduction factor,

SRF = stress condition.

The rock quality can range from Q=0.001 to Q=1000 on a logarithmic rock mass quality in Figure 2. System and it is an engineering system facilitating the design of tunnel supports (Barton N 1988)

Table 1 Rating of Q system parameters

Parameters	Rating	
	Min	Max.
2 joint set number	0.5	20
joint roughness number	1	4
4 joint alteration number	0.25	20
5 Stress reduction factor	(HVS)	1
6 Stress condition	0.5	400

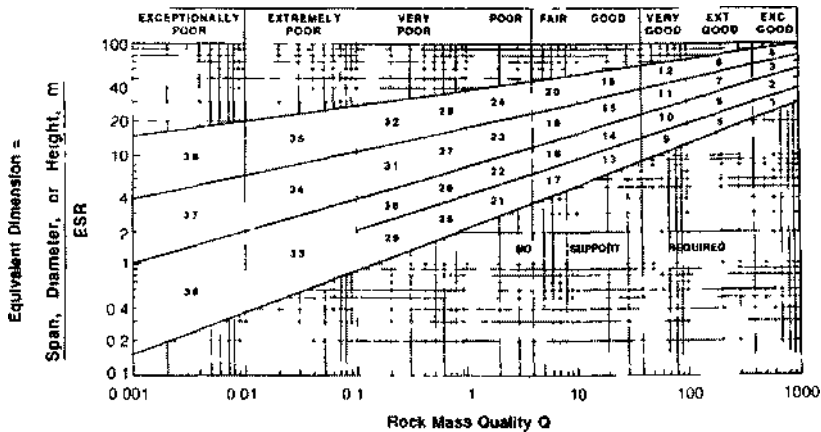


Figure 2 Q system equivalent dimension versus rock mass quality (After Barton et al, 1974)

3.2 MRMR Classification System Sub knowledge base

The classification system known as the mining rock mass rating (MRMR) system was introduced in 1974 as development of the CSIR geomechanical classification system

The development is based on the concept of in situ and adjusted ratings, the parameters and values being related to complex mining situations. Since that time, there have been modifications and improvements and the system has been used successfully in mining projects in Canada, Chile, South Africa and USA (Laubscher 1990)

This system employs the following parameters,

- Uniaxial Compressive Strength (UCS)
- Rock quality designation (RQD) %
- Joint Spacing
- Assessment of joint condition
  - o Joint waviness
  - o Joint roughness
  - o Joint wall alteration
  - o Joint filling

The rates and meaning of the parameters are given in Table 2-3

Table 2 Parameters value of MRMR system

Parameters	Rating	
	Min	Max
UCS (MPa)	1	20
RQD (%)	0	100
Joint Spacing	0	20
Joint Condition	0	40

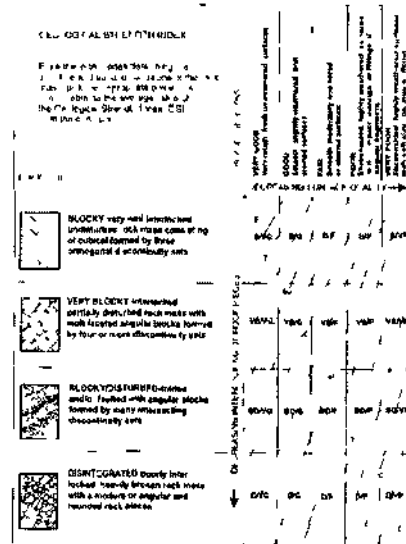
Table 1 Meaning of the ratings

Rating	Description
100-81	Very Good
80-61	Good
60-41	Fair
40-21	Poor
20-0	Very Poor

Table 4 Killing of GSI parameters (Aroglu E, Yüksel A 1999)

Figure 1 Characterization of rock masses on the basis of

Uniaxial Compressive Strength (UCS) (MPa)	100-80	60-40	25-10	1-5	1	1/2	1/3
RQD (%)	25	22	7	4	2	1	0
Joint Spacing (m)	10-100	25-40	10-25	2-50	<2		
Joint Condition	20	17	13	8	3		
Uniaxial Compressive Strength (UCS) (MPa)	5-10	1-3	0.3-1	0.1-0.3	0.05		
Joint Condition	20	25	20	10	5		
Uniaxial Compressive Strength (UCS) (MPa)	25	20	12	7	0		



in situ locking and surface condition of discontinuities GSI classification

3.3 GSI Sub knowledgebase

Determination of the strength of closely jointed rock masses is difficult since the size of representative specimens is too large for laboratory testing. This difficulty can be overcome by using the Hoek-Brown failure criterion. Since its introduction in 1980, the criterion has been refined and expanded over the years, particularly due to some limitations in its application to poor quality rock masses. In the latest version, the geological strength index (GSI) was introduced into the criterion by its originators. However, the GSI classification scheme, in its existing form, leads to rough estimates of the GSI values. Another particular issue is the use of undisturbed and disturbed rock mass categories for determining the parameters in the criterion, for which clear guidelines are lacking. Furthermore, the data supporting some of these revisions, particularly

the latest one, have not been published, making it difficult to judge their validity (Sönmez et al. 1999).

The following four parameters are used to classify a rock mass using the GSI (RMR<sub>76</sub>):

- Uniaxial Compressive Strength(UCS) or point-load index(PL) of rock
- Rock quality designation (RQD) %
- Spacing of discontinuities
- Condition of discontinuities

The GSI=RMR<sub>76</sub> classification is presented in Figure 3 (Sofianos et al. 2002). The rating of the parameters is given in Table 4.

If GSI is less than 18, the following equation is used

$$GSI = 9 \ln(Q') + 44 \quad (2)$$

$$Q' = \frac{RQD}{J_n} * \frac{J_r}{J_u} \quad (3)$$

#### 4 DESCRIPTION OF THE PROGRAM

Computer software known as ClassMass has been developed to help engineers in designing mining project. ClassMass describes the knowledge base structures. It describes the main components of the system and their operation. The initial system was purely interactive. A number of support features have been provided. These include a user interface, an explanation facility and a knowledge base editor. ClassMass's user interface contains two groups of features; menus and help screens or windows. ClassMass is menu driven; all the options available to user are presented in screen forms or windows for selection of using the keyboard cursor keys or a mouse. Help and explanation facilities are provided to the user throughout the consolation.

##### 4.1 Create or open data base file

It requires a database file to be created for the data entered into the programme and recorded at the end of the programme. The created dbase file is Microsoft Access based and it can easily be exported to the other database programs.

##### 4.2 Input data

The data is input into the main knowledge base and sub knowledge bases. Firstly, the code of the borehole, depth limits, formation and lithology are en-

tered and finally the RQD values regarding this lithology are input. All these data are saved under the main knowledge base and controlled. Then, data are input for the desired rock mass classifications. These data are also saved and controlled by the sub knowledge bases they belong to. The data input into the programme is given in the Figures 4, 5, 6.

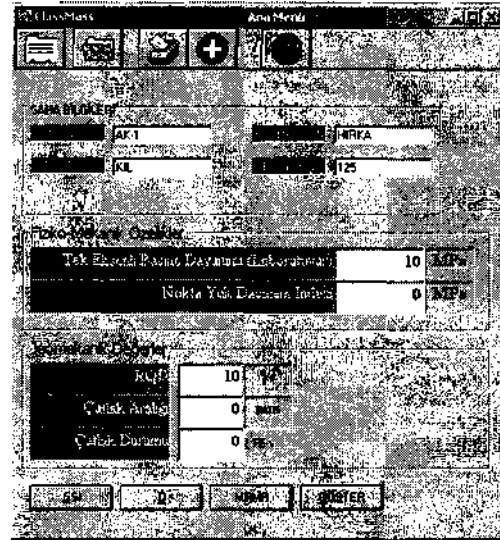


Figure 4. Input data of main knowledgebase and GSI sub knowledgebase.

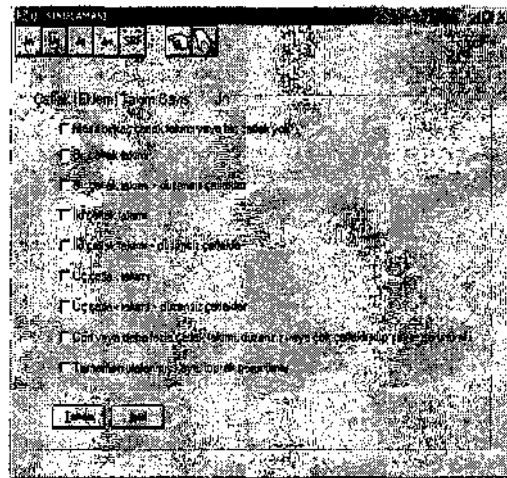


Figure 5. Input data of Q system sub knowledgebase.

KAYI	DATA	KURSU
PARCALANIR	Yuva lat vepa kuyak	0
DANANNE YIKIRIK	pe calar colikende tepik kuyak	0
ALTIYERISTON FOS	Parcalanir tepik de calanir kuyak	0
KAYI KAYI		

Figure 6 Input data of MRMR system sub knowledgebase

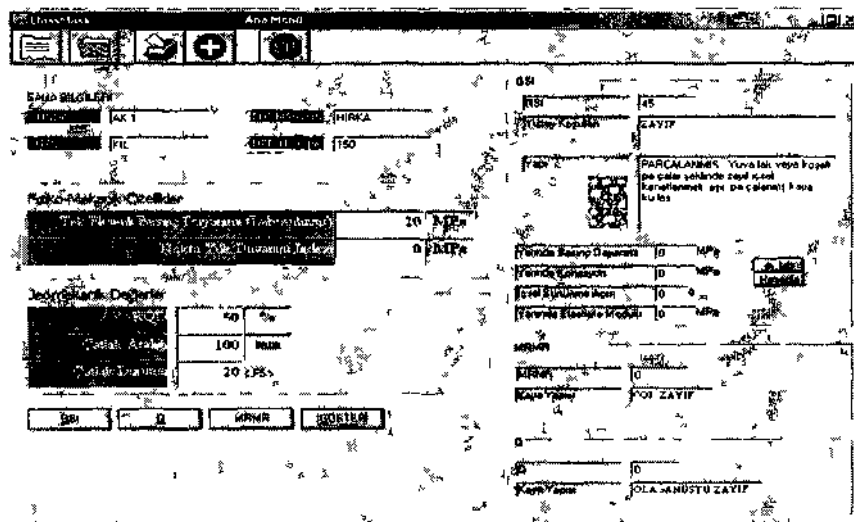


Figure 7 Display output of the ClassMass

#### 4.3 Output data

The program saves the rock mass classification values within the dbase file opened at the beginning phase of the program. These savings are presented to the user in 3 forms. The first of all is the sheet appealing screen print, the second is the one sent to the printer and the last one is the form of export file system converted into various formats in order to be used in other programs. The data output from the program is given in the Figure 7

#### 5 CONCLUSIONS

Rock mass classification is one of the only approaches to estimating large-scale rock mass properties. In

the mining industry, the GSI, Q and MRMR classification system from the basis of many empirical design methods, as well as the basis of failure criteria used in many numerical modeling programs.

In this study, a computer program, ClassMass developed and described by Dehoimanli and Onargan was employed. It examines the structure of the individual knowledge bases created (or each major and minor parameter for rock mass classification). ClassMass is ultimately developed to assist geotechnical engineers in designing underground openings more easily. The user must provide geomechanical parameters and laboratory results to ClassMass. Therefore, engineers should investigate these factors in detail to obtain a good result from the system. An example of input data is given in Table 5. These observations are tried to prove with the geotechnical data obtained from the boreholes.

Table 5 Typical input form used for rock mass classification

Depth (m)	Core Location			Joint Characteristics			Description	RMR	RQD %	Joint Frequency (Joints/m)					Spacing (cm)	Joint Roughness (JRC)	Joint Apertures (JPA)	Weathering	Water	Groundwater Conditions
	25	50	75	Fracture	Discontinuity	Day				1-5	10	15	20	25						
340 to 350.55	0.4			W			Greenish grey claystone	116	84.3	1.73					21			Wet	Flow	General
350.55 to 365.05	0.4			2-B-W	am	1-3	Light grey claystone	111	86.1	2.70				27	P-S-S	R	HW	Wet	Flow	General
365.05 to 380.55	0.4			1-W	Clay	am	Light grey claystone	121	105.7		12.0			7.7	P-S	1/2-S	R	HW	Wet	Flow
380.55 to 390.05	0.4			1-W	Clay	am	Light grey claystone	121	109.5		3.20			21.2	P-S-R	C	HW	Wet	Flow	General

RI MARKS	Discontinuity Roughness	Joint Alteration	Lithological Description
1	1.5-2.0 mm	1	Solid, fresh, unaltered
2	2.0-5.0 mm	2	Slightly altered
3	5.0-10.0 mm	3	Altered, siliceous
4	10.0-20.0 mm	4	Altered, siliceous, clayey
5	> 20.0 mm	5	Altered, siliceous, clayey, highly jointed
6	1.5-2.0 mm	6	Slightly altered, siliceous
7	2.0-5.0 mm	7	Altered, siliceous, clayey
8	5.0-10.0 mm	8	Altered, siliceous, clayey, highly jointed
9	10.0-20.0 mm	9	Altered, siliceous, clayey, highly jointed, highly fractured
10	> 20.0 mm	10	Altered, siliceous, clayey, highly jointed, highly fractured, highly jointed

REFERENCES

Anoglu T, Yüksel A 1999 *Timel ve yealtu mühendislik sapaktı nida çozümlü ptiski tme beton problemleri I* İstanbul TMMOB Maden Mühendisleri Odası

Ballou N 1988 Rock mass classification and tunnel reinforcement selection the Q-system *PIIK SvnpRock Claw Eni; Puup ASTM Special Tihmuil Pub* 984 pp 59-84

Bieniawski Z T 1989 *Etü;ueetm\; link maw ilawjiiatiiiis* Canada John Wiley&Sons

Laubschei D H 1990 A geomechanics classification system for the rating of rock mass in mine design *J S Ap lust Mm Metali \ol* 90 pp 27-271

Milne D, Hadjigeorgiou J, Pakalnis R 1998 Rock mass characterization for underground hard rock mines *Tünelimi; and Unde;ionnd Spate Tetlionnt;\ Vol M* pp 38V-191

Moon V, Russell G, Stewart M 2001 The value of rock mass classification system for weak rock masses a case example from Huntly New Zealand *Eng/meinn Getting Vol 61* pp 51-67

Soriano A I, Halakatevakis N 2002 Equivalent tunneling Mohi-Coulomb strength parameters for given Hoek-Brown ones *hit lain Of Hoik Meilumit\ aiul Milling Saence\ Vol V* pp H1-M7

Sonnitz H, Ulusay R 1999 Modifications to the geological index (GSI) and then applicability to stability of slopes *Join Of Raik Meilum\ and Minini; Sueiut\ Vol 16* pp 741-760



## Determination of the Optimum Cement Content for Paste Backfill Samples

E. Yılmaz, A. Kesimal, B. Erçikti & İ. Alp

Department of Mining Engineering, Karadeniz Technical University, Trabzon, Turkey

**ABSTRACT:** In this study, the effect of cement content between, 3 and 7 wt %, on the mechanical strength of the paste backfill was examined at different size of slump between 6" and 7". The paste backfill samples were prepared using the tailings sample A and B. They were subjected to the unconfined compressive strength test at predetermined curing periods. The results showed that the optimum cement content of the paste backfill sample A was found to be 7 wt% at a 7.0" slump value resulting in a compressive strength of 1.387 MPa at 28 days curing period. With 7 wt% binder, the highest compressive strength of 0.8J2 MPa at a 6.0" slump value was determined for the paste backfill mixture prepared for the tailings sample B for 28 days curing period. The differences observed in the compressive strengths and slump consistencies for paste backfill samples A and B could be attributed both tailings samples to have different characteristics such as particle size, chemical and mineralogical composition.

### I INTRODUCTION

The process of mining involves the removal and recovery of economically valuable minerals from the earth's crust. The resulting voids are usually filled with waste materials by a process known as backfilling. Backfilling has long been an integral part of underground mining. The underground placement of backfill falls into two categories-backfill required for ground support and underground disposal of tailings (Thomas et al. 1979, Edwards 1992). Waste materials used as a backfill material include waste development rock, deslimed and whole mill tailings, quarried and crushed aggregate, and metallurgical process tailings (like slag) (Grice 1998, Yılmaz et al. 2003).

The development and utilization of paste backfill technology has been evolving over the last two decades around the world and especially in Canada. Due to the low operating costs involved and high strength acquisition of paste backfill compared with the other backfilling methods (rock fill and hydraulic fill), the use of paste backfill has steadily increased in recent years (Landriault et al. 1993, Landriault 1995).

The disposal of mine tailings underground reduces the environmental impact and provides a material that can be used to improve both ground conditions and the economics of mining. A significant environmental benefit of the paste backfill, especially when tailings are acid generating, is the possibility of placing a large amount of

tailings up to 100% to underground. This significantly reduces the oxidation risk and other environmental effects (Weaver et al. 1970, Brackebusch 1994, Strömberg 1997, Benzaazoua et al. 1999 and 2002).

Various binder materials are used to increase the support potential and stability of paste backfill. Portland cements are often used alone or with the addition of natural or artificial additives having specific hydraulic properties in cemented paste backfill. The additives are used to increase the durability and the strength of the mixture, and appreciably reduce the binder costs (Viles et al. 1989, Naylor et al. 1997, Hassani et al. 2001, Ouellet and Hassani 2002).

The characteristics of mechanical and rheological of paste backfill are connected to the physical, chemical, and mineralogical characterization of tailings, binder type and ratio used (Lamos and Clark 1989, Ouellet and Hassani 2002, Chew 1999).

In this study, at 28-day curing period, the effect of cement content between 3 and 7 wt% on the mechanical strength of the paste backfill was examined at different size of slump between 6" and 7". The paste backfill samples were prepared using the tailings sample A and B.

Tailings sample A consists of pyrite and chalcopyrite, and less than 10% sphalerite. Tailings sample B consists of pyrite, chalcopyrite and sphalerite.

## 2 MATERIAL

In order to better understand the effect of the material composition of mill tailings on the mechanical strength of paste backfill, a series of unconfined compressive strength (UCS) tests was conducted in detail. For this reason, about 800 kg representative samples of tailings were obtained from a suitable disc filter. In addition, authors examined the main components of each tailings such as grain size distribution, specific gravity, chemical and mineralogical composition, and rheological properties.

### 2.1 Tailings Material Determination

The tailings were sized by using a Maslersizer S Ver. 2.15 (Malvern Instruments Ltd, UK) particle size analyser and the results are shown on Figure 1.

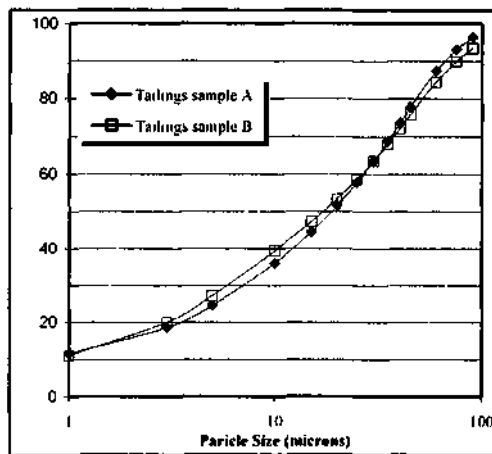


Figure 1 Particle size distribution of tailings samples A and B.

The grain size distribution of tailings is closely similar. Tailings sample A was found to have approximately 52 wt% finer than 20 (µm and tailings sample B was found to have approximately 54 wt% finer than 20 (µm, which indicates that both tailings can be classified as a medium size tailings material (Kesimaletal.2002).

These tailings generally produce a good paste fill, but typically have lower strength than the coarse tailings because of a higher water/cement ratio (Landriault2001).

The specific gravity of the tailings was also measured using picnometer. The results indicated that tailings sample A had a specific gravity of 4.82 and tailings sample B had a specific gravity of 4.10.

In addition, the main chemical element of the two tailings was determined by atomic absorption spectrometry, spectro photometer, and wet chemical analysis and are listed in Table 1.

Table 1. Chemical composition of tailings samples A and B.

Element (symbol)	Tailings sample A	Tailings sample B (%)
MgO	0.45	1.00
Al <sub>2</sub> O <sub>3</sub>	1.44	3.90
SiO <sub>2</sub>	3.26	10.88
CaO	0.74	1.43
Fe <sub>2</sub> O <sub>3</sub>	57.00	43.67
S <sup>2-</sup>	2.24	3.68
K <sub>2</sub> O	0.14	0.24
Na <sub>2</sub> O	0.26	0.22
NiO	0.13	0.17
TiO <sub>2</sub>	1.04	0.68
Cr <sub>2</sub> O <sub>3</sub>	0.04	0.03
Mn <sub>2</sub> O <sub>3</sub>	0.02	0.10
P <sub>2</sub> O <sub>5</sub>	0.08	0.13
Loss on ignition	31.55	27.72
Total	98.49	93.85

The presence of sulphur species within cementitious material can cause a deterioration in quality for construction works (e.g., mortars and concrete in the building trade) (Ducic and Miletic 1987, Bernier et al. 1999, Santhanam et al. 2001). It has been observed in many sulphide-rich backfills.

The high sulphide and low cement contents enhance the reaction. Calcium-rich cements like ordinary portland cement have many disadvantages, especially at a long term due to their weak resistance to sulphate attack on the cement bonds (Ouellet et al. 1998, Benzaazoua et al. 1999).

The mineralogical composition of the tailings materials of A and B was determined by X-ray diffraction analysis (XRD), which provides determination of the crystalline mineral assemblage of a sample (Fig. 2 and 3). The relative proportions of the minerals are based on peak height.

The major mineral identified in tailings samples A and B is pyrite. The results are summarised in Table 2 identified as major, minor and trace quantities. (Table 2).

Table 2. Mineralogical composition for tailings.

Crystalline Mineral Assemblage (*)			
Sample Type	Major	Minor	Trace
Tailings sample A	pyrite	dolomite	sphalerite. barite
Tailings sample B	pyrite	kaolinite. dolomite	barite. sphalerite

\* relative proportions based on peak height.

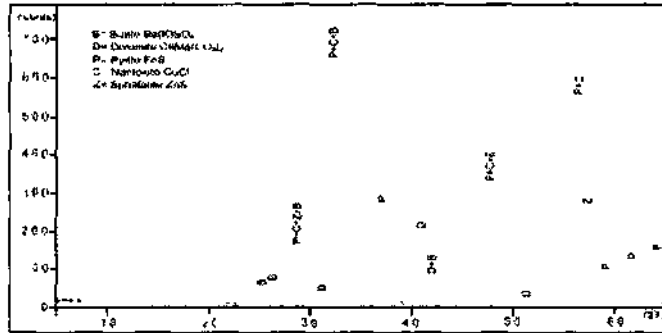


Figure 2. XRD analysis for tailings sample A.

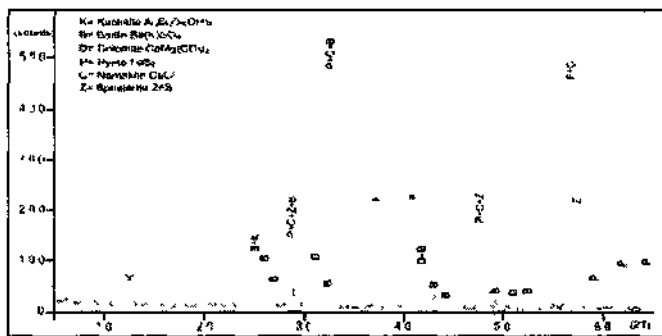


Figure 1 XRD analysis for tailings sample B.

A series of tests was conducted to determine the solids content of specific slump values for both tailings. For this reason, uncemented mill tailings were mixed at slump consistencies of between 5.4" and 7.4". Thus, solids content of each tailings samples was determined. Figure 4 indicates a relationship between solids content and slump consistencies.

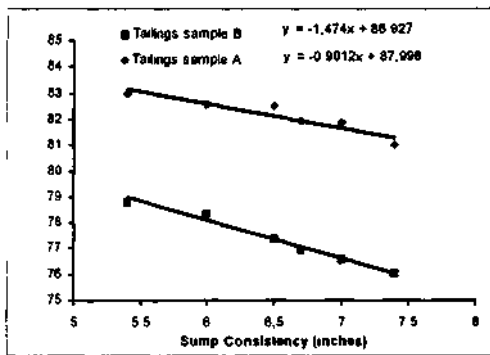


Figure 4. Solids content vs slump for ladings A and B.

A series of Theological index tests was performed to gain an appreciation of the tailings potential for

pipeline transport and to determine tailings properties. The index testing consists of a series of water retention, settling and modified slump cone tests designed to assess the colloidal properties of an uncemented material. In general, a granular material must have at least 15wt% finer than 20 microns to produce sufficient colloidal water retention to create paste-flow properties and can be transported through a borehole/pipeline by a fluid material with paste How properties (Landriault 2001).

The rheological index test results for tailings samples A and B are presented at Figure 5.

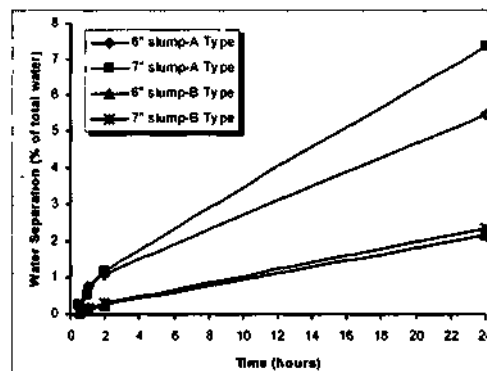


Figure 5. Water separation vs time for tailings A and B.

### 2.2 Binder characteristics

Various binder types are used to increase the durability and the strength of the mixture. Backfill strength and curing period are directly dependent on the binder quality and their content. The increase in cement content generally results in a higher strength of paste backfill. In this study, PKÇ/B 32.5-R type Unye portland composite cement was used as binder. The main chemical elements of PKÇ/B type binder are listed in Table 3.

Table 3. Chemical composition of Unye portland cement.

Chemical Composition	PKÇ/B 32.5-R (%)
SiO <sub>2</sub>	32.27
Insoluble residue	26.3 X
Soluble SiO <sub>2</sub>	6.49
Al <sub>2</sub> O <sub>3</sub>	8.91
Fe <sub>2</sub> O <sub>3</sub>	3.83
CaO	44.02
MgO	1.41
SO <sub>3</sub>	1.99
Loss on ignition	4.06
Undetermined	2.91
Free CaO	0.26
Total	97.09

Binder costs can be a significant contribution to the operating costs of the mine (Grice 1998). Pozzolanic products such as fly ash and blast furnace slags can be used to increase the strength of backfill and reduce the binder consumption (Hassani et al. 2001, Ouellet and Hassani 2002). Portland composite cement is a hydraulic binder which consists of 21-35 wt% additives (blast furnace slag, silica, natural and industrial pozzolan, fly ash), 65-79 wt% clinker, 5 wt% minor additives, and calcium sulphate as the setting regulator (UÇS 2002).

## 3 METHODS

### 3.1 Paste backfill mixture preparation

Two different paste backfill mixtures were prepared for tailings samples A and B. Proportions of between 3 and 7 wt% binder types and slump values between 6" and 7" were chosen for the tailings samples to make the various mixtures of paste backfill. Water was added to bring the mix to the desired slump prior to casting the cylinders. Lake water was used as mixing-water.

HOBART A 200 model mixer (ASTM C-305) was used to homogenize paste backfill mixture consisted of tailings samples, cement and water (Fig. 6).



Figure 6 Hobart Mixer

The final slump, which corresponds to the height between the top of an initial state of the paste (moulded into a 6.0" height conic cylinders) and its final state (after removing the cone) was measured using the standardized ASTM C143-90 (Fig. 7).

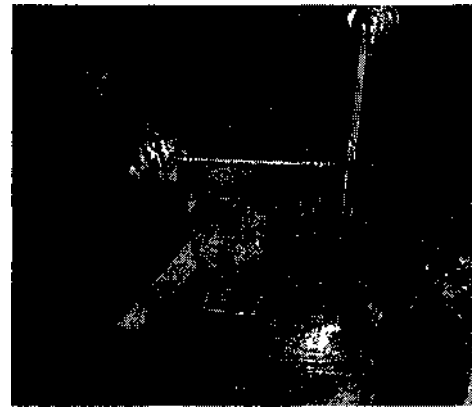


Figure 7. Détermination of slump value.

### 3.2 Casting paste backfill cylinders

The paste backfill mixtures were poured into plastic-cylinders with a diameter of 4" and a height of 8". Between seven and nine small diameter holes were drilled in the bottom of each cylinder mould so that excess water could drain and to simulate the free

drainage that may occur when paste backfill was placed in a slope (Fig 8)



Figure 8 Plastic cylinder used in the tests

After pouring the different mixtures into the cylinders they were sealed and cured in a humidity chamber maintained at approximately 95% humidity and 25°C temperature (this is similar to underground mine conditions) for 28 days curing period. After the curing period, paste backfill specimens were tested by UCS tests.

#### 4.1 Uniaxial compressive strength tests

A total of 135 backfill samples (78 and 57 samples for tailings sample A and B, respectively) were conducted to uniaxial compression strength (UCS) tests using a digital mechanical press (ELE Multiplex 50) having a normal loading capacity of 50 kN and a displacement rate of 1 mm per minute (Fig 9).

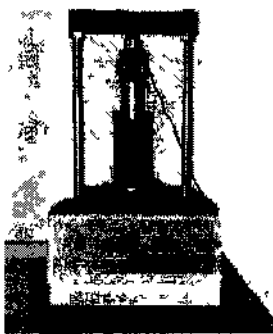


Figure 9 ELE Multiplex 50

The two ends of the samples were first rectified to get plane surface before running the tests. The specimen's height-to-diameter ratio was 2. Three cylinders were tested for each cement and curing period for the paste poured at between 6' and 7"

slump consistencies and the results averaged to provide representative results.

## 4 RESULTS

The aim of these strength tests mainly was to obtain optimum cement content and slump value between paste backfill samples A and B poured the different mixtures.

### 4.1 Results of paste backfill tailings sample A

The UCS test results obtained from tailings sample A is shown in Figure 10.

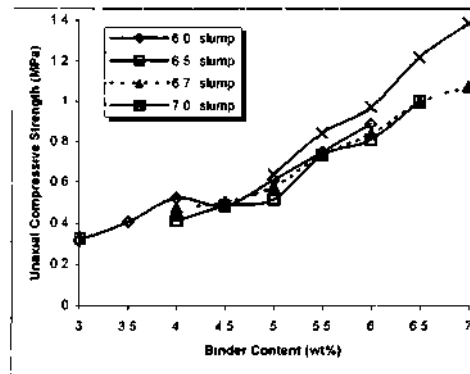


Figure 10 UCS test results for paste backfill sample A at 28 curing period

From the Figure 10, the maximum value of UCS obtained with the paste backfill sample A is always proportional to the binder proportion at a given slump value (6.0", 6.5", 6.7", 7.0").

The paste backfill sample at 7" slump value and 7 wt% of cement content produced higher strength acquisition than that of the other slump values after 28 days curing period. It reached a value of about 1.387 MPa.

### 4.2 Results of paste backfill tailings sample B

The UCS test results obtained from tailings sample B is presented at Figure 11.

With 6.0" slump value, the paste backfill sample B having 7 wt% binder produced the highest strength of 0.812 MPa after 28 days of curing period. However, with 7.0" slump value, the strength acquisition of the paste backfill sample B is lower than that of the paste backfill sample A with the same slump value.

The required water addition for hydrated phases of the cement was 21.625 wt% for the paste backfill sample B having 6.0" slump value and 7 wt% binder. This was 17.450 wt% for the paste backfill sample A having the same slump value and binder.

content. In other words, the paste backfill sample B seemed to have more water retention compared with the paste backfill sample A and therefore resulted in low strength acquisition.

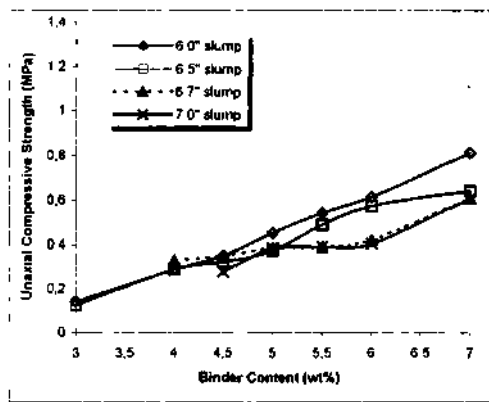


Figure 11. UCS test results for paste backfill sample B at 28 days curing period.

The UCS test results showed that the paste backfill sample A produced strengths approximately between 1.5 and 2.5 times that of the paste backfill sample B at the same binder content and slump value.

#### 4.3 Mineralogical and chemical characteristics

The tailings sample A is dominated by iron oxide,  $Fe_2O_3$  (57%). Minor quantities of silicon dioxide,  $SiO_2$  (3.26%) and aluminium oxide,  $Al_2O_3$  (1.44%) were detected as well as trace amounts of magnesium, calcium, potassium, sodium, nickel, titanium, chromium, manganese and phosphorous oxides (all less than 2%).

The tailings sample B are also dominated by iron oxide,  $Fe_2O_3$  (43.67%) and minor quantities of silicon dioxide,  $SiO_2$  (10.88%) and aluminium oxide,  $Al_2O_3$  (3.90%), together with trace amounts of magnesium, calcium, potassium, sodium, nickel, titanium, chromium, manganese and phosphorous oxides (all less than 2%).

The tailings samples A and B have more enough pyrite minerals according to the chemical analysis results. This means that the presence of sulphide minerals within cemented composites as well as the soluble sulphates have a deleterious effect on the strength of paste backfill due to sulphate attack at a long time. In addition, the tailings sample B seems to have higher silicate content than that of the tailings sample A. This makes the tailings sample B retain more water and affects negatively by reducing the strength of the paste backfill at a long term.

## 5 CONCLUSIONS

The purpose of this study was to investigate the effect of binder and tailings chemistry on the UCS of paste backfill after curing period of 28 days using tailings sample A and B.

According to the UCS test results, the paste backfill sample A with 7" slump value resulted in a higher strength acquisition than other slump consistencies. With a mixture containing 7 wt% cement content, cylinders poured with 7" slump indicated the highest strength development compared with other slump consistencies after 28 days curing period. This can be attributed to the need of potential water content (18.125 wt%) of 7 wt% cement content for binder hydration. In this point, it reached the highest UCS value of 1.387 MPa.

The paste backfill sample B with 6" slump value produced higher strengths. At 28 days curing period the UCS of 6" slump reached a value of 0.82 MPa. However, the UCS results of the backfill sample B with 7" slump were much lower than those achieved for the backfill sample A with 7" slump. This could be interpreted the water retention of the backfill sample B.

Both tailings samples are sulphide-rich in terms of mineralogical characteristic. Therefore, they had a deleterious effect on the strength of paste backfill generating acid in the presence of water and oxygen.

Additionally, this study highlighted that the mechanical and rheological properties of cemented paste backfill depended on physical, chemical and mineralogical properties of the mill tailings, binder types and their proportions.

## REFERENCES

- ASTM C305. 1996. Standard practice for mechanical mixing of hydraulic cement pastes and mortars of plastic consistency. ASTM Standards.
- ASTM C143-90. 1994. Standard test method for slump of hydraulic cement concrete. Annual book of ASTM Standards. Vol. 04.
- Benzaazoua. M., Belem. T., Bussière. B., 2002. Chemical factors that influence the performance of mine sulphidic paste backfill. *Cement and Concrete Research*. 32: 1133-1144.
- Benzaazoua. M., Ouellet. J., Servant. S., Newman, K., Verbürg. R., 1999. Cementitious backfill with high sulfur content: Physical, chemical and mineralogical characterization. *Cement and Concrete Research*. 29: 719-725.
- Bernier. R.L., Li. M.G., Mootman. A., 1999. Effects of tailings and binder geochemistry on the physical strength of paste backfill, in: Goldsack, Belzile, Yearwood, Hall (Eds.). *Sudbury'99. Mining and the Environment II*. 3: 1113-1122.

- Brackebusch, F.W. 1994. Basics of paste backfill systems. *Mining Engineering* . 46:10: 1175-1178.
- Chew, J.L. 1999. A parametric study of the factors affecting the application of post-consumer waste glass as an alternative cementing agent in paste backfill, M.Sc. Thesis. Queen's University. Canada.
- Ducic, V. Miletic, S. 1987. Sulphate corrosion resistance of blended cement mortars. *Durability Builtl Mater.* 4: 343-356.
- Edwards, F.. 1992. Backfilling in underground mines. AIME Annual General Meeting, Canada.
- Hassani, F.P., Ouellet, J., Hossein, M.. 2001. Strength development in underground high-sulphate paste backfill operation. *CIM Bulletin.* 94: 1050: 57-62.
- Grice, T. 1998. Underground mining with backfill. The 2nd Annual Summit-Mine Tailings Disposal Systems. Busbane. Australia.
- Kesimal, A. Alp. I. Yilmaz, E. Erçikdi, B. 2002 Optimization of test results obtained from different size slumps with varying cement contents for Cayeh Mine's clastic and spec ore tailings. K.T.U. Engineering and Architecture Faculty. Revolving Fund Project. Trabzon.
- Lamos, A.W., Clark, I.H.. 1989. The influence of material composition and sample geometry on the strength of cemented backfill, in: Hassani, et al. (Eds.). *Innovation in Mining Backfill Technology.* A.A. Balkema. Rotterdam. pp. 89-94.
- Landriault, D.. 1995. Paste backfill mix design for Canadian underground hard rock mining. *Proceedings of the 97th Annual General Meeting of the CIM Rack Met hanics and Strata Control Session.* Halifax. Nova Scotia.
- Landriault, D., Lidkea, W.. 1993. Paste fill and high density slurry fill. *Proceedings of the International Congiess on Mine Design.* Queens University. Canada.
- Landriault, D.. 2001. Backfill in underground mining, in: W.A. Hustrulid (Eds.). *Underground Mining Methods Engineering Fundamentals and International Case Studies.* SME. pp. 608-609.
- Thomas, E.G., Nantel, J.H., Notely, K.R.. 1979. Fill technology in underground metalliferous mines. *International Academic Services Limited.* Kingston. Ontario. 293 pages.
- Naylor, J., Farmery, R.A., Tenbergen, R.A.. 1997. Paste backfill at the Macassa mine with flash paste production in a paste production and storage mechanism. *Proceedings of the 29th Annual Meeting of the Canadian Mineral Processors,* Ottawa. Ontario, pp. 408-420.
- Ouellet, J., Bidwell, T.J., Servant, S.. 1998. Physical and mechanical characterisation of paste backfill by laboratory and in situ testing, in: M.Bloss (Ed.). *Proceedings of the Sixth International Symposium on Mining with Backfill, MinefillIX.* Brisbane. Australia, pp. 249-1253.
- Ouellet, J., Hassani, F.. 2002. Chemistry of paste backfill. *Proceedings 34th Annual Meeting of the Canadian Mineral Processors.* CIM. Canada.
- Santhanam, M., Cohen, M.D., Olek, J.. 2001. Sulfate attack research whither now?. *Cement and Concrete Research.* 31:6:845-851.
- Stromberg, B.. 1997. Weathering kinetics of sulphidic mining waste: an assessment of geomechanical process in the Aitik mining waste rock deposit. *AFR-Report 159.* Department of Chemistry. Inorganic Chemistry. Royal Institute of Technology. Stockholm. Sweden.
- UÇS. 2002. Ünye Çimento Sanayii ve Ticaret AŞ.. Portland çimento ürün katalogları. Ordu. Türkiye <http://www.unvecimento.com.tr/>
- Viles, R.F., Davis, R.TR, Boily, M.S.. 1989. New material technologies applied in mining with backfill, in: F. Hassani, et al. (Eds.). *Innovation in Mining Backfill Technology.* A.A. Balkema. Rotterdam, pp. 95-101.
- Weaver, W.S., Luka, R.. 1970. Laboratory studies of cement-stabihzed mine tailings. *Can. Min. Metal Bull.* 64: 988-1001.
- Yilmaz, E., Kesimal, A., Deveci, H., Erçikdi, B.. 2003 The factors affecting the performance of Paste Backfill; physical, chemical and mineralogical characterization. *The first Engineering Sciences Congress for Young Researcher (MBGAK0.İ),* 17-20 February 2003. (in Turkish).

